The Pennsylvania State University
The Graduate School
Department of Energy and Mineral Engineering

FACTORS AFFECTING HYDRAULICALLY FRACTURED WELL PERFORMANCE IN THE MARCELLUS SHALE GAS RESERVOIRS

A Thesis in
Energy and Mineral Engineering
by

Tunde A. Osholake

© 2010 Tunde A. Osholake

Submitted in Partial Fulfillment
of the Requirements
for the Degree of

Master of Science

December 2010

The thesis of Tunde A. Osholake was reviewed and approved* by the following:

John Yilin Wang
Assistant Professor of Petroleum and Natural Gas Engineering
Thesis Co-Adviser

Turgay Ertekin
Professor of Petroleum and Natural Gas Engineering;
George E. Trimble Chair in Earth and Mineral Sciences;
Undergraduate Program Officer of Petroleum and Natural Gas Engineering
Thesis Co-Adviser

Terry Engelder
Distinguished Professor of Geosciences

R. Larry Grayson
Professor of Energy and Mineral Engineering;
Graduate Program Officer for Energy and Mineral Engineering

*Signatures are on file in the Graduate School.

ABSTRACT

Unconventional reservoirs such as shale, hydrates, tight sand, ultra tight sand and coal bed methane reservoirs serves as alternative sources to meet the increasing demand for energy here in the US and all over the world. The exploitation of unconventional gas reservoirs has become an integral part of the North American gas supply. The economic viability of many unconventional gas developments hinges on the effective stimulation of extremely low permeability reservoir rocks. With improve drilling and stimulation technologies, many unconventional plays have become realistic contributors to the energy budget. The Marcellus shale reservoir contains large amount of natural gas resources and its proximity to high demand markets along the East Coast of the United States makes it an attractive target for energy development. According to Arthur et al (2008), the estimated original gas in place in the Marcellus shale is 1,500 TCF (Trillion Cubic Foot) which when compared to other shale plays in the United States almost doubles the estimated gas in place associated with other shale reservoirs. So, it is crucial for exploration and production companies to invest in the Marcellus shale.

Hydraulic fracturing technique is the stimulation method of choice in shale gas reservoirs. Even though hydraulic fracturing technique improves ultimate gas recovery, they are several factors that occur after hydraulic fracture treatment that impacts the production of natural gas from a hydraulically fractured shale gas well. These factors include: multi phase flow of gas and water, proppant crushing, proppant diagenesis, interaction of fracture fluid with reservoir particles, relative permeability, capillary pressure, reservoir permeability change, operational conditions, and reservoir heterogeneity among others.

This research study was undertaken to quantify the impact of selected post hydraulic fracture factors that affects shale gas wells. With the use of commercial reservoir simulation software that models cumulative production and production flow rate from a vertical well located in a 160 acre Marcellus shale gas reservoir, we are able to quantify how much impact this various factors will have on the ultimate gas recovered from the reservoir under consideration. An ideal case single phase flow was simulated and was used as the base result for which simulation results of other factors was compared.

The new knowledge from this research should enable engineers to better design fracture treatments and helps operators manage the wells in the Marcellus shale formation. The observation and recommendations will also be useful for further studies in this area.

TABLE OF CONTENTS

LIST OF FIGURES vi

LIST OF TABLES viii

ACKNOWLEDGEMENTS ix

CHAPTER 1 1

INTRODUCTION 1

CHAPTER 2 4

LITERATURE REVIEW 4

2.1 Multiple phase flow 5

2.2 Interaction of fracture fluid and reservoir particles 11

2.3 Proppant Crushing 19

2.4 Proppant diagenesis 24

2.5 Reservoir Compaction 28

2.6 Operational Condition 33

CHAPTER 3 34

PROBLEM STATEMENT 34

CHAPTER 4 35

MODEL DESCRIPTION 35

CHAPTER 5 44

SIMULATION RESULTS AND ANALYSES 44

5.1 Ideal Single Phase Flow 45

5.2 The Effect of Multiphase Flow on Production 49

5.3 The Effect of Proppant Crushing on Production 53

5.4 The Effect of Proppant Diagenesis on Production 56

5.5 The Effect of Reservoir Compaction on Production 62

5.6 The Effect of Operational Condition on Production 67

5.7 The Effect of Addition of All Factors on Production 71

5.8 The Effect of Proppants on Gas Recovery 75

CHAPTER 6 78

CONCLUSIONS AND RECOMMENDATION 78

REFERENCES 80

APPENDIX 83

LIST OF FIGURES

Figure 1: The model approach to developing shale gas reservoirs (Schlumberger 2007) 3
Figure 2: Full capillary pressure curve (Dake 1997) 6
Figure 3: Multiplier of pressure drop vs. fraction flow of liquid for two gas rates (Palisch 2007) 10
Figure 4: A Marcellus shale well flowback analysis major cation trend (Blauch et al. 2009) 13
Figure 5: A Marcellus shale well flowback analysis anion trend (Blauch et al. 2009) 13
Figure 6: A Marcellus shale well flowback monovalent ion trend (Blauch et al. 2009) 14
Figure 7: A Marcellus shale well flowback divalent cation trend (Blauch et al. 2009) 15
Figure 8: A Marcellus shale well flowback Barium trend (Blauch et al. 2009) 16
Figure 9: Illustration of crushing in sand and ceramic proppant at same closure stress (Palisch et al. 2007) 20
Figure 10: Disassembled Cooke conductivity cell for used in the modified API RP-61 to measure proppant conductivity (Palisch et al. 2007) 22
Figure 11: Illustration of crushing in sand and ceramic proppant at same closure stress (Palisch et al. 2007) 23
Figure 12: Schematic of proppant pack diagenesis process over time (Lee et al. 2009) 25
Figure 13: Experimental set-up for permeability and compaction test of shale cores (Reyes 2000) 29
Figure 14: Schematic of the fracture well model 36
Figure 15: 160 acre drainage area with a hydraulically vertical well located at the top corner ... 37
Figure 16: Relative permeability curve for the gas phase 40
Figure 17: Relative permeability curve for the water phase 40
Figure 18: Dual porosity model 41
Figure 19: Proppant transport scenarios (Cipolla et al. 2009) 43
Figure 20: Cumulative gas production of various proppants with different hydraulic fracture conductivity 46
Figure 21: Gas flow rate of various proppants with different hydraulic fracture conductivity. ... 47
Figure 22: Water injected and water produce from highly and lowly conductive hydraulic fracture. 49
Figure 23: Cumulative gas production from high and low conductivity hydraulic fracture 50
Figure 24: Gas production rate from high and low conductivity hydraulic fracture 51
Figure 25: Proppant crushing effect on gas recovery for selected proppants. 54
Figure 26: Proppant crushing effect on gas production rate for selected proppants. 55
Figure 27: Plot showing proppant pack permeability decrease over time (Lee et al. 2009) 56
Figure 28: Proppant diagenesis effect on selected proppants (highly conductive hydraulic fracture). 58
Figure 29: Proppant diagenesis effect on selected proppants (lowly conductive hydraulic fracture). 59
Figure 30: Gas flow rate of selected proppants (High conductivity hydraulic fracture). 60

Figure 31: Proppant diagenesis effect on selected proppants (low conductivity hydraulic fracture)....... 61
Figure 32: Reservoir compaction effect on selected proppants (Highly conductive hydraulic fracture)....... 63
Figure 33: Reservoir compaction effect on selected proppants (low conductive hydraulic fracture)....... 64
Figure 34: Reservoir compaction effect on yearly gas production rate for selected proppants (high and low conductivity hydraulic fracture). 66
Figure 35: Effect of several BHP on overall gas production (high permeability fracture)....... 67
Figure 36: Effect of several BHP on overall gas production (low permeability fracture)....... 68
Figure 37: Effect of several BHP on overall water production (high conductivity fracture) 69
Figure 38: Effect of several BHP on overall water production (low conductivity fracture) 70
Figure 39: Cumulative impact of various effects on overall gas recovery. 71
Figure 40: Cumulative impact of various effects on gas production rate. 72
Figure 41: Cumulative impact of various effects on overall gas recovery. 73
Figure 42: Cumulative impact of various effects on gas production rate. 74
Figure 43: Effects of proppants on overall gas production. 75
Figure 44: Effects of proppants on gas production rate. 76
Figure 45: Effect of 20-40 ceramic proppant on cumulative production....... 83
Figure 46: Effect of 20-40 ceramic proppant on gas production rate 84
Figure 47: Effect of 20-40 multicoated sand proppant on cumulative gas production....... 85
Figure 48: Effect of 20-40 multicoated sand proppant on gas production rate 86
Figure 49: Effect of 40-70 Ceramic proppant on cumulative gas production 87
Figure 50: Effect of 40-70 ceramic proppant on gas production rate 88
Figure 51: Effect of 40-70 multicoated sand proppant on cumulative gas production....... 89
Figure 52: Effect of 40-70 multicoated sand proppant on gas production rate 90

LIST OF TABLES

Table 1: Comparison of data for the gas shale in the United States (Arthur et al 2008) 2
Table 2: A Marcellus shale well late stage flowback water chemical data characterization data (Blauch et al. 2009) 17
Table 3: Table describe the mineral composition and location of shale cores in this study (Reyes 2000) 31
Table 4: Gas permeability test result for Wapanuka shale (Reyes 2000) 32
Table 5: Basic reservoir and fracture parameters 38
Table 6: PVT table 39
Table 7: Proppant pack permeability of different proppants 46
Table 8: Pressure vs. permeability multiplier of different proppants used in our model.............. 53
Table 9: Table showing proppant pack permeability decrease with time..................................... 57
Table 10: Permeability multiplier table employed in modeling compaction effect...................... 62
Table 11: Table showing overall gas recovery associated with 4 proppants. 77

ACKNOWLEDGEMENTS

First and foremost, I thank God, who has given me the strength, the knowledge and wisdom and understanding necessary to succeed in all my life endeavors, especially in my graduate career here at Penn State University. I will like to thank the department of Energy and Mineral Engineering for given me opportunity to come and study at this great and prestigious institution.

I will personally like to thank Dr. Turgay Ertekin for all the help and guidance he has given me since my first day at Penn State. His contributions have been immense in the successful completion of my graduate study. I would like to express my profound gratitude to my academic and research advisor, Dr. John Yilin Wang for his relentless effort in providing support and guidance during the course of this study. I would also like to thank Dr. Terry Engelder for serving on my thesis committee. I will like to thank everyone in my research group 3 S laboratories for their help during the course of my research study. I like to thank the folks at Computer Modeling Group for their support in using the reservoir simulation software CMG necessary for my research.

Most importantly, I like to thank my immediate family; Tunde Osholake Sr., Iyabode Osholake, Olaitan Osholake, Olawunmi Osholake. I will not be where I am today without their love, support, advice, encouragement, motivation, guidance, provisions. They have given me the gift of Education which is the greatest gift of all. I also like my brother in law Akinade Eboda, my nephew Adedayo Eboda and the rest of my extended family.

I wish to take the opportunity to thank all the friends I have acquired here at Penn State for making my stay here in State College worthwhile and my entire friends from back home in New Jersey, Georgia, Oklahoma, and Nigeria. Thank you all for your friendship, support and guidance over the years.

Thank you all and God bless.

CHAPTER 1

INTRODUCTION

The depletion of conventional oil and gas reservoirs in the US and also the rise in energy demand has led to the energy industry searching for alternative energy sources to meet the demand. Early history of the petroleum industry shows that most of the hydrocarbon energy sources were produced from conventional oil and gas reservoirs. Unconventional reservoirs such as shale, hydrates, tight sand and coal bed serves as alternatives sources to meet the increasing demand for energy.

Shale gas reservoirs are organic-rich formations and are apparently the source rock as well as the reservoir. Gas is stored in the limited pore space of the rock and sizeable fraction of gas is adsorbed on the organic material (Cipolla 2009). According to Arthur et al (2008), the estimated natural gas potential in shale reservoirs is between 50 to 1,500 TCF. Shale reservoirs exhibit extremely low permeability in the range of 10 to 1000 nano - Darcy (10^{-6} md) and thus require effective stimulation strategies in place to produce economically.

Typical shale gas reservoirs exhibit a net thickness of 50 to 600 ft, porosity of 2 to 8%, total organic carbon of 1 to 14 % and are found at depths ranging from 1,000 to 13,000 ft. There are various shale gas plays across the US including the Barnett shale, the Woodford shale, the Fayetteville shale, the Haynesville shale and the Marcellus shale among others. In this research, we are focused more on the Marcellus shale.

Marcellus shale gas reservoir is located across the eastern part of the United States running across the southern tier and the Finger Lakes regions of New York, in the northern and western part of Pennsylvania, the eastern part of Ohio through the western part of Maryland, and throughout most of West Virginia. The shale reservoir contains largely untapped natural gas resource and its proximity to market along the East Coast of the United States makes it an attractive target for energy development.

Typical properties of the Marcellus are as follows: estimated basin area of 95,000 square miles, found at depth ranging from 4,000 to 8,500 ft, net thickness of 50 to 200 ft, total organic carbon of 3 to 12 %, total porosity of 10%, and original gas in place of 1,500 TCF. A comparison of the Marcellus and other shale plays in the U.S is shown in the table below.

	Barnett	Fayetteville	Haynesville	Marcellus	Woodford	Antrim	New Albany
Estimated Basin Area (sq. miles)	5,000	9,000	9,000	95,000	11,000	12,000	43,500
Depth (ft)	6,500 to 8,500	1,000 to 7,000	10,500 to 13,500	4,000 to 8,500	6,000 to 11,000	600 to 2,200	500 to 2,000
Net Thickness (ft)	100 to 600	20 to 200	200 to 300	50 to 200	120 to 220	70 to 120	50 to 100
Total Organic Carbon (%)	4.5	4.0 – 9.8	0.5 – 4.0	3 – 12	1 – 14	1 – 20	1 – 25
Total Porosity (%)	4 – 5	2 – 8	8 – 9	10	3 – 9	9	10 – 14
Gas Content (Scf/ton)	300 to 350	60 to 220	100 to 330	60 to 100	200 to 300	40 to 100	40 to 80
Original gas in place (TCF)	327	52	717	1,500	52	76	160
Well spacing (acres)	60 to 160	80 to 160	40 to 560	40 to 160	640	40 to 160	80
Reserves (TCF)	44	41.6	251	262 to 500	11.4	20	19.2
Water produced (bbl/day)	0	0	0	0	0	5 – 500	5 – 500

Table 1: Comparison of data for the gas shale in the United States (Arthur et al 2008)

As we can see, Marcellus shale compared to all other shale has approximately 750 TCF original gases in place more than any other shale play in the United State. These statistical estimates makes Marcellus shale a reasonable reservoir to explore and produce from.

According to Schlumberger, the modeling approach to developing shale gas reservoirs efficiently requires an extensive program of technical evaluation. This approach includes identifying and quantifying the resources, determining the appropriate benchmark for recovery factors. The following step is the reservoir simulation, then evaluating various stimulation strategies to optimize well performance. From individual well optimization, attention is focused on optimization of the field. The figure below shows the integrated model approach to achieve unparalleled results in shale gas recovery.

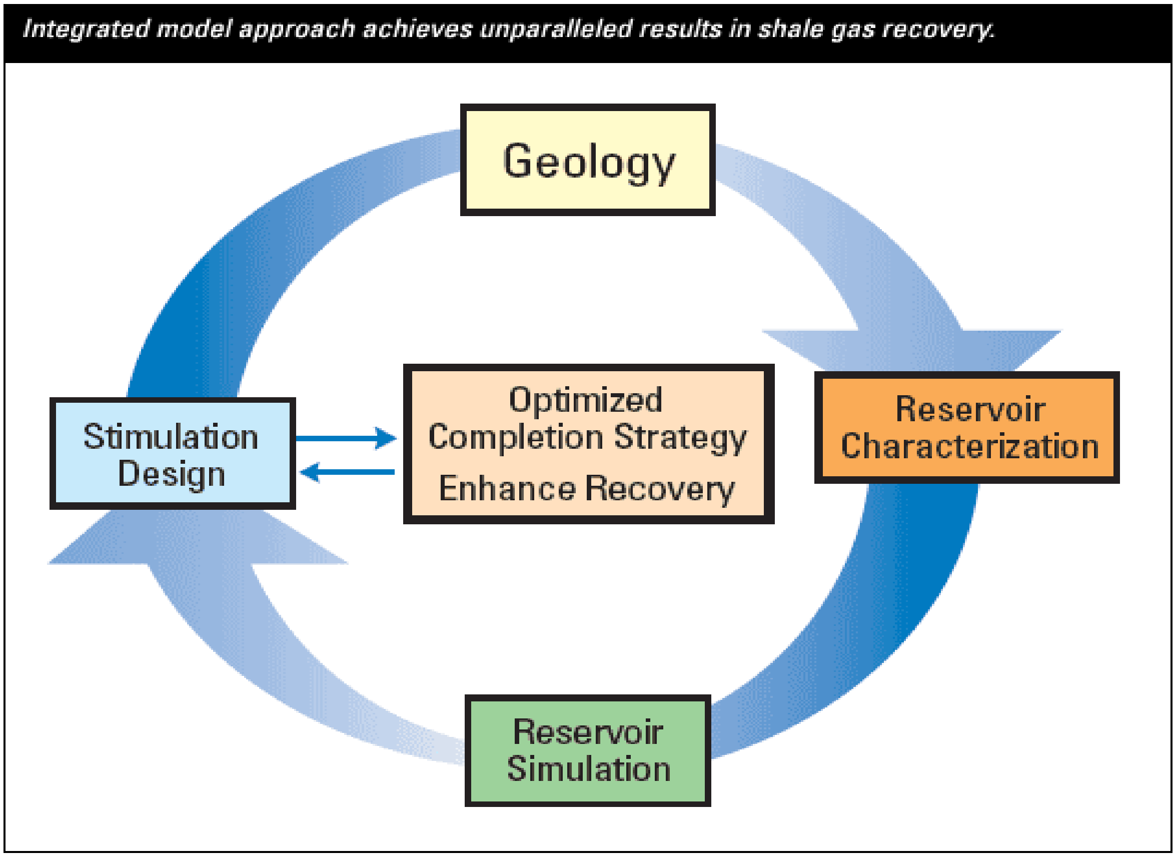
Integrated model approach achieves unparalleled results in shale gas recovery.
Geology
Stimulation Design
Optimized Completion Strategy
Enhance Recovery
Reservoir Characterization
Reservoir Simulation

Figure 1: The model approach to developing shale gas reservoirs (Schlumberger 2007)

From Figure 1, we can see that geology; reservoir characterization; reservoir simulation; and stimulation design all play important roles in successful shale gas recovery. Accurate geologic exploration, accurate reservoir characterization facilitates accurate reservoir simulation which is instrumental in developing effective stimulation design that plays a significant role in the ultimate gas recovered from any given shale reservoir.

CHAPTER 2

LITERATURE REVIEW

Hydraulic fracturing has been widely used in the industry. Hydraulic fracturing tends to increase the productivity of shale gas wells if applied successfully, but there are various factors affecting the effectiveness of the treatment. These factors impact the fracture cleanup process and the ultimate gas recovery. These factors includes: multiphase (gas and water) flow, proppant crushing, proppant diagenesis, relative permeability, capillary pressure, reservoir permeability change, operational conditions, reservoir heterogeneity, and fracture fluid interaction with reservoir particles among others.

The goal of this research study is to develop a reservoir model that will quantify how much impact these factors have on ultimate gas recovery and gas production rate from a shale gas reservoir with particular focus on the Marcellus shale. Before an accurate reservoir model can be built; it is essential to develop a critical understanding for the selected factors that will be studied in this research. Various articles have been reviewed and summarized in this section.

2.1 Multiple phase flow

Multiphase flow is the simultaneous flow of different phases such as gas, oil and water. Clean up process is a period of controlled production, generally following a stimulation treatment, during which time treatment fluids return from the reservoir formation. During cleanup process, multiphase flow of gas and fracture fluid occurs in the created fracture and the reservoir. When simultaneous flow of different phases (gas and water) occurs in a hydraulic fracture, factors such as relative permeability, capillary pressure, and wettability inside the fracture and the reservoir will play important roles in the fracture fluid cleanup behavior and long term gas production in shale gas reservoir.

To understand how relative permeability, wettability, and capillary pressure can affect cleanup process and gas production from shale gas reservoir, a brief explanation of these factors is given from literature.

According to Dake (1997), wettability describes the relative preference of a rock to be covered by a certain phase. Rock is defined to be water-wet if the rock has more affinity for water than for oil or gas. In that case, a major part of the rock surface in the pores will be covered with a water layer. Wettability is affected by the minerals present in the pores. For example, clean sandstone (quartz) is strongly water-wet, but sandstone reservoir rock is usually found to be intermediate-wet; which implies that some pores are water wet and other pores are oil or gas wet. In reality, extreme water-wetness or extreme oil-wetness is rare. But particularly for a gas-liquid systems, it can be safely assumed that gas is always the non-wetting phase. Basic reservoir properties like relative permeability, capillary pressure, saturation, and resistivity depends robustly on wettability of the reservoir rock.

Dake (1997) defined capillary pressure (P_c) as the pressure difference between the non-wetting phase and the wetting phase as a function of the wetting-phase saturation. For gas-water systems in porous rock, gas is generally considered to be the non-wetting phase. Therefore, capillary pressure equation for a gas-water system is defined as:

$$P_c\,(sw) = P_g - P_w \qquad (1)$$

In reservoir engineering, capillary pressure is an important parameter for simulation studies and analysis, especially for heterogeneous reservoirs. In many cases the inflow of water needs to be modeled, so particularly the imbibitions capillary pressure is of importance.

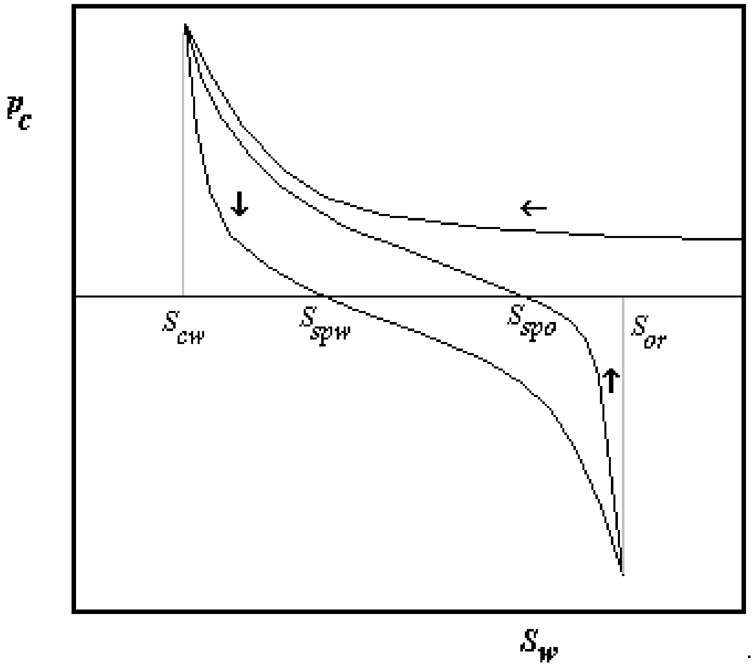

Figure 2: Full capillary pressure curve (Dake 1997)

Figure 2 shows a typical capillary pressure curve for a gas-water system in a porous media. The capillary pressure curve consists of three curves: a primary drainage, a primary imbibition, and a second drainage curve.

For the primary drainage curve, when water saturation equals (*Sw* = 1), an "entrance" pressure (threshold pressure) needs to be exceeded before gas can enter the core sample and then reach a plateau. With decreasing water saturations, the capillary pressure rises to a higher value. The capillary pressure goes to infinity at the connate water saturation (*Scw*).

For the primary imbibitions curve, when the gas pressure is slowly decreased, water will spontaneously imbibe and the saturation will increase. The capillary pressure decreases, and is smaller than the drainage capillary pressure at the same water saturation, an effect called capillary hysteresis. When the gas pressure is equal to the water pressure, capillary pressure is zero (*pc* = 0), the saturation reaches the spontaneous water imbibitions saturation. Increasing the water saturation from this point can be accomplished only by forcing the water in, hence by increasing the water pressure above the gas pressure. An ever higher water pressure is required to force more gas out to reach the residual gas saturation. Capillary pressure (*pc*) goes to minus infinity at water saturations near (*1 – Sgr*) (residual gas saturation). In summary, a negative capillary pressure implies the need for a larger water injection pressure than the gas-phase pressure for the displacement of gas, the non-wetting phase out (Dake 1997).

For the second drainage curve, when the water pressure is slowly decreased, the non-wetting phase (gas), will spontaneously imbibe and the water saturation will decrease. The capillary pressure will be larger than the imbibition capillary pressure for the same saturation because of the capillary hysteresis. At *pc* = 0, the capillary pressure curve crosses the spontaneous gas-imbibition saturation. More water can only be removed by increasing the gas pressure (also *pc*)—a forced drainage process. The capillary pressure approaches infinity around connate water saturation (Dake, 1997). As already discussed, wettability determines the distribution of fluids in the porous rock and affects parameters like connate water and residual saturation. The capillary pressure also depends strongly on the wettability. In the extreme water-wet situation, the drainage and the imbibition capillary pressure are positive over the whole saturation range. Water will spontaneously imbibe from *Scw* to (1 – *Sor*). A kind of inverse situation holds for an extremely oil-wet system; the drainage as well as the imbibition capillary pressure are negative.

Multi-phase flow through porous media is governed by the interplay between capillary, viscous, and gravitational forces. The flow regime can be characterized by the capillary number and the bond number. Capillary forces usually dominate in reservoir flow. Even though the actual flow is driven by viscous or gravitational forces, the flow paths at the pore scale are determined by the capillary forces.

Dake (1997) defined permeability as the single-phase fluid conductivity of a porous material. From Darcy's law, the permeability K of the material is defined as:

$$K = \frac{q\mu L}{A\,\Delta P} \qquad (2)$$

Where μ is the viscosity of the fluid, which is forced to flow, at flow rate q, through a porous medium, of length L and with cross section A, such that the pressure difference across the length of the porous medium is ΔP.

In case of two or more fluids flowing simultaneously through a porous medium, a relative permeability for each of the fluids can be defined. It describes the extent to which one fluid is hindered by the other. The relative permeability is defined by setting-up the Darcy equation individually for each phase (i) that flows in the pore space:

$$q_i = \left(\frac{Kk_{ri}}{\mu_i} \right) A \frac{\Delta p_i}{\Delta x} \qquad (3)$$

In the above equation, q_i is the flow rate of phase i, k_{ri} is the relative permeability of phase i, μ_i is the viscosity of phase i, and P_i is the pressure drop within the phase i. The term in brackets is denoted as the mobility of the phase i. ($K* k_{ri}$) represents the total permeability of phase i.

From various definitions of wettability, capillary pressure, saturations and relative permeability, we can see that all this parameters play a significant role when it comes to multiple phase flow (fracture fluid cleanup) in a porous media (shale gas reservoir).

According to Palisch et al. (2007), multiphase effects have been described in many ways but various researchers consistently describe that pressure loss in a fracture may increase by an order of magnitude when more than one phase (gas and liquid) are mobile within the fracture. Various researchers in their studies describe the pressure loss measured in a fracture when two or more phases are mobile significantly increase as compared to pressure losses associated with single phase flow.

Palisch et al. (2007) explained that at least three phenomena will contribute to multi phase pressure losses. They are: alteration of fluid saturation, relative permeability changes, and phase interaction between fluids.

Alteration of fluid saturation simply explains that as the saturation of one phase increases, it reduces the flow area available to the other phase. As with the case of hydraulic fracture process, if we assume that gas saturation in the reservoir is 100% initially before fracturing process begins, as the process proceeds and reservoir rock are being opened, the saturation of liquid begins to rise from 0% to ideally 30% and the saturation of gas phase begins to decrease from 100% to ideally 70%, then the flow area available to the gas phase has been altered by 30% and can lead to decrease in gas production.

Relative permeability changes explain that as the saturation of one phase increases (fracture fluid), the permeability relative to the other phase (gas) decreases. In gas wells, as the water saturation increases in the fracture, the gas permeability in the fracture will decrease when the proppant becomes wetted with liquid. Palisch et al (2007) noted that even though both scenario of alteration of fluid saturation and relative permeability change can be significant, it does not explains the drastic losses that have been observed in many gas wells as they begin to cut small percentage of water. It is however the third phenomena that causes most of the multiphase pressure losses.

The phase interaction between fluids (gas-water) explains the concept of mobility differences. As two phase moves through a porous media at drastically different velocities, they begin to interfere with the flow of each other, yielding a very inefficient flow regime. This is particularly evident in gas-water flow. The impact of multiphase flow is illustrated in Figure 3 which shows the multiplier of pressure drop caused by very small increase of water in a low rate gas situation

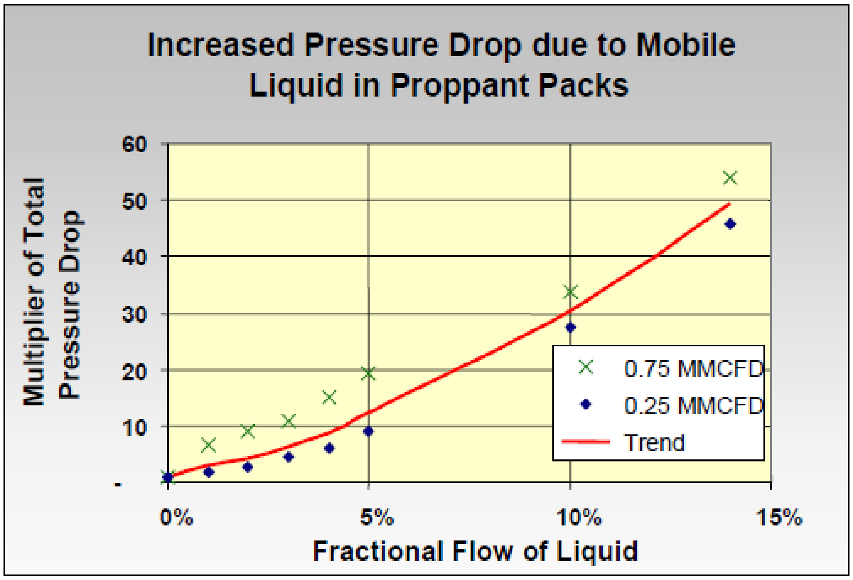

Figure 3: Multiplier of pressure drop vs. fraction flow of liquid for two gas rates (Palisch 2007)

In conclusion, multiphase flow occurring in a hydraulically fractured well can significantly reduce the fracture fluid cleanup and long term gas production in shale gas reservoir due to several reservoir parameters such as wettability, capillary pressure and relative permeability.

2.2 Interaction of fracture fluid and reservoir particles

Shale reservoirs are characterized by extremely low permeability rocks. To make hydrocarbon production from shale reservoirs economical, hydraulic fracture stimulation with large volumes of proppant is applied. Upon flowback, large volumes of fluid must be managed to minimize impairment to gas production. Post fracture flowback fluid produced from the well consists of potentially damaging formation products that have the potential to cause production impairment by yielding damaging precipitates within the fracture, perforation and wellbore. This constituent can also make waste water disposal expensive and challenging.

According to Blauch (2010), potentially damaging formation substances picked up down hole by fracturing fluids includes: soluble salts; metal ions such as iron, barium, strontium, calcium, and magnesium; solubilized sulfate such as gypsum, anhydrite and celistite; scale and gas forming microbes; and significant levels of anions including carbonate, bi-carbonate, sulfate, and chlorides.

During fracture cleanup process, post fracture flowback fluid will interact with the proppant pack in the created fracture before it reaches the wellbore. During this process, part of the material dissolved by the flowback fluid will interact with the proppant pack in the created fracture, perforations, piping and surface equipments. The interaction of the materials from the formation and the proppant pack becomes a detriment to the proppant pack permeability, porosity and conductivity. The interaction of produced formation material can create scale formation in the perforation, piping, and surface equipment. Reduction in proppant pack porosity, permeability or conductivity and formation of scale in perforation, piping and surface equipment adversely affects hydrocarbon production.

To reduce the formation of geochemical precipitates, bacteria damage and other problems encountered due to dissolved constituent, appropriate geochemical control agents, bacterial control agents, iron control polymers, scale control agent are added to the initial fracture fluid. To effectively quantify how much impact formation substances have on total gas production in the Marcellus shale, it is important to identify all the dissolved constituent of post fracture fluid, the respective concentrations, the dominating constituent and the impact on fracture porosity, permeability or conductivity.

Studies conducted by Blauch et al. (2009) on the Marcellus shale post fracture flowback water includes nineteen samples of post fracture flowback water collected from a Marcellus shale gas well in southwestern Pennsylvania. Analyses were run on each sample to determine the constituents and the concentration of each. Results were compiled, and the trends from observation are presented by Blauch et al. (2009) in the publication “Marcellus Shale Post-Frac Flowback Water”. The important conclusions that Blauch described are as follows:

1. The amount of dissolved constituent increased as flowback progressed (Figure 4). Both sodium and calcium show similar trend as well.
2. Sodium and calcium are most concentrated cations (Figure 4).
3. Alkalinity and pH dropped as flow back progressed, potentially explaining the rise of calcium levels
4. Sulfate scaling is likely as calcium is rising while sulfate is dropping (Figure 4 and Figure 5).
5. Figure 6 shows a monovalent ion trend; Figure 7 illustrates a divalent cation trend.
6. As shown in Figure 8, the sharp rise in barium levels in the latter stage of flowback (at about 30% load recovery) suggests potential barium sulfate scale formation during the last potion of the flowback. The solubility of barium sulfate is very low and it can be a very aggressive scale.
7. Iron content in the flowback increased as flowback progressed (Table 2).
8. Chemical composition of these waters can be classified as highly saline.
9. With cations such as Mg, Sr, and Ba, chemical signatures of the waters are consistent with evaporate and carbonate rich source.

Plots and table below shows the data gathered from the analysis of the well by Blauch et al. (2009)

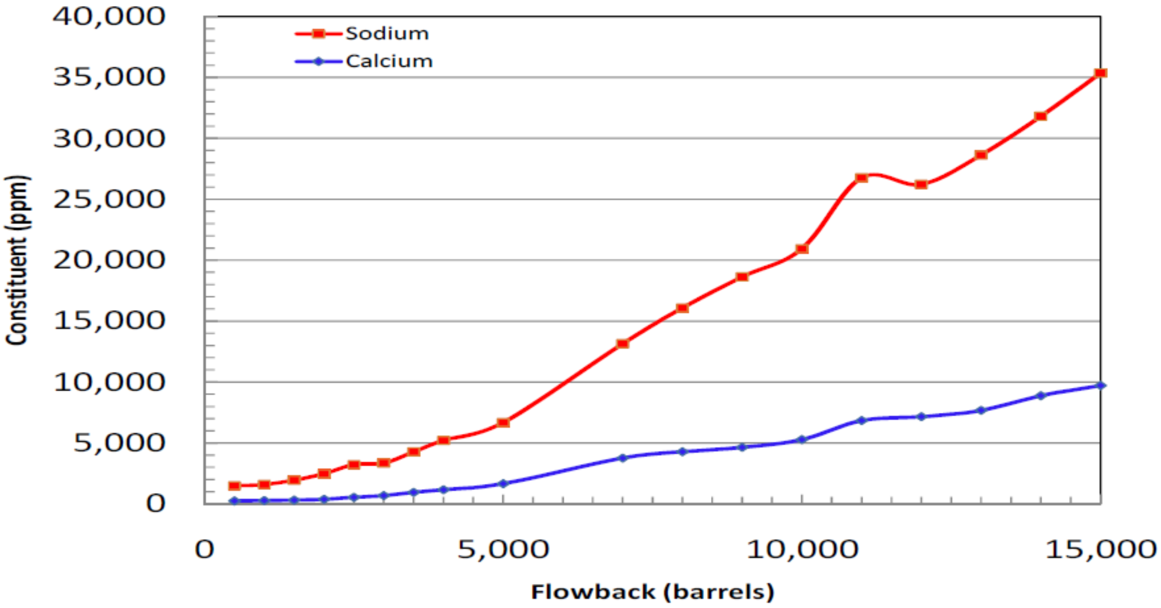

Figure 4: A Marcellus shale well flowback analysis major cation trend (Blauch et al. 2009)

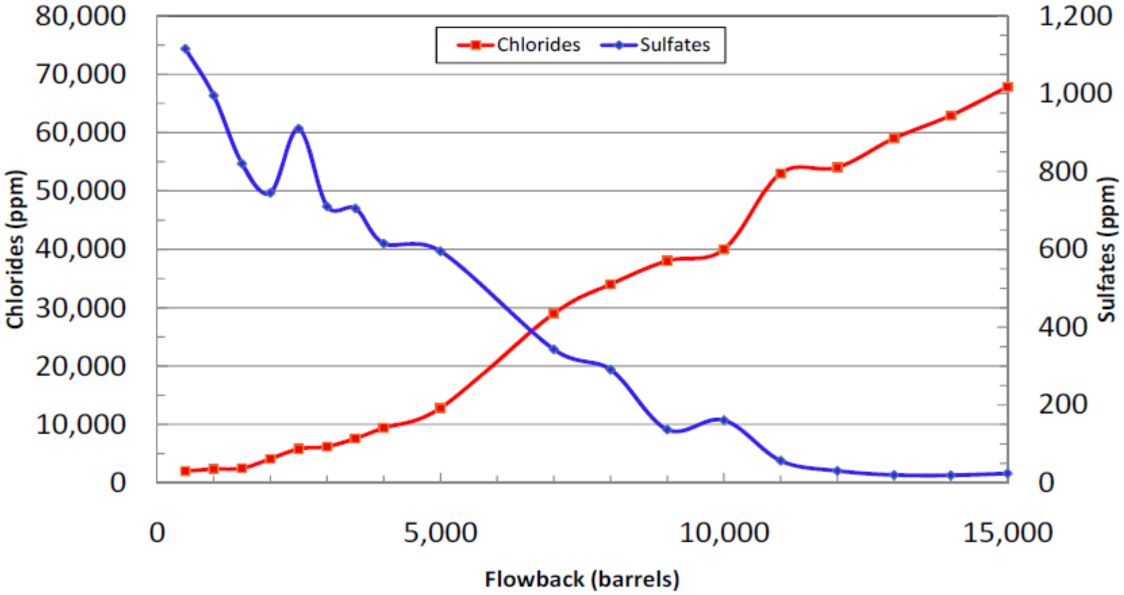

Figure 5: A Marcellus shale well flowback analysis anion trend (Blauch et al. 2009)

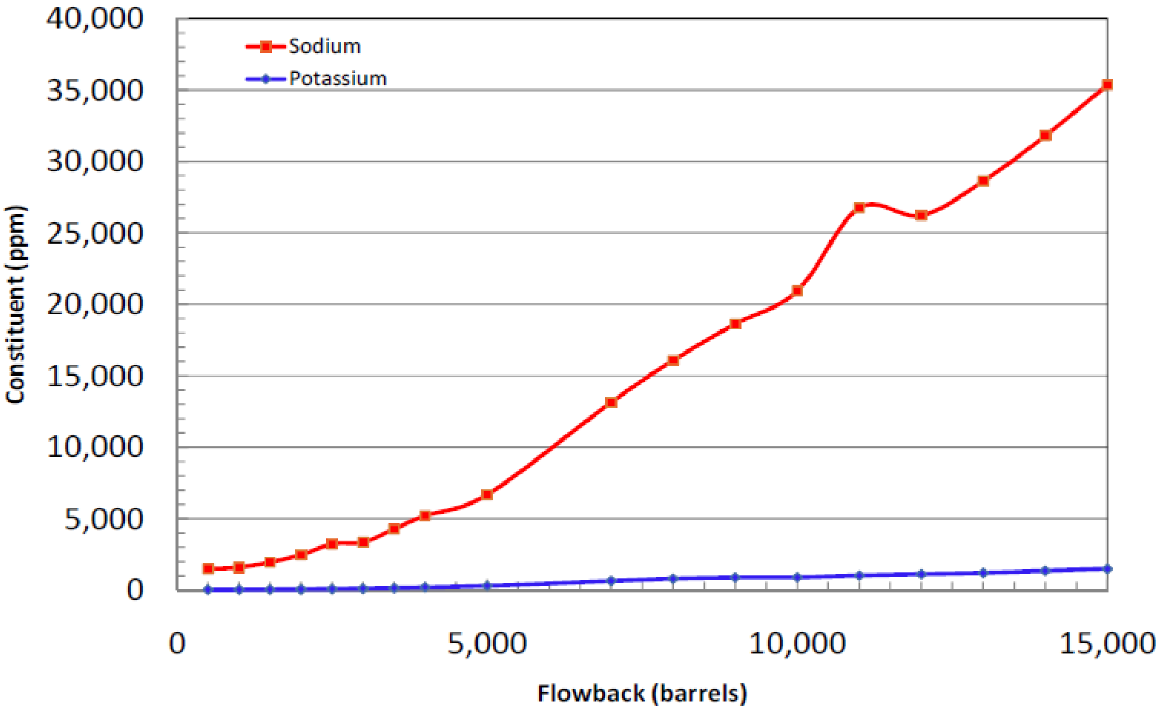

Figure 6: A Marcellus shale well flowback monovalent ion trend (Blauch et al. 2009)

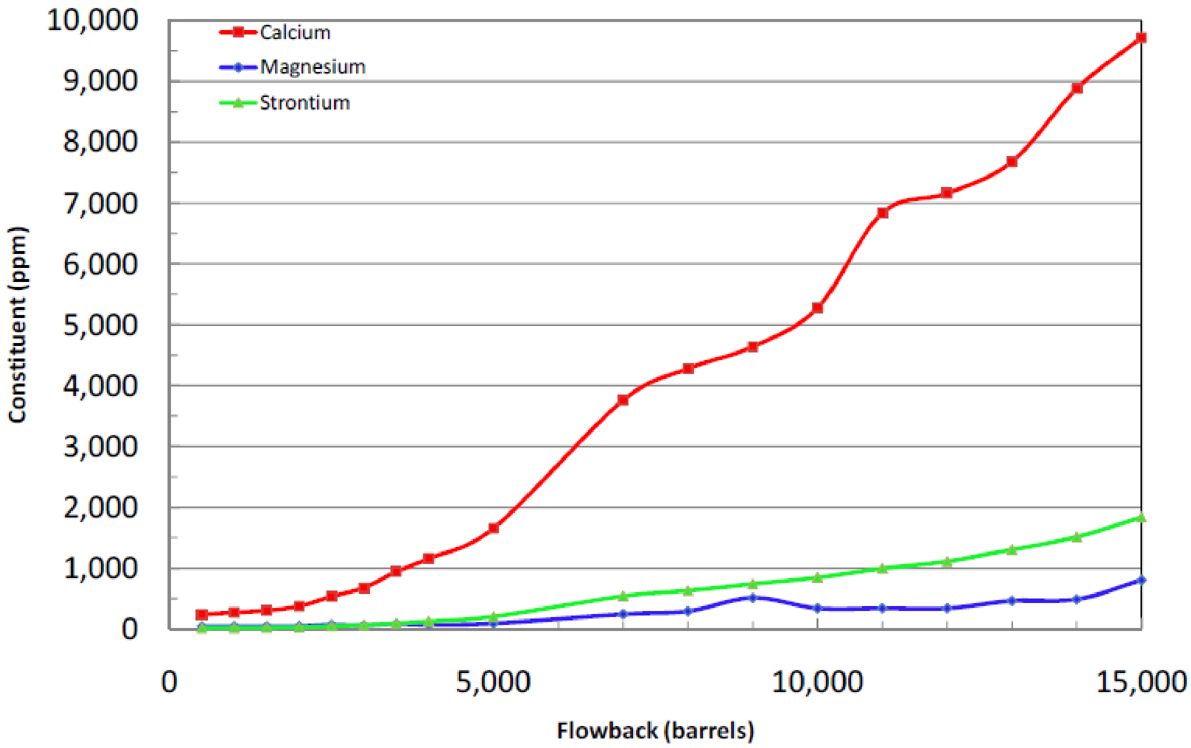

Figure 7: A Marcellus shale well flowback divalent cation trend (Blauch et al. 2009)

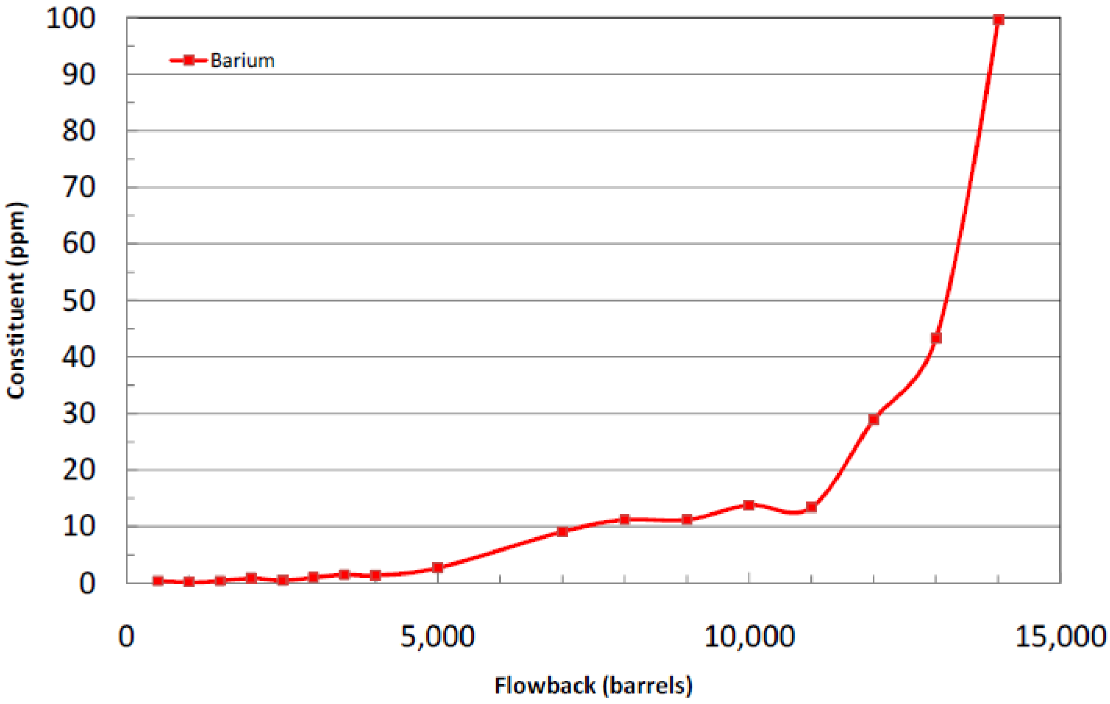

Figure 8: A Marcellus shale well flowback Barium trend (Blauch et al. 2009)

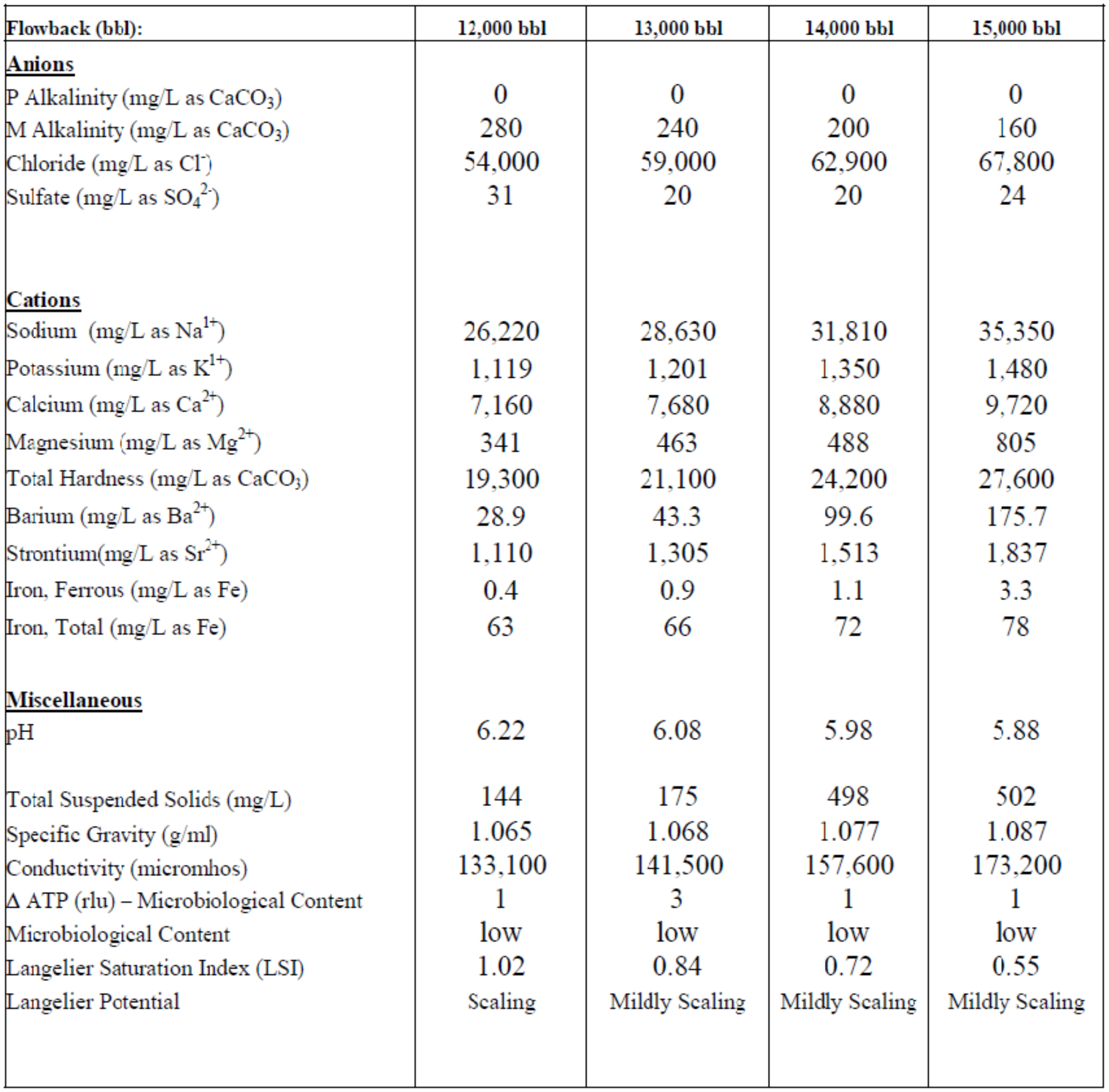

Flowback (bbl):	12,000 bbl	13,000 bbl	14,000 bbl	15,000 bbl
Anions				
P Alkalinity (mg/L as $CaCO_3$)	0	0	0	0
M Alkalinity (mg/L as $CaCO_3$)	280	240	200	160
Chloride (mg/L as Cl^-)	54,000	59,000	62,900	67,800
Sulfate (mg/L as SO_4^{2-})	31	20	20	24
Cations				
Sodium (mg/L as Na^{1+})	26,220	28,630	31,810	35,350
Potassium (mg/L as K^{1+})	1,119	1,201	1,350	1,480
Calcium (mg/L as Ca^{2+})	7,160	7,680	8,880	9,720
Magnesium (mg/L as Mg^{2+})	341	463	488	805
Total Hardness (mg/L as $CaCO_3$)	19,300	21,100	24,200	27,600
Barium (mg/L as Ba^{2+})	28.9	43.3	99.6	175.7
Strontium(mg/L as Sr^{2+})	1,110	1,305	1,513	1,837
Iron, Ferrous (mg/L as Fe)	0.4	0.9	1.1	3.3
Iron, Total (mg/L as Fe)	63	66	72	78
Miscellaneous				
pH	6.22	6.08	5.98	5.88
Total Suspended Solids (mg/L)	144	175	498	502
Specific Gravity (g/ml)	1.065	1.068	1.077	1.087
Conductivity (micromhos)	133,100	141,500	157,600	173,200
Δ ATP (rlu) – Microbiological Content	1	3	1	1
Microbiological Content	low	low	low	low
Langelier Saturation Index (LSI)	1.02	0.84	0.72	0.55
Langelier Potential	Scaling	Mildly Scaling	Mildly Scaling	Mildly Scaling

Table 2: A Marcellus shale well late stage flowback water chemical data characterization data (Blauch et al. 2009)

Most of the data gathered in Blauch articles show a similar trend in terms of the concentration of constituents. From literature review, we are able to draw a conclusion that sodium and calcium are the most concentrated cations; chlorides are the most concentrated anion. These ions will be the dominating constituents that affect fracture conductivity, porosity and permeability in hydraulically created fractures. Also scaling of perforation, pipes and well resulting from the reaction of formation products can significantly decrease the production from Marcellus shale gas reservoir.

To be able to simulate and quantify how much ion precipitation in hydraulically created fracture, we need to find data that relate either the conductivity or the permeability response of created fracture with the amount of ions present in the fracture.

2.3 Proppant Crushing

According to Weaver et al (2007), proppant crushing can occur at several sites during fracturing operation. Cracking and chipping of proppants can occur during the transportation of proppants pack from the manufacturing site to the place of final use which is the fracturing site. Efforts should be taken to minimize the exposure of proppant to chipping and cracking during the transportation process.

However the type of proppant crushing that we are concerned with in this research is the crushing that occurs when the proppant has been transported into the created hydraulic fracture and it is exposed to closure stress from the overburden formation layers. The major source of proppant crushing is formation closure, particularly where the proppant is not well distributed. Conductivity examinations conducted on proppant pack indicates that crushing is most prevalent at the interface and less significant toward the center of the pack.

There are two primary sources of fines within a hydraulic fracture. Fines are generated either from the proppant pack or the reservoir itself. Reservoir fines can be generated due to spalling as proppant embeds into the fracture surface while proppant fines are generated due to proppant crushing.

According to Palisch et al. (2007), while all proppants experience crushing, the way they crush is dependent on their substrate. When sand based proppant crushes, it shatters similar to a drinking glass and it breaks into so many small fragments. On the other hand, most ceramic based proppant cleave like a brick. Figure 9 shows this difference.

Fines generated falls into three size categories which includes: particles too large to penetrate the proppant pack, particles small enough to enter the proppant pack but large enough to subsequently plug the pore throat of the proppant pack, and lastly, particles small enough to flow through the proppant pack all the way to the wellbore.

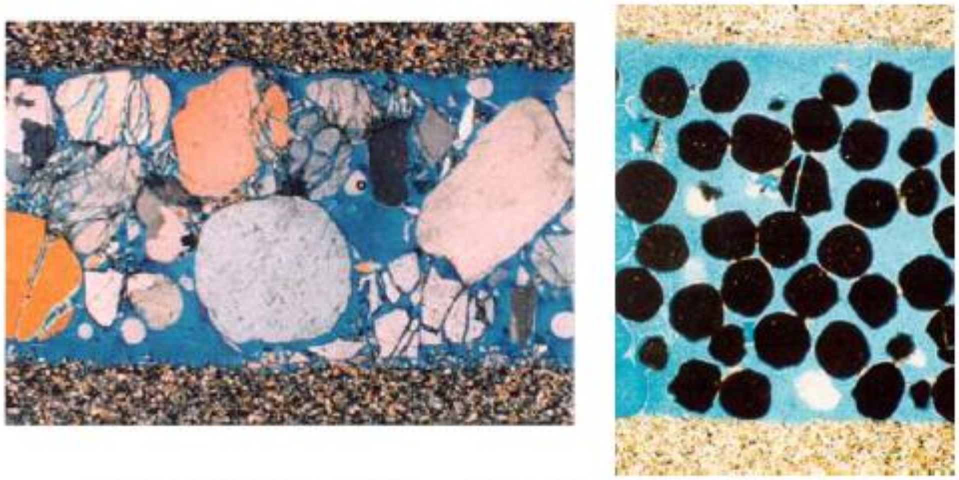

12/20 Hickory/Brady Sand at 8000 psi.

Intermediate Density Ceramic at 8000 psi.

Figure 9: Illustration of crushing in sand and ceramic proppant at same closure stress (Palisch et al. 2007)

The fines that are too large as well as those that are small enough to flow through the proppant pack are not damaging to the pack. However, particles small enough to enter the proppant pack but large enough to subsequently plug the pore throat of the proppant pack are detrimental to the proppant pack conductivity.

When proppants are crushed and they produce fines that can plug the proppant pack, the porosity of the proppant pack is reduced which subsequently reduces the permeability of the proppant pack. Permeability reduction in the proppant pack will therefore reduce the fracture conductivity. The relationship between fracture conductivity and proppant pack permeability is shown in the equation 4 below.

$$\text{Conductivity} = k_{frac} * w_{frac} \qquad (4)$$

Where k_{frac} is the fracture permeability and w_{frac} is the fracture width created by the hydraulic fracture. As we can see there is a direct relationship between fracture or proppant pack permeability and fracture conductivity.

In order to understand realistic conductivity, it is essential to understand how conductivity of proppant pack is measured and reported.

According to Palisch et al. (2007), years ago the American Petroleum Institute (API) developed standard procedures for measuring the conductivity of proppant in the lab using Cooke's conductivity cell. These procedures were documented in API RP-61. The condition for the test includes:

- Steel pistons,
- 2 lb/ft^2 proppant loading,
- Ambient temperature,
- Stress maintained for 15 minutes, and
- 2% KCl fluid pumped at 2 ml/min.

The primary goal of the test was to provide a way to compare the performance of proppants in a way that was practical and repeatable. To substantially improve the RP-61 test, minor modifications were made to the test in 1987 by a consortium sponsored by StimLab. Three main modifications that were proposed include:

- Replacing the steel piston with Ohio Sandstone
- Increasing the temperature to 150 or 250° F, and
- Maintaining the stress for 50 hours

Figure 10 illustrates the Cooke conductivity cell updated for use in the API RP-61 test.

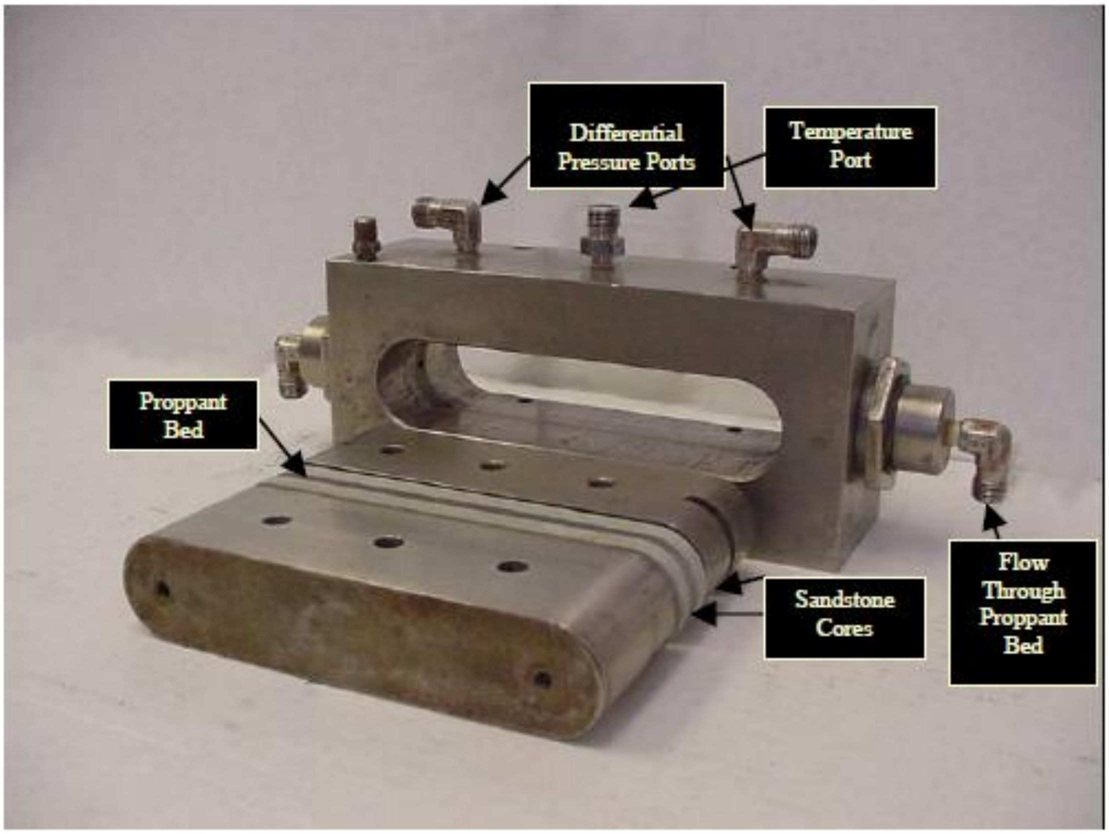
Differential Pressure Ports
Temperature Port
Proppant Bed
Flow Through Proppant Bed
Sandstone Cores

Figure 10: Disassembled Cooke conductivity cell for used in the modified API RP-61 to measure proppant conductivity (Palisch et al. 2007)

These changes was useful in the reduction of the over prediction of proppant pack conductivity from the original test by as much as 85% depending on proppant quality and test conditions. Figure 11 shows the conductivity comparison between APR-RP61 and modified RP-61 tests for a high quality and low quality ceramic proppant.

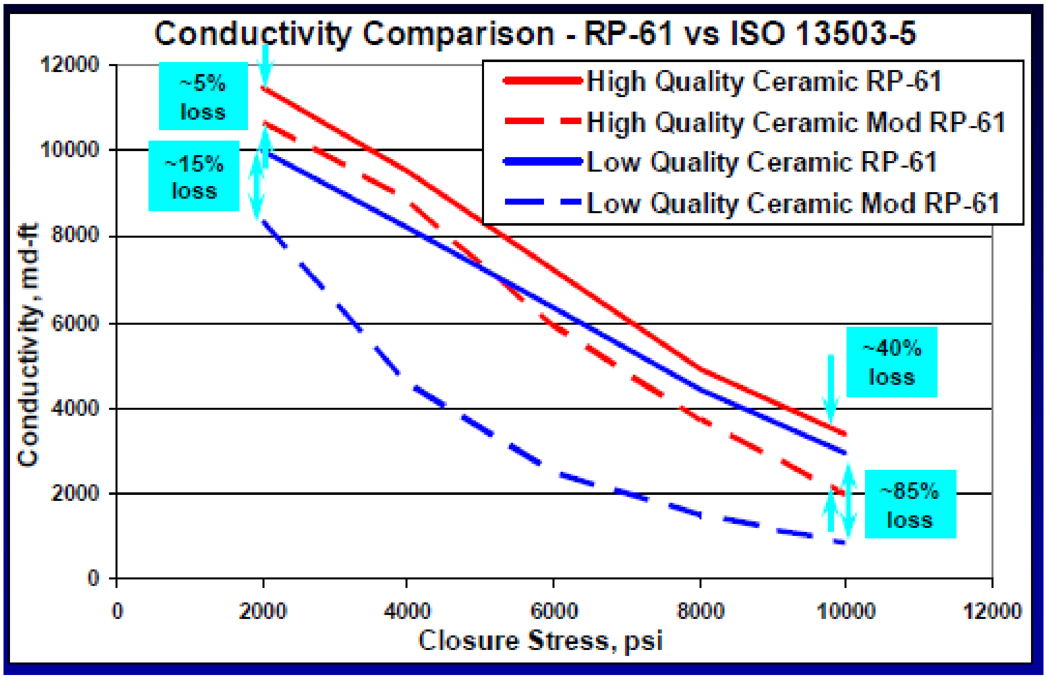

Figure 11: Illustration of crushing in sand and ceramic proppant at same closure stress (Palisch et al. 2007)

The industry has generally accepted this modified API test as the testing standard. The test has also recently been approved by the International Organization for Standardization (ISO). Conductivities measured using the modified API test are normally reported in service companies or proppant manufacturing literature and called “reference”, “laminar” or “baseline” conductivities. These conductivity values are typically used as inputs in fracture flow and propagation models. The setback with the results generated by reservoir production prediction models that make use of this conductivity values is the over prediction of hydrocarbon production. This is because the conductivity measured using the laboratory tests gives ideal prediction of proppant conductivity.

The proppants that we use in our study are the ceramic based Carbo-lite proppants of sizes 20/40 mesh and 40/70 mesh and 100 mesh sand manufactured by Carbo Ceramics and the multi coated sand based proppants of sizes 20/40 mesh, 40/70 mesh and 100 mesh manufactured by Power Prop Santrol.

2.4 Proppant diagenesis

Diagenesis is defined as the alteration of sediments rock at temperature and pressures that can result in significant changes to the mineralogy and texture. Usually, sediments become compacted as they experience higher overburden loads caused by successive sedimentation and burial. The pore space of the sediments is gradually infilled partially with mineral deposit that cements the particles to form the rock. This process is believed to proceed slowly, requiring geologic time to manifest (Weaver et al. 2007).

As a result of earth diagenesis, permeable sandbeds are converted to low–porosity, low-permeability rock. Most hydrocarbon reservoirs that require hydraulic fracturing to ensure an economic production are matured and have already underwent earth diagenesis. These reservoirs are typically high closure stress and high temperature condition reservoir. When the reservoir rock has been fractured and proppants have been transported into the reservoir rock, conditions are suitable to promote geochemical reactions that cause diagenic reaction to begin filling the porosity of the proppant pack.

According to Lee et al. (2009), proppant placed within hydraulic fractures are subjected to an evolving stress field and to changes in chemical composition of the fluids located in the pore spaces. These stresses will be of the order of the pre-stimulation minimum in situ stress. These bulk stresses are amplified at the grain-grain contacts of granular proppants elevating the potential for stress-corrosion cracking and the chemical potential at the contacts. These reactions are surprisingly faster than what would be expected. A schematic diagram of the process of proppant pack diagenesis is shown in Figure 12. Diagenesis process involves the action of three serial processes: dissolution at grain-grain contact, diffusion at the interfacial water film separating the grains, and precipitation on the pore walls.

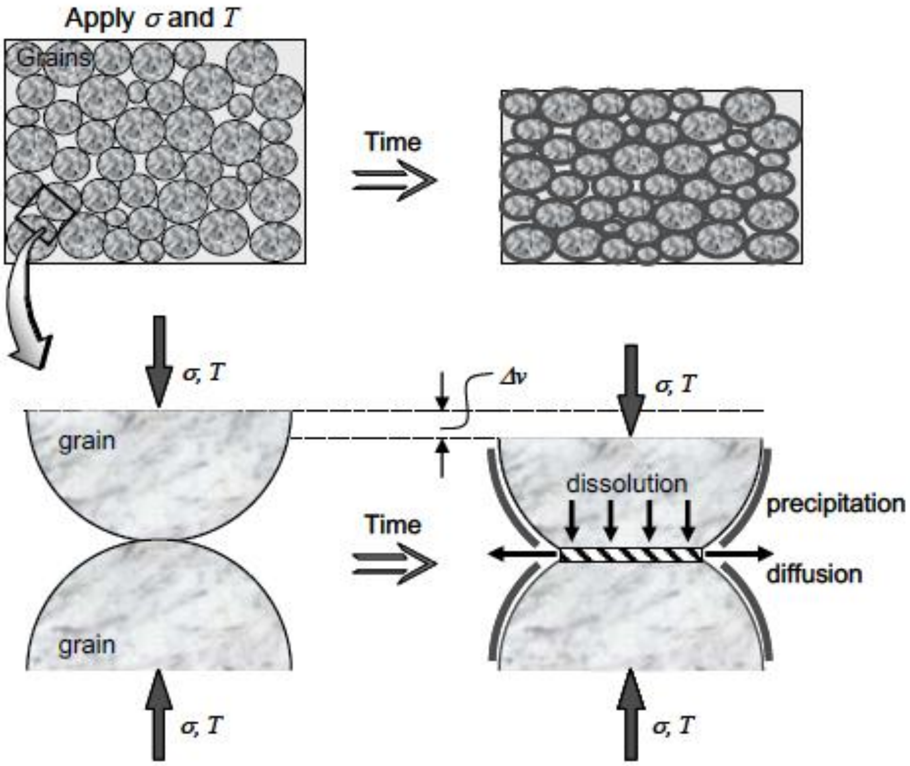

Figure 12: Schematic of proppant pack diagenesis process over time (Lee et al. 2009)

According to Yasuhara et al. (2003), Dissolution at the grain-grain contact provides a source of mass into the pore through the interface, and it is defined in terms of the dissolution mass flux, dM_{diss}/dt, the rate of addition of dissolved mass into solution at the interface.

$$\frac{dM_{diss}}{dt} = \frac{3\pi V_m^2 (\sigma_a - \sigma_c) k_+ \rho_g d_c^2}{4RT}, \tag{5}$$

Where V_m is the molar volume of the solid, σ_a is the disjoining pressure equal to the amount by which the pressure acting at grain-to-grain contacts exceeds the hydrostatic pore pressure, k_+ is the dissolution rate constant of the solid, ρg is the grain density, dc is the diameter of the contacts, R is the gas constant, T is the temperature of the system, and σ_c is the critical stress, which defines stress state where the compaction of grain aggregate will effectively halt.

Yasuhara et al. (2003) further explains that based on the first Fick's law, diffusion along the interface of the grain contacts is defined in terms of the diffusive mass flux dM_{diff}/dt

$$\frac{dM_{diff}}{dt} = \frac{2\pi\,\omega D_b}{\ln\left(d_c/2\varepsilon\right)}\left(C_{int} - C_{pore}\right), \qquad (6)$$

Where, D_b is the diffusion coefficient, and $(C_{int})_{x=\varepsilon}$ and $(C_{pore})_{x=dc/2}$ are concentrations in the interface and pore space, respectively.□ ω is the thickness of the water film trapped at the interface.

According to Yasuhara et al. (2006), the final process of precipitation of solute to the free face of pore wall is defined in terms of the precipitation mass flux, dM_{prec}/dt, the rate of deposition of solute from pore space onto the free walls .

$$\frac{dM_{prec}}{dt} = k_{-}A_{pore}\rho_g V_m\left(\left(\frac{C_{pore}}{C_{eq}}\right)^m - 1\right)^n, \qquad (7)$$

Where, A_{pore} is the nominal area of the void, k_{-} is the precipitation rate constant of the dissolved mineral, and C_{eq} is the equilibrium solubility of the dissolved mineral. m and n are two positive numbers normally constrained by experiment.

The three processes of dissolution, diffusion, and precipitation along with the associated change in geometry, are combined to define the progress of porosity and permeability change with time.

Experiments were conducted by Lee et al. (2009) to understand the transformations that occur in the complex environment within a propped hydraulic fracture. The experiments were conducted to reproduce the hostile environment condition encountered in a diagenic reservoir formation. The principal in situ stress characteristics are of elevated inter-granular stress, high loadings of dissolved constituents with the pore fluids, and elevated temperature coupled with mechanism of pore fluid flushing of the pore space. These characteristics were replicated in two experiments.

The first experiment conducted by Lee et al. (2009) is the furnace experiment. The process of this experiment involves the flow through of simulated reservoir fluid at elevated temperature with the absent of compounding role of inter-granular stress with the hope of capturing the evolution of permeability to be measure directly and followed as a result of mineral dissolution, transport and re-precipitation.

The second experiment, the quad cell experiments conducted by Lee et al. (2009) were conducted at high temperature and with the important action of controlled and applied inter-granular stress but this time with stagnant and no flow through of simulated reservoir fluid. The goal was to measure the evolution of compaction and to infer the evolution of permeability from porosity but including the important influence of the numerous stress related processes that are expected to be important in real reservoirs.

The important conclusion drawn from both the furnace experiment and the quad cell experiment is that the rate of porosity declines most rapidly with an increase in temperature. Porosity decrease is directly proportion to the permeability decrease. Therefore, as temperature and compaction increases in a diagenic reservoir, the proppant pack porosity and permeability decrease significantly.

From this experiment, we are able to generate experimental data relating the relationship between porosity-decrease of a ceramic Carbo-Econoprop proppant (Carbo Ceramics) of varying sizes with time. Another data generated from this experiment is the permeability-decrease of a ceramic Carbo-Econoprop proppant of varying sizes with time. Proppant size of 20/40 mesh, 40/70 mesh and 100 mesh were use to conduct this experiment. We will use this data generated to simulate the effect of proppant diagenesis on total gas production and gas production flow rate in a 160 acre Marcellus shale reservoir with a vertical well on production for a 30 year period.

2.5 Reservoir Compaction

According to Tao et al (2009), fractures are the main channels of production/injection in naturally fractured reservoirs, which make the natural fracture permeability a key parameter to optimizing production in shale gas reservoir. The effective stress increases with the decrease in pore pressure due to production from wells. Increase in the effective stress compact the reservoir rock and reduces reservoir porosity. Decrease in reservoir porosity relates to a decrease in reservoir permeability.

The effect of reservoir compaction on reservoir permeability and natural fracture permeability change has not been studied in sufficient details. In most reservoir simulation models applicable to shale gas reservoirs, reservoir permeability and natural fracture permeability are often treated as a constant during production. However, few investigations have shown that stress has an important effect on the matrix and fracture permeability change during production.

To effectively model the effect of stress dependent permeability change on production in the Marcellus shale, it is essential to conduct laboratory studies on cores from the Marcellus formation. The objective of laboratory test is to simulate actual reservoir condition, actual reservoir stress change and how the permeability of the matrix and fracture of this core changes with increasing effective stress. Laboratory test results are further used in modeling the effect of matrix and fracture permeability change on production from the Marcellus shale reservoir.

Several studies from literature on stress dependent permeability change have predicted permeability change in shale reservoirs using various derived equation in computer models. The difficulty encountered with this kind of study is that derived equations give ideal permeability and porosity change predictions and this causes inaccuracy in the prediction of matrix and fracture permeability change effect on production from a shale reservoir.

Since the Marcellus shale is a recently discovered reservoir, very limited studies have been conducted in the area of stress dependent permeability change. In our studies, we will employ laboratory tests conducted on shale plays that are closely related to the Marcellus in terms of reservoir properties.

Reyes and Osisanya conducted series of compaction and permeability tests on four shale samples. They employed a small scale laboratory pressure vessel that includes innovative testing procedure under simulated down-hole conditions to determine the effect of confining pressure, pore pressure, temperature, and fluid types on the porosity and permeability of the shale cores tested. Figure 13 illustrated below shows the triaxial cell used in the gas permeability tests of shale cores under in-situ stress conditions.

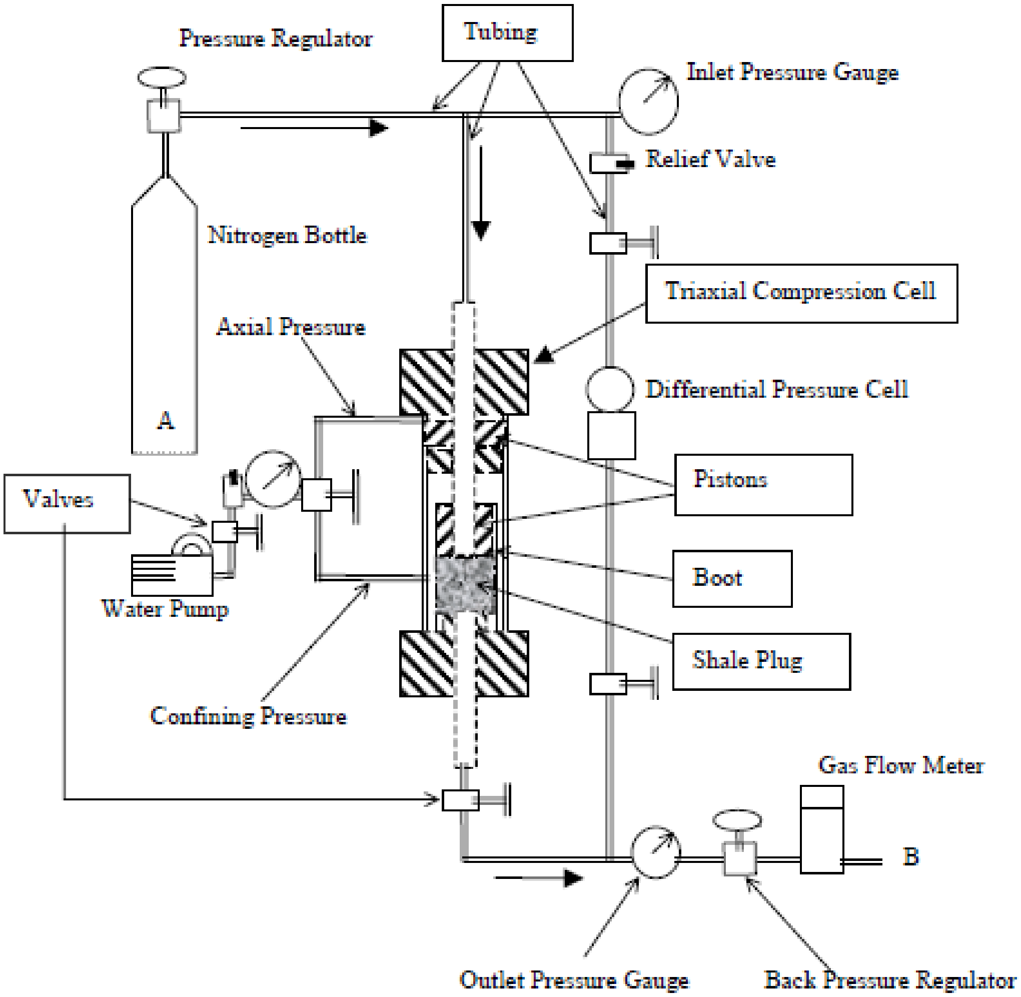
Pressure Regulator
Tubing
Inlet Pressure Gauge
Relief Valve
Nitrogen Bottle
Triaxial Compression Cell
Axial Pressure
Differential Pressure Cell
A
Pistons
Valves
Boot
Water Pump
Shale Plug
Confining Pressure
Gas Flow Meter
B
Outlet Pressure Gauge
Back Pressure Regulator

Figure 13: Experimental set-up for permeability and compaction test of shale cores (Reyes 2000)

The triaxial cell has the capability to apply axial loading and confining pressure using water, and also the pore pressure can be applied using nitrogen gas, oil or water. A boot is used in the equipment to separate pore fluid and confining pressure fluid. Major component of the experimental setup in the study conducted by Reyes and Osisanya are:

- Triaxial compression cell
- Water pump
- Differential pressure pump
- Differential pressure cell
- Positive displacement pump
- Nitrogen cylinder and pressure regulator
- Digital gas flow meters
- High accuracy scale and breaker
- Back pressure regulators
- Calibrated gauges.

The core samples that were employed in this study are from the Wapanuka, Wilcox, Atoka, and Catoosa formations. The different mineral composition and location of each shale formation is described in the table below.

Shale Formation	Location	Mineral Composition
Marcellus Shale	West Virginia, Ohio, New York, Pennsylvania	Calcite, quartz, illite, kaolonite, chlorite, halite, pyrite, mica
Wapanuka Shale	Pittsburgh, Oklahoma	Calcite, quartz, illite, kaolonite, chlorite, siderite, orthoclase, dolomite, albite
Wilcox Shale	Seminole, Oklahoma	Quatz, dolomite, smectite, siderite, albite, anhydrite, oligioclase, pyrite, kaolinite
Atoka Shale	Washita, Oklahoma	Quartz, dolomite, siderite, albite, chlorite, orthoclase, pyrite, oligioclase, kaolinite, smectite
Catoosa Shale	Tulsa, Oklahoma	Illite, quartz, dolomite, chlorite, oligioclase, albite, siderite, orthoclase, kaolinite, smectite

Table 3: Table describe the mineral composition and location of shale cores in this study (Reyes 2000)

From Table 3, we can see that Marcellus shale and Wapanuka shale have very similar mineral composition, so we will employ the compaction and permeability test result generated for Wapanuka shale in our numerical model.

The permeability testing procedure involves placing the core plug samples in the triaxial cell, then axial and confining pressure were applied to the required test valve. The pore pressure was gradually increased to establish gas flow, but keeping the differential pressure between confining and pore pressures greater than 300 psi. Finally, when steady state conditions for gas flow were reached, the flow rates were measured. At constant flow rate, gas permeability was determined at different values of hydrostatic pressure below the fracture limit of the rock sample. Permeability value calculations were done using Darcy’s law as a function of effective stress.

The compaction test was similar to the permeability test but now calculations were carried out to measure the porosity change of the core samples with respect to confining or effective stress.

In the experiments conducted by Reyes and Osisanya, compaction and permeability tests were conducted on core samples from the shale formation listed above. Since Wapanuka shale has close similarity to the Marcellus shale as compared to the rest of the shale used in this work, the result of the test conducted on Wapanuka shale is shown in the table below and will be employed in our model. To improve the accuracy of our model, it will be beneficiary to conduct compaction and permeability test on shale cores specifically from the Marcellus shale reservoir.

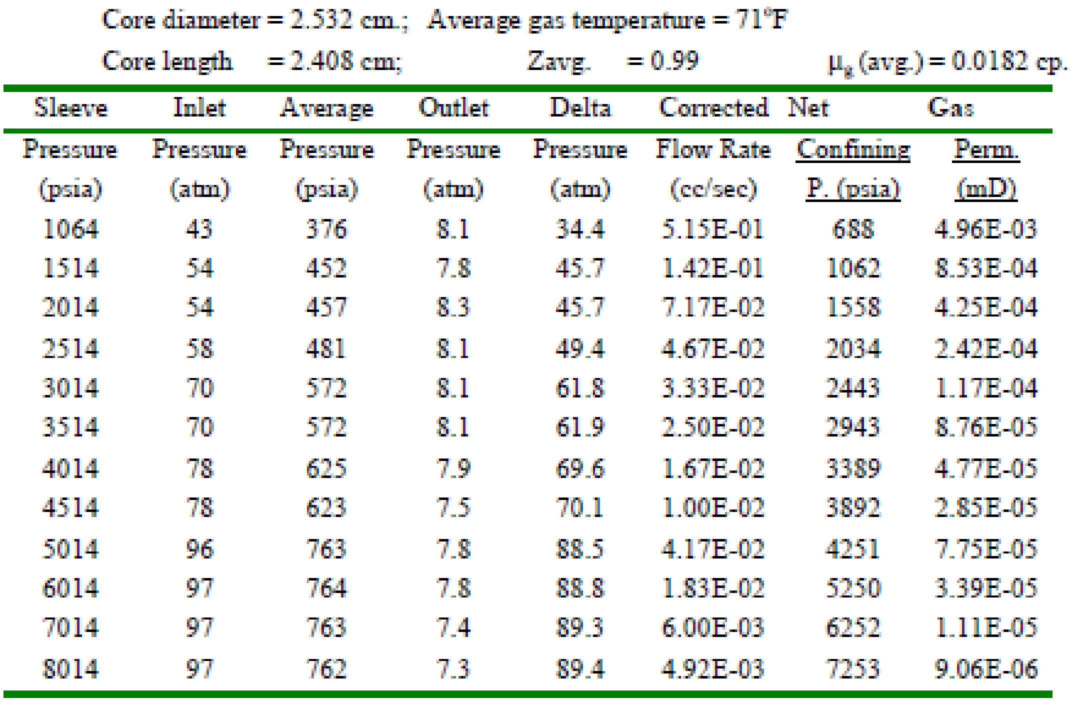

Core diameter = 2.532 cm.; Average gas temperature = 71°F

Core length = 2.408 cm; Zavg. = 0.99 μ_g (avg.) = 0.0182 cp.

Sleeve Pressure (psia)	Inlet Pressure (atm)	Average Pressure (psia)	Outlet Pressure (atm)	Delta Pressure (atm)	Corrected Flow Rate (cc/sec)	Net Confining P. (psia)	Gas Perm. (mD)
1064	43	376	8.1	34.4	5.15E-01	688	4.96E-03
1514	54	452	7.8	45.7	1.42E-01	1062	8.53E-04
2014	54	457	8.3	45.7	7.17E-02	1558	4.25E-04
2514	58	481	8.1	49.4	4.67E-02	2034	2.42E-04
3014	70	572	8.1	61.8	3.33E-02	2443	1.17E-04
3514	70	572	8.1	61.9	2.50E-02	2943	8.76E-05
4014	78	625	7.9	69.6	1.67E-02	3389	4.77E-05
4514	78	623	7.5	70.1	1.00E-02	3892	2.85E-05
5014	96	763	7.8	88.5	4.17E-02	4251	7.75E-05
6014	97	764	7.8	88.8	1.83E-02	5250	3.39E-05
7014	97	763	7.4	89.3	6.00E-03	6252	1.11E-05
8014	97	762	7.3	89.4	4.92E-03	7253	9.06E-06

Table 4: Gas permeability test result for Wapanuka shale (Reyes 2000)

As we can see from the results of the laboratory experiment conducted on Wapanuka shale, as confining stress (effective stress) of which the core is subjected to increases, the permeability of the core reduces.

2.6 Operational Condition

According to Crafton (2008), clear evidence is becoming available that shows that ultimate gas well performance is extremely sensitive to the early time well production management during the flowback period. Production management problem is aggravated by the plasticity of shale gas reservoirs. Many aspects of stimulation treatment impact the recovery performance of gas wells producing from shale reservoirs.

Various papers from literature have explained the adverse consequence of shut-ins during initial well cleanup after hydraulic fracturing treatment. The fracturing fluid recovery and productivity of a hydraulically fractured gas well are also affected by the well flow rate at initial well clean up. According to Sherman and Holditch (1991), flow of a well at high flow rates in an attempt to increase production increases the risk of rapid and excessive closure stresses. Excessive closure stress above the strength of the propping agent causes severe crushing to proppant pack and subsequent decrease in fracture conductivity.

Crafton (2008) gave a review of various articles that have been published in literature. These papers demonstrated the adverse consequences of shut-ins during initial well cleaning after fracture stimulation. The papers discussed the potential values or liabilities associated with stimulation fluid flowback rates ranging from a few tenths of a barrel per minute to five barrel per minute.

In this study, we will use the method of operating the fractured well at several BHP to simulate the effect of operational condition on gas production from a hydraulically fractured Marcellus shale gas well.

CHAPTER 3

PROBLEM STATEMENT

With improved drilling and completion technologies during the past ten years, the development of unconventional shale oil and gas resources becomes viable and more and more important to the industry. Extensive engineering effort, manpower, horsepower and capital have been spent on producing shale gas in the U.S. However, the fundamentals for completing and stimulating shale gas wells are not well understood yet, current completion and stimulation methods are not optimized, and simulation technologies for shale gas reservoirs are far from satisfactory. It is critical for the industry to develop models and methodologies for the accurate simulation of ultimate production from a shale gas reservoir and then to develop optimal completion and stimulation technologies for a particular shale play.

Even though hydraulic fracturing technique, which is the stimulation technique of choice that is in extensive use in the industry today, has made production from shale gas reservoirs more economically viable; there are post fracturing factors associated with hydraulic fracturing that however causes rapid decrease in production after 6 month to a year of when initial production began. To understand this, it is critical to accurately simulate production from the field. Most shale gas reservoir simulation models that are in use at the moment over predict the production of gas from shale gas reservoirs. One of the reasons for this is that these models do not incorporate post hydraulic fracturing factors that negatively impact gas production in their model.

The objective of this research is to develop a model to quantify the effects of selected important factors on the ultimate gas recovery from a Marcellus shale gas reservoir.

CHAPTER 4

MODEL DESCRIPTION

In this section, we will describe the base model; reservoir, fracture and fluid properties; and the flow and storage mechanism employed in our model. We will also describe how we have modeled the hydraulic fracture process and the proppant placement within the hydraulic fracture in our model.

Base Model

We used a two-dimensional, three-phase black oil reservoir simulator developed by Computer Modeling Group (CMG) to model selected factors affecting performances of a hydraulically fractured vertical well in the Marcellus shale gas reservoir. Initially, our reservoir is gas saturated and later hydraulically fractured with fractured fluid. The two phase present in our model is the gas phase and the water phase which represents the injected fracture fluid. The oil phase is not in existence in our model. Figure 14 shows a schematic of the fractured well model used in this study. Initially, we have a square reservoir with an area of 160 acres with a hydraulically fractured well located in the center. We have simulated just ¼ of the drainage area from a fractured well because of the symmetry of the well configuration. We assume that the fracture extends an equal distance on two sides of the wellbore and fully penetrates the formation.

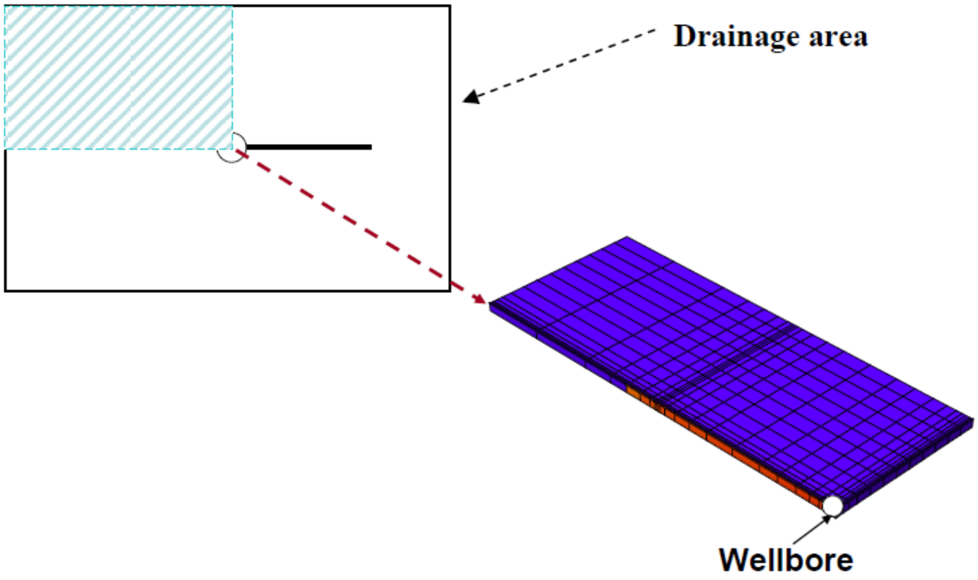

Figure 14: Schematic of the fracture well model

The area we have simulated is a square 40 acre drainage area with a hydraulically fractured vertical well located at the top edge of the formation. The created hydraulic fracture haft length is 500 ft, propagating from the wellbore into the x and y direction of our drainage area. Figure 15 shows the modified model employed in our study. The width of the hydraulic fracture is assumed to be constant from the well bore tip, while the porosity of the hydraulic fracture is 30%. The reservoir is assumed to be homogeneous and isotropic.

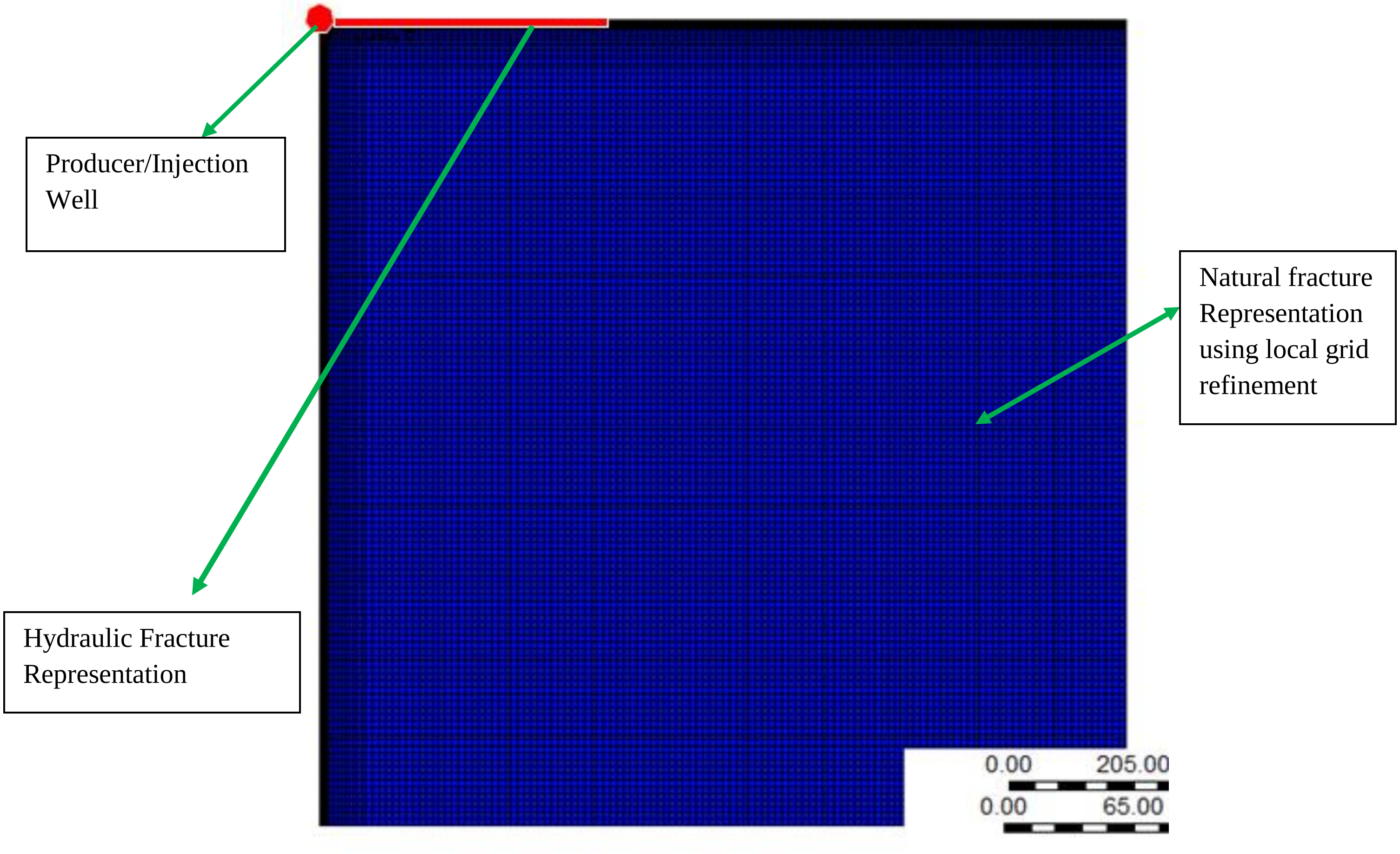
Producer/Injection Well
Natural fracture Representation using local grid refinement
Hydraulic Fracture Representation
0.00
205.00
0.00
65.00

Figure 15: 160 acre drainage area with a hydraulically vertical well located at the top corner

For our model, we created a non-uniform 30 by 30 by 1 grid system. Then we locally refined each grid block created into a 5 by 5 by 1 grid system; this is done to capture the natural fracture system within the matrix block. We varied the grid dimensions in the fracture direction, this is because the grids are very small in the fracture plane near the wellbore, increase towards the middle of the propped fracture half length and then decreases until the tip of the propped fracture, and it increases again to the drainage boundary.

The wellbore is located in the 1 by 1 by 1 cell block as shown in Figure 15 above. We operate the well at a constant bottom hole pressure (BHP). All of our simulation results, which includes gas production rate, cumulative gas production are presented as just 1/4 of drainage area because of our simulation configuration and strategy. However, the real gas production for the 160 acre area should be four time our results.

Reservoir, Fracture and Fluid Properties

Since Marcellus shale reservoir is a shale play that extends through various states in the east coast of the United States, the reservoir characteristic of the Marcellus shale at various location differs. We have decided to use average values of various published articles regarding the reservoir characteristics of the Marcellus shale in building our model. Basic reservoir parameters that we have utilized in our model are shown in the table below.

Reservoir Parameters and Units	Numerical Values
Drainage Area, ft	40
Thickness, ft	300
Matrix Porosity, %	3.0
Matrix Permeability, md	0.0001
Natural Fracture Conductivity, md-ft	4
Reservoir Pressure, psi	3,000
Reservoir Temperature, Deg F	130
Bottom Hole Flowing Pressure, psi	1000
Fracture Half Length, ft	500
Fracture Fluid, gallons	172,000
Initial Gas Saturation	1.00
Initial Water Saturation	0
Well Radius, ft	0.125

Table 5: Basic reservoir and fracture parameters

For the duration of our work, we kept most of the reservoir values in Table 5 constant. The only situation when we change a certain reservoir value is when we are conducting a parametric study using this value.

The relative permeability curves and PVT table that were employed in our model are shown in Figure 16, Figure 17 and Table 6.

Pressure (psi)	**Solution Gas Ratio (SCF/STB)**	**Formation Volume factor of Oil (RB/STB)**	**Gas Compressibility Factor**	**Viscosity Oil (Centipose)**	**Viscosity Gas (Centipose)**
14.7	0	1	1	1.2	0.02
400	165	1.012	1	1.17	0.02
800	335	1.0255	1	1.14	0.02
1200	500	1.038	1	1.11	0.02
1600	665	1.051	1	1.08	0.02
2000	828	1.063	1	1.06	0.02
2400	985	1.075	1	1.03	0.02
2800	1130	1.087	1	1	0.02
3200	1270	1.0985	1	0.98	0.02
3600	1390	1.11	1	0.95	0.02
4000	1500	1.12	1	0.94	0.02
9000	1510	1.121	1	0.93	0.02

Table 6: PVT table

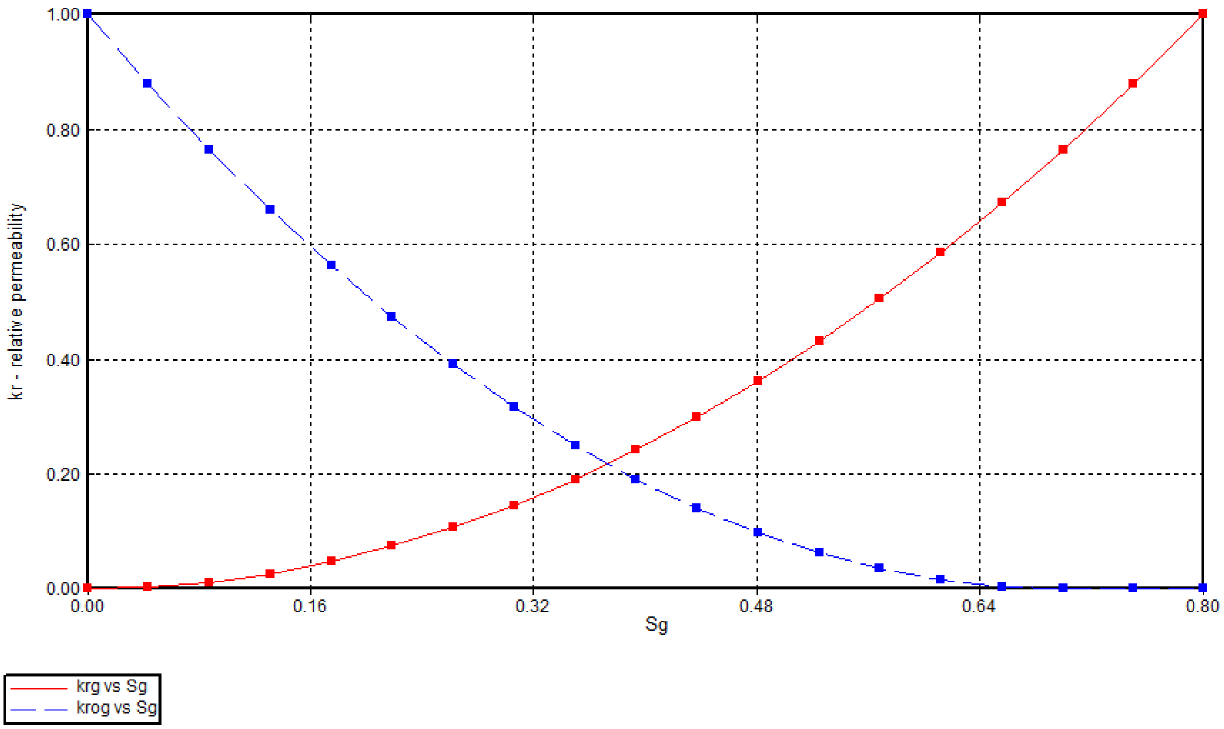

Figure 16: Relative permeability curve for the gas phase

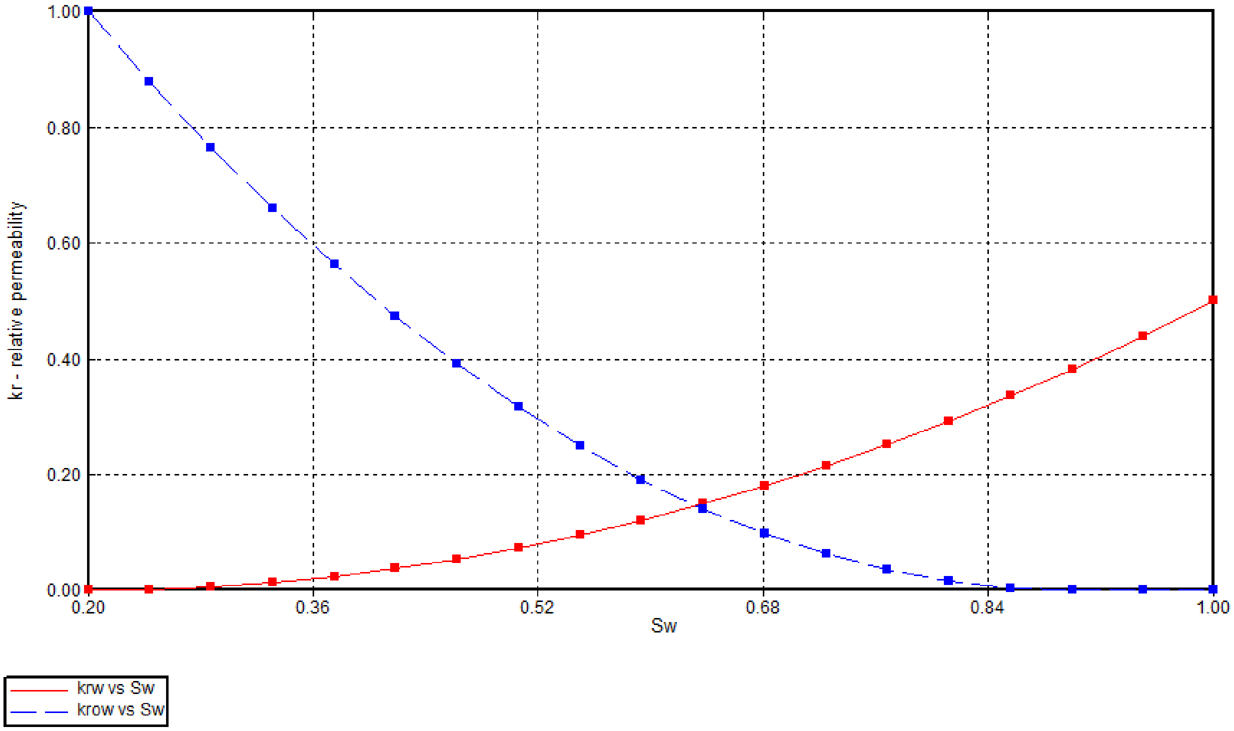

Figure 17: Relative permeability curve for the water phase

Flow and Storage Mechanism

Our reservoir model is a double porosity, double permeability locally refined grid model (DΦ-DK-LGR**).** We have two storage mechanisms in our model, Gas is assumed to be stored in the matrix block and in the existing natural fracture system within the system. The advantage of using a double porosity model is the increased speed in computation as compared to other models. The disadvantage of using a double porosity model is the disregard for the third storage mechanism associated with shale gas, which is the adsorbed gas on shale particle. Although production from desorption accounts for 15 % of overall gas production, desorption gas recovery do not begin until the late time of the gas well or at reservoir pressures lower than 600 psi. We are producing our well at bottom hole pressure of 1000 psi, so for our simulation, gas desorption does not contribute to our overall gas recovery.

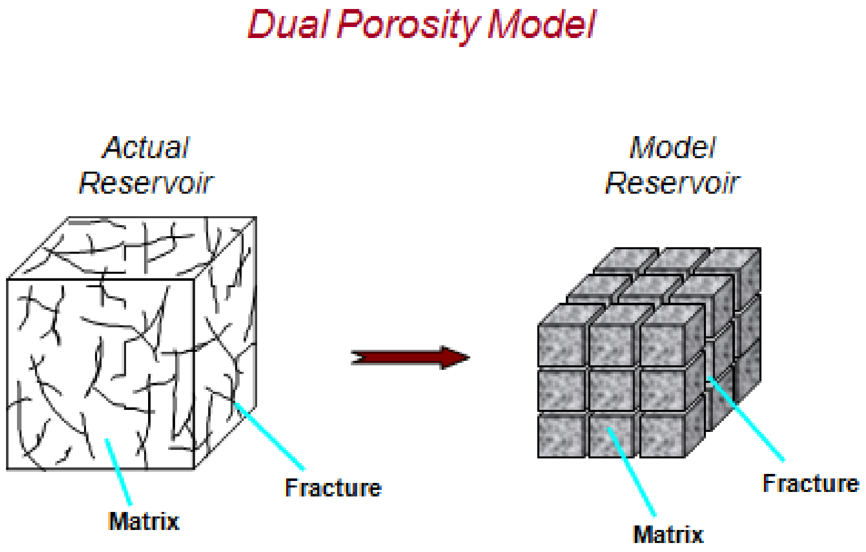

Figure 18: Dual porosity model

The flow mechanism employed in our model includes Darcy flow and the transient non Darcy flow. The transient non Darcy flow is used to represent the behavior within the natural fracture and the hydraulic fracture and the Darcy flow is used to represent the flow behavior from the matrix block into the natural fractures.

We locally refined the matrix grid blocks in our model to represent the natural fractures systems that are located within each matrix block. Although local refinement increases computational time, it improves the accuracy of our model.

Hydraulic Fracture and Proppant Placement Representation

According to Cipolla (2009), micro seismic mapping can provide significant insight into fracture growth in shale gas reservoirs, however the overall effectiveness of stimulation treatment is difficult to determine from M.S. mapping alone because the location of proppant and distribution of conductivity within the fracture network cannot be measured.

In order to effectively represent the flow capacity and the conductivity of the hydraulic fractures created, we need to answer three key questions:

- Where is the proppant within the fracture network?
- What is the conductivity of the propped fracture network?
- What is the conductivity of the un-propped fracture network?

Proppant transport within the natural fractures cannot be modeled reliably when fracture growth is complex, making it very difficult to predict the location of the proppant within the fracture network. Location of proppants within the fracture network can be estimated by the use of two limiting scenarios which are:

- The proppant is evenly and uniformly distributed throughout the complex fracture system
- The proppant is concentrated in a dominant primary fracture that is connected to un-propped complex fracture network.

We have decided to employ the second scenario in our model; we created a hydraulic fracture system which is highly conductive compared to the surrounding un-propped fracture network. The advantage of this is that if the proppant is concentrated in a dominant primary fracture, the average proppant concentration would be significantly greater and this should result in much higher conductivity in the primary fracture, which implies a better connection between the fracture system and the wellbore. We expect this is the case from cross linked gel or gel fracture treatment in the Marcellus shale.

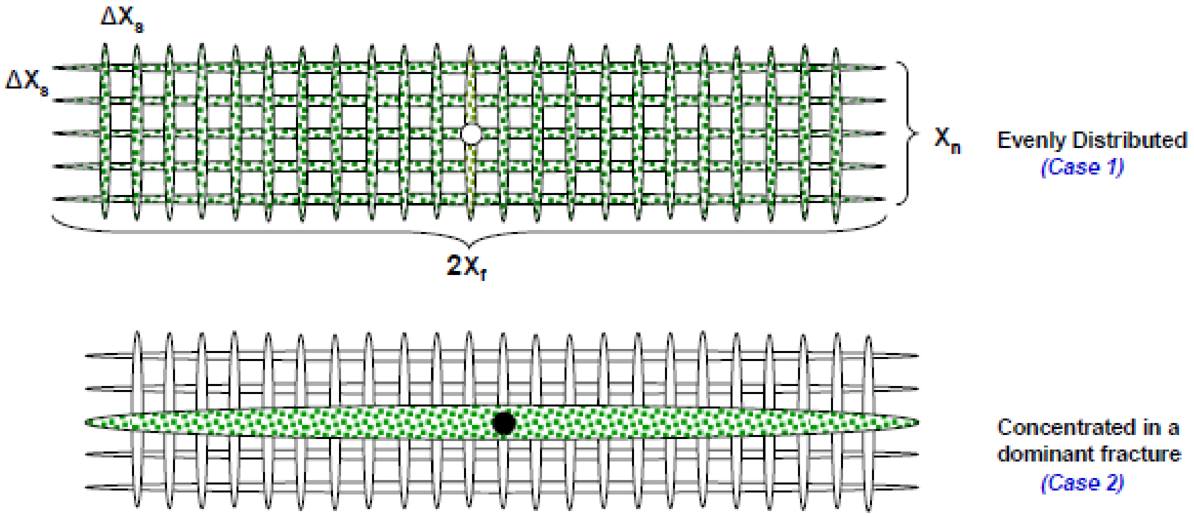
ΔX_s
ΔX_s
X_n
Evenly Distributed
(Case 1)
$2X_f$
Concentrated in a
dominant fracture
(Case 2)

Figure 19: Proppant transport scenarios (Cipolla et al. 2009)

It is important to realize that well productivity in shale reservoirs is dominated by the conductivity of the natural fracture system. If the natural fracture conductivity is very low, then the reservoir system maybe uneconomic to produce even after a hydraulic fracture process has taken place.

We have validated our reservoir simulation model with field data on the Marcellus shale that we have obtained from companies currently operating in the Marcellus shale.

CHAPTER 5

SIMULATION RESULTS AND ANALYSES

In this research, we have studied several post-hydraulic fracturing factors that affect the ultimate gas recovery from a hydraulically fractured shale gas well. The factors that have been studied includes: ideal single phase flow, multiphase (gas and water) flow, proppant crushing, proppant diagenesis, reservoir compaction, operational conditions.

We have developed a reservoir model to simulate the production and gas flow rate for a 30 year production period from the Marcellus shale gas reservoir. The base model has been modified to capture the impact of several post-hydraulic fracture factors on ultimate gas recovery. Using the ideal single phase flow as the base model, we conducted two kinds of analyses.

First, we did a case by case study for each factor by comparing predicted gas production using the single phase model and the predicted gas production using the modified case by case model. From the comparison study, we are able to quantify the impact that each factors individually have on ultimate gas recovery and gas flow rate for a 30 year production period.

Second, we conducted a study that quantifies the impact of all the factors additively on ultimate gas recovery. Starting from the single phase base model, I added multi-phase flow, then added proppant crushing effect, then added proppant diagenesis effect, then added reservoir compaction effect, and at last I added operational condition effect. Some results are analyzed in this chapter. All other are included in the appendix.

It should be noted that in this chapter, we refer to the fracture conductivity associated with 12,500 md-ft proppant as the high conductivity fracture and likewise, we refer to the fracture conductivity generated by the 0.4 md-ft proppant as the low conductivity fracture.

5.1 Ideal Single Phase Flow

We begin our reservoir simulation study by building an ideal single phase flow model. Gas phase saturation is 100 % in the reservoir. For every computer run we conducted in this research, we have made the ideal single phase run as the base case for each run. As we develop a model for the several factors associated with the post-hydraulic fracturing production decline in the Marcellus shale reservoir, we can compare each case to the base case (ideal single phase flow) to evaluate its effect on the ultimate gas recovery and yearly gas flow rate. The results of the simulation runs for the ideal single phase flow effect are shown in Figure 20 and Figure 21. We present our result in graphs of cumulative gas sc (ft^3) vs. time (date), and gas rate sc (ft^3/day) vs. time (date).

For the ideal single phase flow simulation, we used various proppants with the specific proppant pack permeability associated with each proppant to define the hydraulic fracture conductivity property of our model. We used both ceramic and multicoated sand proppants. The ceramic proppant were developed by Carbo-Ceramics. All the properties of the ceramics proppant that were employed in our model were obtained from the Carbo- Ceramics website. The multicoated sand proppant we used were developed by Power Prop Santrol. All the properties of the multicoated sand proppant employed in our model were obtained from the Power Prop Santrol website. We used the proppant pack permeability associated with 20-40 mesh carbolite ceramic proppant, 40-70 mesh carbolite ceramic proppant, 100 mesh carbolite ceramic proppant, 20-40 mesh multicoated sand proppant, 40-70 mesh multicoated sand proppant, and 100 mesh multicoated sand proppant in our model. The table 7 below shows the proppant pack conductivity associated with each proppant at no closure stress employed in our study.

Proppant type	Proppant Pack Conductivity (mD-ft)
20-40 mesh carbolite ceramic proppant	12,500
40-70 mesh carbolite ceramic proppant	2,740
100 mesh carbolite ceramic proppant	852
20-40 mesh multicoated sand proppant	6,171
40-70 mesh multicoated sand proppant	1639
100 mesh multicoated sand proppant	759

Table 7: Proppant pack permeability of different proppants

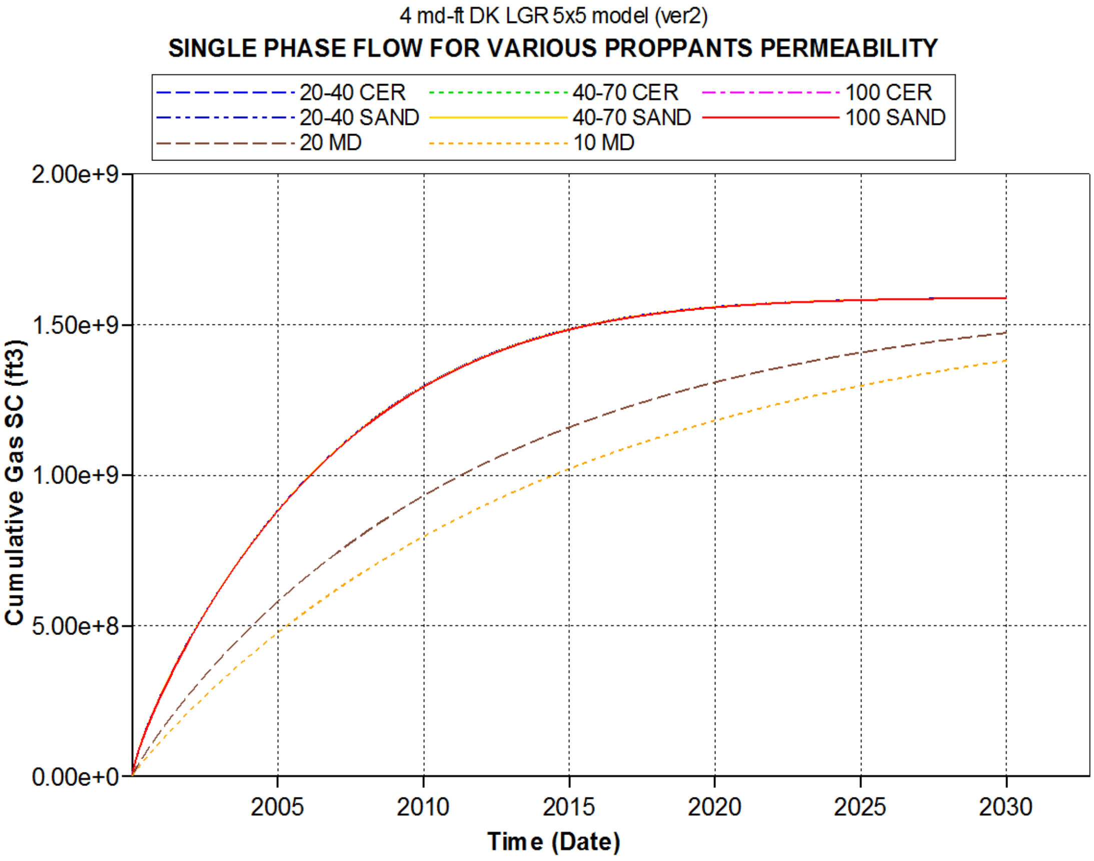

Figure 20: Cumulative gas production of various proppants with different hydraulic fracture conductivity.

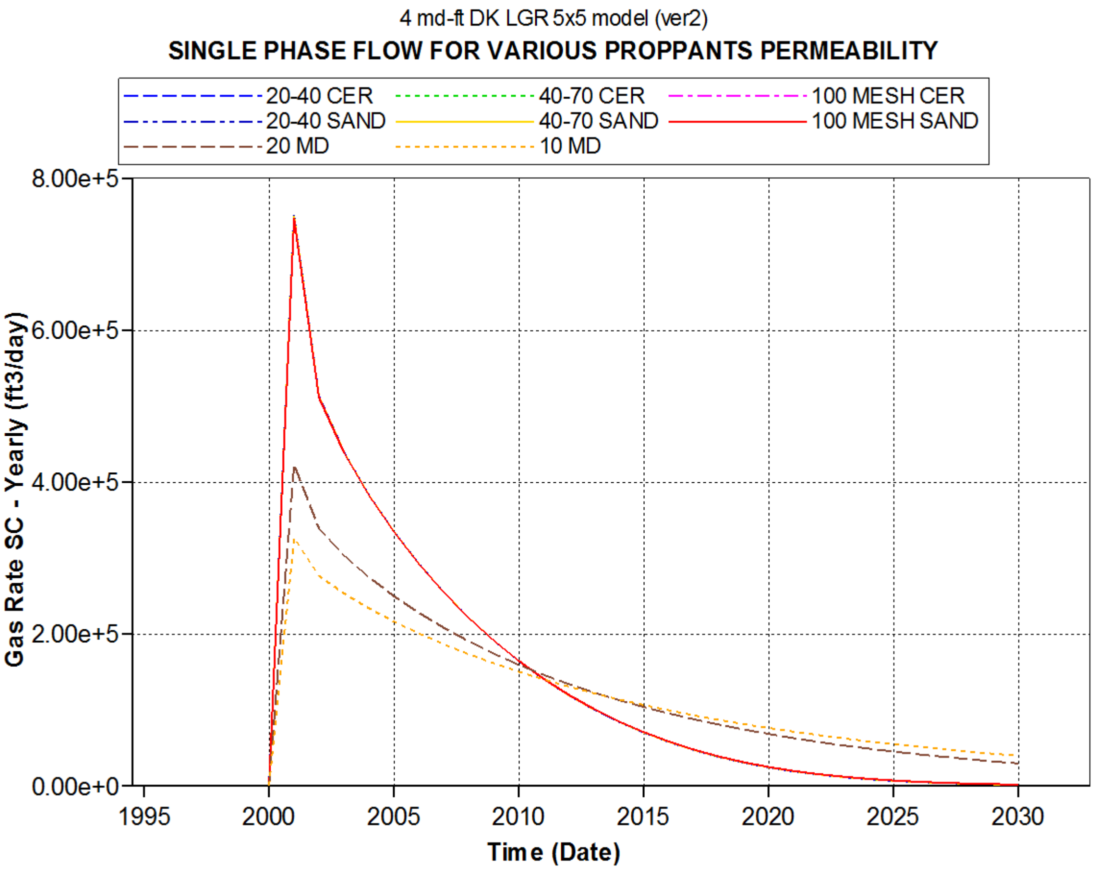

Figure 21: Gas flow rate of various proppants with different hydraulic fracture conductivity.

Figure 20 and Figure 21 shows that cumulative gas production and the gas flow rate curve associated with each of the six proppant are the same (plots of the six proppants listed in Table 7 lies underneath each other in Figure 20 and Figure 21). The reason for this result is because at any conductivity above the infinite proppant pack conductivity of our model, there will be little or no change to the ultimate gas recovered. The permeability associated with each of the proppant pack we used is the ideal values generated from laboratory tests conducted by Carbo-Ceramic and Power-Prop Santrol. Realistically, when this proppants are pumped into the actual Marcellus shale reservoir, it is possible to experience significant decrease (up to ninety percent decrease) in the conductivity and permeability properties of the proppant pack. To realistically simulate the behavior of our proppant pack in an actual reservoir, we conducted simulation runs of which the permeability of the proppant pack with in the hydraulic fracture is 20 md and 10 md. As we can see from figure 20, the overall gas recovery is approximately

1.5BCF and1.4 BCF for 20 md and 10 md respectively. This shows that the optimum proppant pack permeability within the hydraulic fracture at which the maximum recovery is attained is close to 20 md. This is because the difference between overall recovery associated with very high permeability and 20 md proppant pack permeability is about 0.1 BCF.

In conclusion, using expensive proppants or bigger proppants does not necessary imply significant increase in the ultimate gas recovery, a proppant that will give maximum hydraulic fracture conductivity at the least expensive price should be used in creating the hydraulic fracture in the Marcellus shale gas well.

5.2 The Effect of Multiphase Flow on Production

To simulate the effect of multiphase flow on gas production in shale gas reservoirs, the assumption we made was that a hydraulic fracture has been created, and the fracture fluid used to create the hydraulic fracture has the same properties as the formation water. The exact amount of fracture fluid was injected and leaked off into the reservoir to create water saturation around the vicinity of the hydraulic fracture. Pressure of the water phase temporarily reduces the gas flow into the fracture and into the wellbore. The well takes time to clean up the fracture fluid before gas starts to flow at maximum capacity.

To create the hydraulic fracture, 172,000 gallons of fracture fluid is injected into the formation. Then the well is shut in for two hours before flow back of the fracture fluid begins at a rate of 40 (bbl/hr).

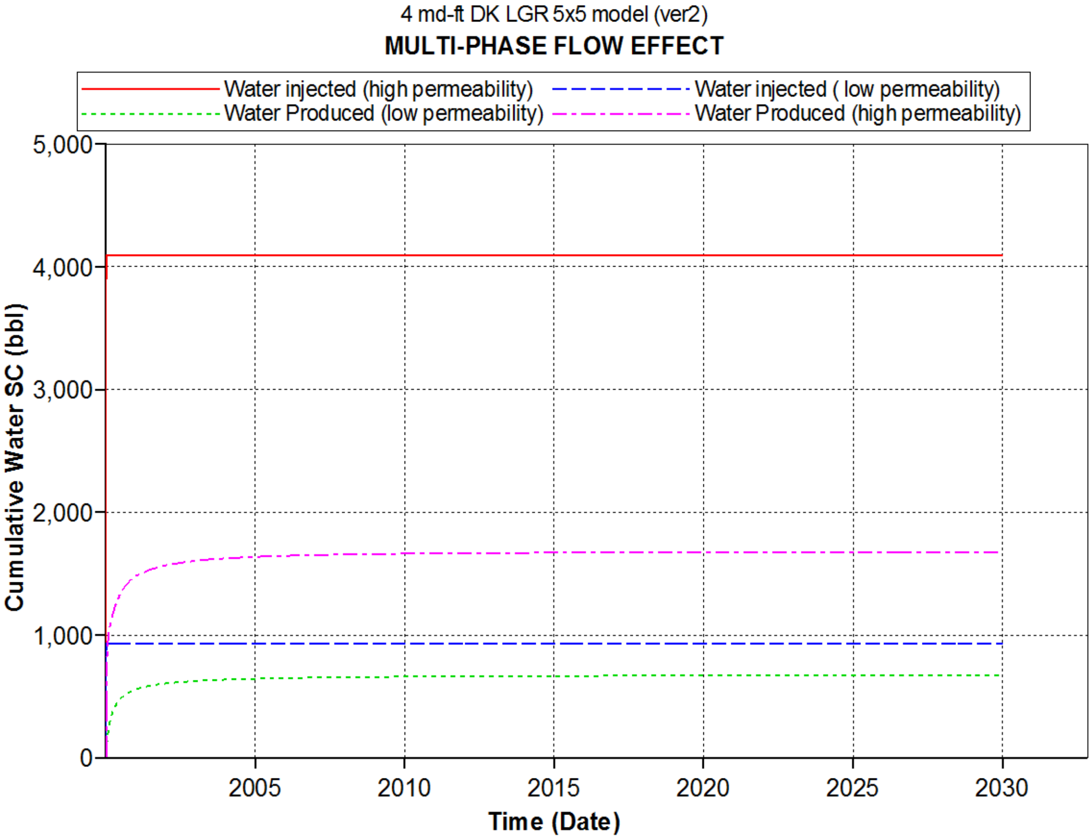

Figure 22: Water injected and water produce from highly and lowly conductive hydraulic fracture.

As in the case of the single phase flow, we ran simulation for 2 cases, the highly conductive and the low conductive hydraulic fracture cases. Highly conductivity case occurs when the conductivity of the hydraulic fracture created is high (12,500 md-ft) and the lowly conductive case occurs when the permeability of the hydraulic fracture created is low (0.4 md-ft).

Figure 22 shows that we are able to inject 4,090 bbl of fracture fluid into our formation when the hydraulic fracture conductivity is 12,500 md-ft and we are able to inject 929 bbl of fracture fluid into the formation when the hydraulic fracture conductivity is 0.4 md-ft. We are able to flowback 1,675 bbl (40%) of fracture fluid when hydraulic fracture conductivity is high and we are able to flowback 673 bbl (72%) of fracture fluid when hydraulic fracture conductivity is low over a period of 30 years. Most of the water flown back is produced during the first month of production.

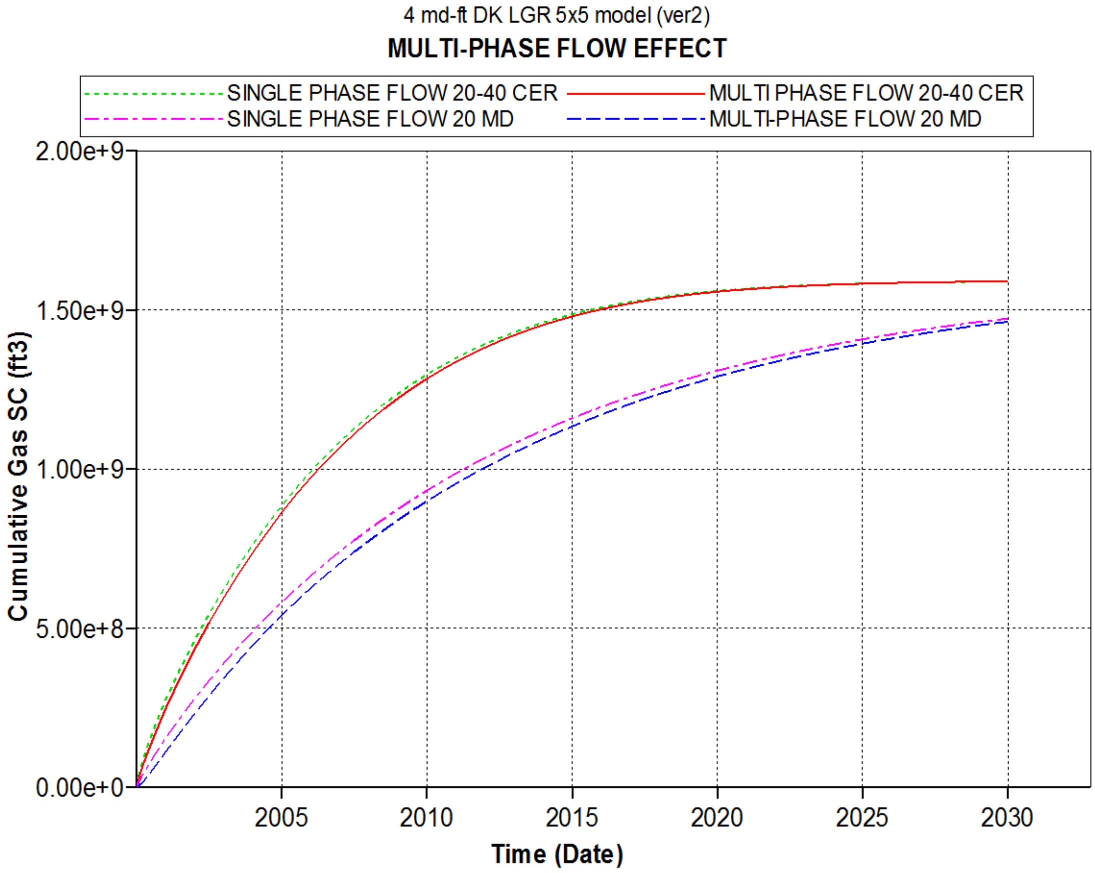

Figure 23: Cumulative gas production from high and low conductivity hydraulic fracture

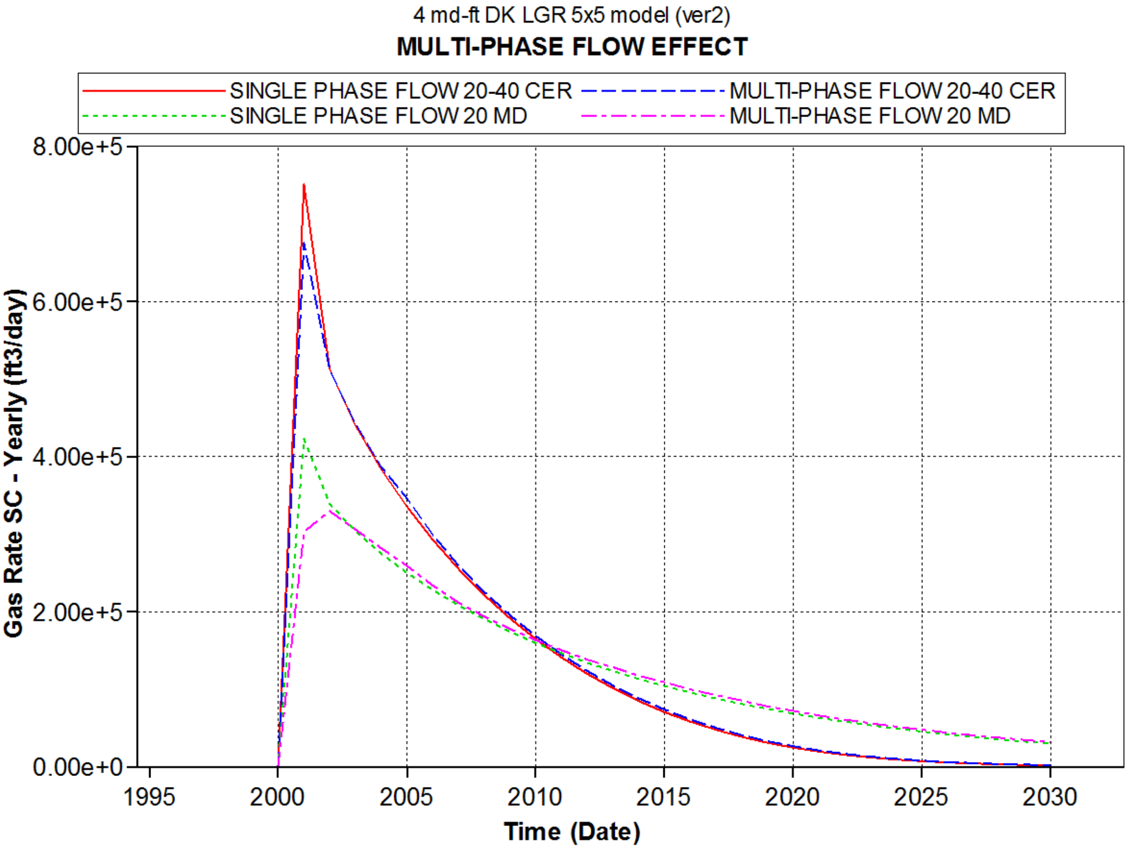

Figure 24: Gas production rate from high and low conductivity hydraulic fracture

Figure 23 and Figure 24 show the cumulative production and the gas production rate for the high conductivity and low conductivity hydraulic fracture cases. From the plots, we can see that the overall recovery for 30 year is slightly decreased when multiphase flow effect is compared to the ideal single phase effect. Decrease in production is more significant when the conductivity of the hydraulic fracture is lower. As one can see, when the hydraulic fracture conductivity is low, there is approximately 10.2 MMSCF decrease in cumulative production and when the hydraulic conductivity is high, there is a 0.5 MMSCF decrease in cumulative production. Gas production rates drops faster when multiphase flow effect occurs, however the drop in gas production rates is more noticeable when the hydraulic fracture is less conductive. At later years, the gas production rate is higher when a low conductivity hydraulic fracture is created as compared to the case of a high conductivity hydraulic fracture.

The conclusion drawn from this study is that when high conductivity hydraulic fracture is created, the impact of multiple phase flow effect on cumulative gas production is less as compared to the case when a low conductivity hydraulic fracture is created.

5.3 The Effect of Proppant Crushing on Production

It is well know that the values of hydraulic fracture conductivity will decrease as the value of closure pressure on the proppant pack increases. We have modified the ideal single phase model to account for this effect known as proppant crushing. The proppant crushing data used was obtained from conductivity tests on proppants that were conducted by Carbo-Ceramics and Power Prop Santrol. We used ceramic proppants and multicoated sand proppants in our simulation runs. 20-40 mesh carbolite ceramic proppant, 40-70 mesh carbolite ceramic proppant, 20-40 mesh multicoated sand proppant, and 40-70 mesh multicoated sand proppant, were employed. The pressure vs. permeability multiplier for the 4 types of proppant is shown in table 8 below.

Net Pressure (psi)	Conductivity multiplier 20-40 ceramic	Conductivity multiplier 40-70 ceramic	Conductivity multiplier 20-40 sand	Conductivity multiplier 40-70 sand
0	1	1	1	1
2,000	0.87	0.7941	0.8428	0.8706
4,000	0.61	0.5882	0.6855	0.7412
6,000	0.35	0.4706	0.5535	0.5882
8,000	0.17	0.3529	0.3742	0.4824
10,000	0.09	0.2059	0.239	0.2824
12,000	0.05	0.1471	0.1289	0.1882

Table 8: Pressure vs. permeability multiplier of different proppants used in our model

As one can observe from the table 8, at different closure stress, the proppant pack conductivity of the four proppant reduces from the initial conductivity shown in Table 8 (single phase) to a value derived by multiplying the initial proppant pack conductivity by the conductivity multiplier. The ceramic proppants tends to lose strength quicker than the multicoated sand proppant as the net pressure increases. This trend is exhibited in the plot of cumulative production and gas production rate vs. time.

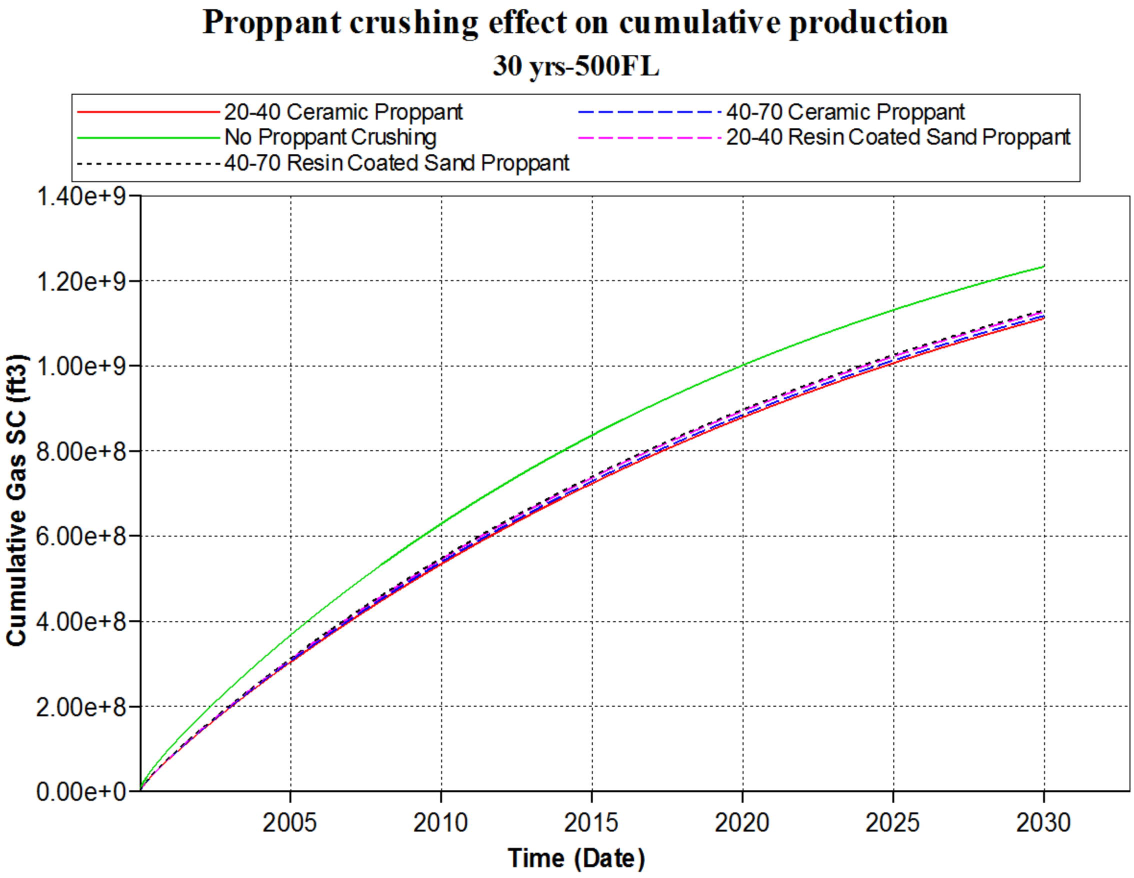

Figure 25: Proppant crushing effect on gas recovery for selected proppants.

As one can see from figure 25, when proppant crushing effect is incorporated into the ideal single phase model, a decrease in the overall gas recovery is experienced. Gas production for a 30 year period is decreased from approximately 1.22 BCF to approximately 1.15 BCF. Even though the difference in production for the various proppants we employed in our simulation runs is not pronounced, we can see the effect of proppant crushing on the overall gas recovery associated with using each proppants. From Figure 25 we observe that the gas recovery associated with using a 20-40 ceramic proppant is slightly less as compared to using 20-40 multicoated sand proppant. It is also observed that 40-70 ceramic proppant gives a slightly higher gas recovery than gas recovery associated with the 20-40 ceramics proppant. This is also true for the overall gas recovery associated with 20-40 and 40-70 multicoated proppants. We are not able to simulate the effect of proppant crushing on overall gas production when a proppant pack that creates a lowly conductive hydraulic fracture is used. This is because we do not have any conductivity data for this low conductivity proppant.

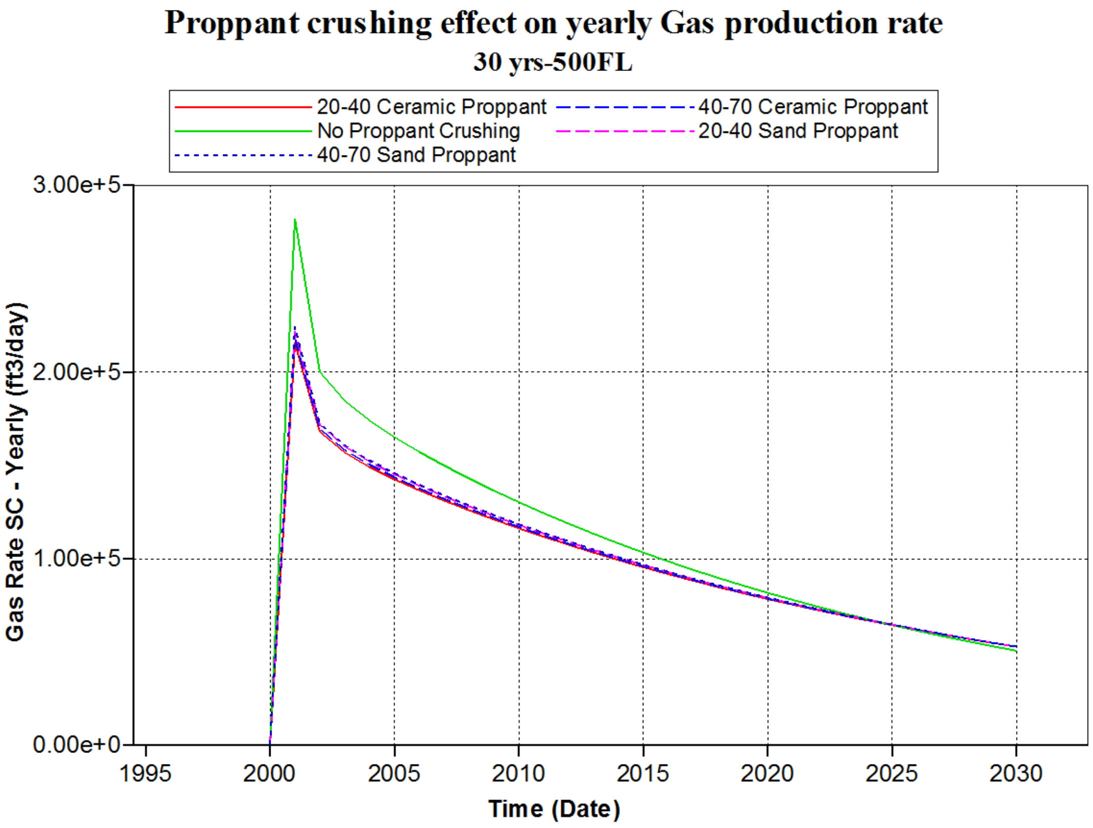

Figure 26: Proppant crushing effect on gas production rate for selected proppants.

Similar to the trend observed from Figure 26, proppant crushing causes a decrease in the gas production rates that is generated for each of the four proppants we used. Using a 20-40 multicoated sand proppant gives the highest initial production rates of the four proppant used in our study. Over time, the production rate associated with 20-40 multicoated sand proppant becomes less than that of the other 3 proppants. This is because at early times, more gas is produced and the gas depletion in the reservoir proceeds quicker when using 20-40 multicoated sand proppant as compared to the rest of the proppants.

5.4 The Effect of Proppant Diagenesis on Production

Proppant diagenesis is a process that occurs with time. The conductivity of the hydraulic fracture decreases as proppant diagenesis process progresses. We have modeled the effect of proppant diagenesis by incorporating data from a proppant pack permeability change with time table into our ideal single phase model. Lab experiment data that we used in our model was from the lab experiment work conducted by Lee et al. (2009). Proppants that were used in our model includes 20-40, 40-70 and 100 mesh Carbo-Econoprop proppant by Carbo Ceramics. There was no diagenesis lab experiment data for sand proppants from literature. From the plot derived by Lee et al. (2009), we were able to generate a time vs. proppant pack permeability multiplier table.

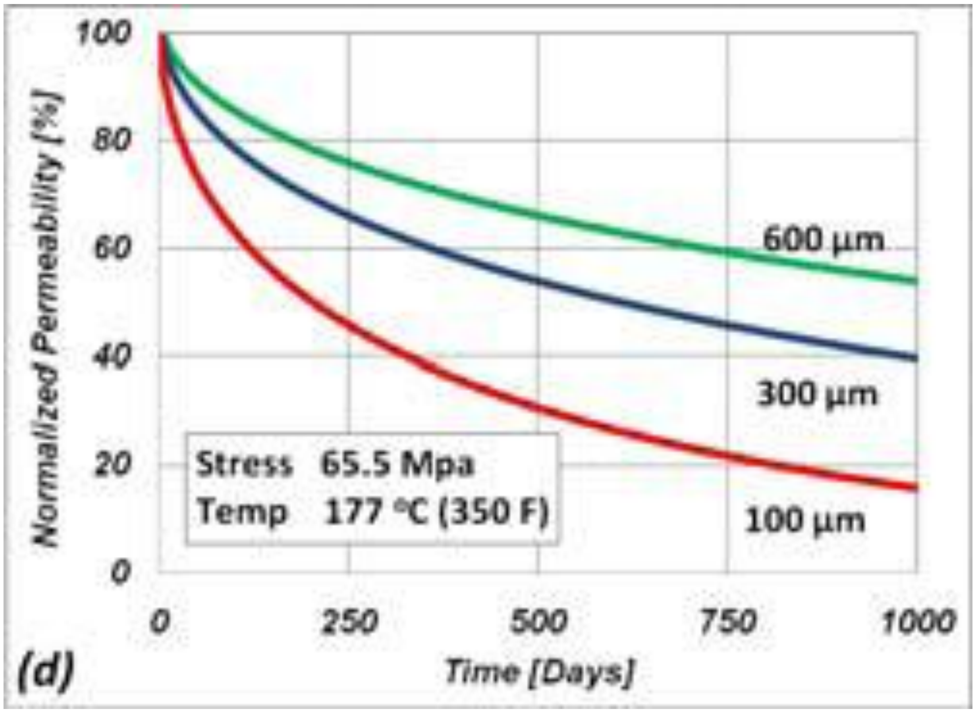

Figure 27: Plot showing proppant pack permeability decrease over time (Lee et al. 2009)

The 600 µm size particle is equivalent to 20-40 Carbo-Econoprop proppant, 300 µm size particle is equivalent to 40-70 Carbo-Econoprop proppant, and the 100 µm size particle is equivalent to the 100 mesh Carbo-Econoprop proppant.

The Table 9 showing the time vs. proppant pack permeability multiplier data is shown below.

TIME (days)	20-40 Carbo-Econoprop proppant	40-70 Carbo-Econoprop proppant	100 Carbo-Econoprop proppant
0	1	1	1
125	0.84	0.76	0.59
250	0.77	0.65	0.45
375	0.7	0.59	0.36
500	0.66	0.53	0.3
625	0.63	0.49	0.25
750	0.59	0.45	0.21
875	0.57	0.42	0.18
1000	0.55	0.39	0.16

Table 9: Table showing proppant pack permeability decrease with time

From Table 9, we observe that proppant diagenesis effect is more predominant as the proppant size decreases. The rate of permeability decrease experienced with a proppant size of 20-40 mesh is less severe as compared to the proppant size of 100 mesh ceramic proppant. This trend shown in Table 9 is expected to affect the overall gas recovery from a Marcellus shale gas well depending on what proppant size is selected.

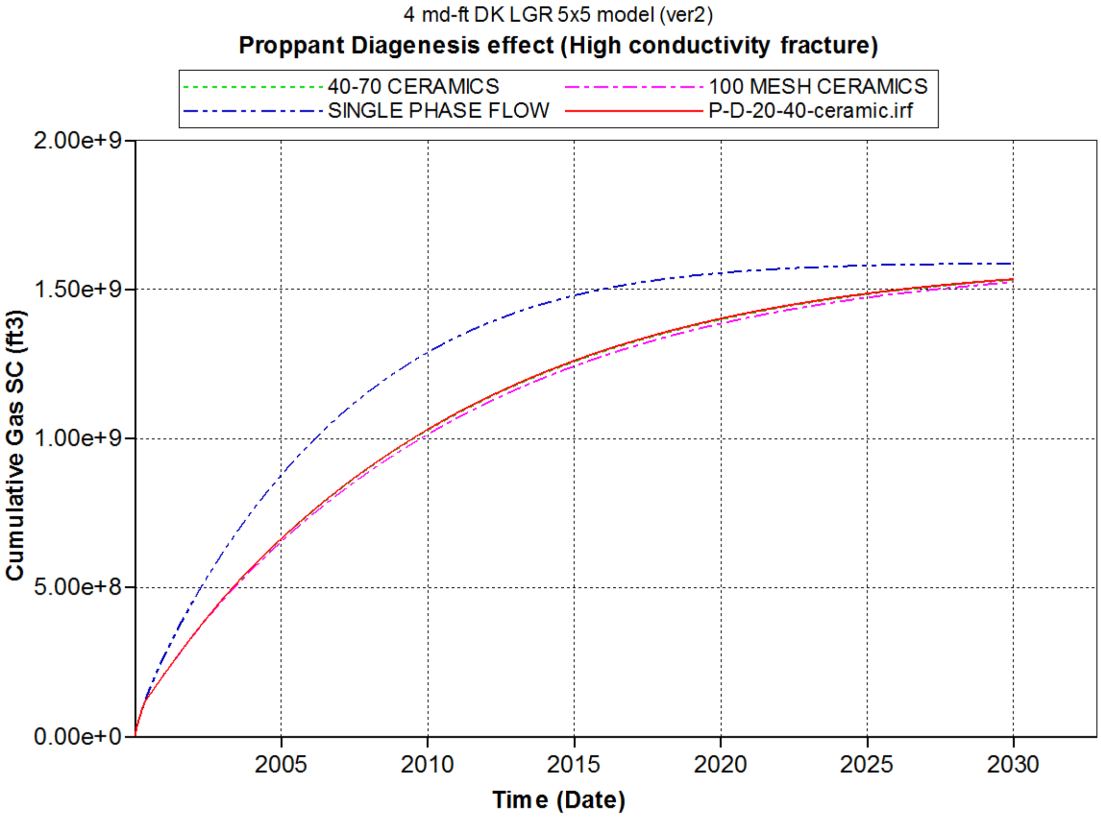

Figure 28: Proppant diagenesis effect on selected proppants (highly conductive hydraulic fracture).

Figure 28 shows the overall gas recovered over a 30 year period from a Marcellus shale gas well using 3 different sizes of proppants that provide high conductivity hydraulic fracture. As expected from the trends of Table 9, using a 20-40 ceramic proppant will give the maximum gas recovery, while using a 100 mesh ceramic proppant will give the least gas recovery for a 30 year period. The difference in overall gas recovered is not easily noticeable. This is because the hydraulic fractures created by the 3 kinds of proppants are highly conductive.

Difference in overall gas production using the three kinds of proppant listed in Table 9 above is noticeable when we assume a lowly conductive hydraulic fracture is created.

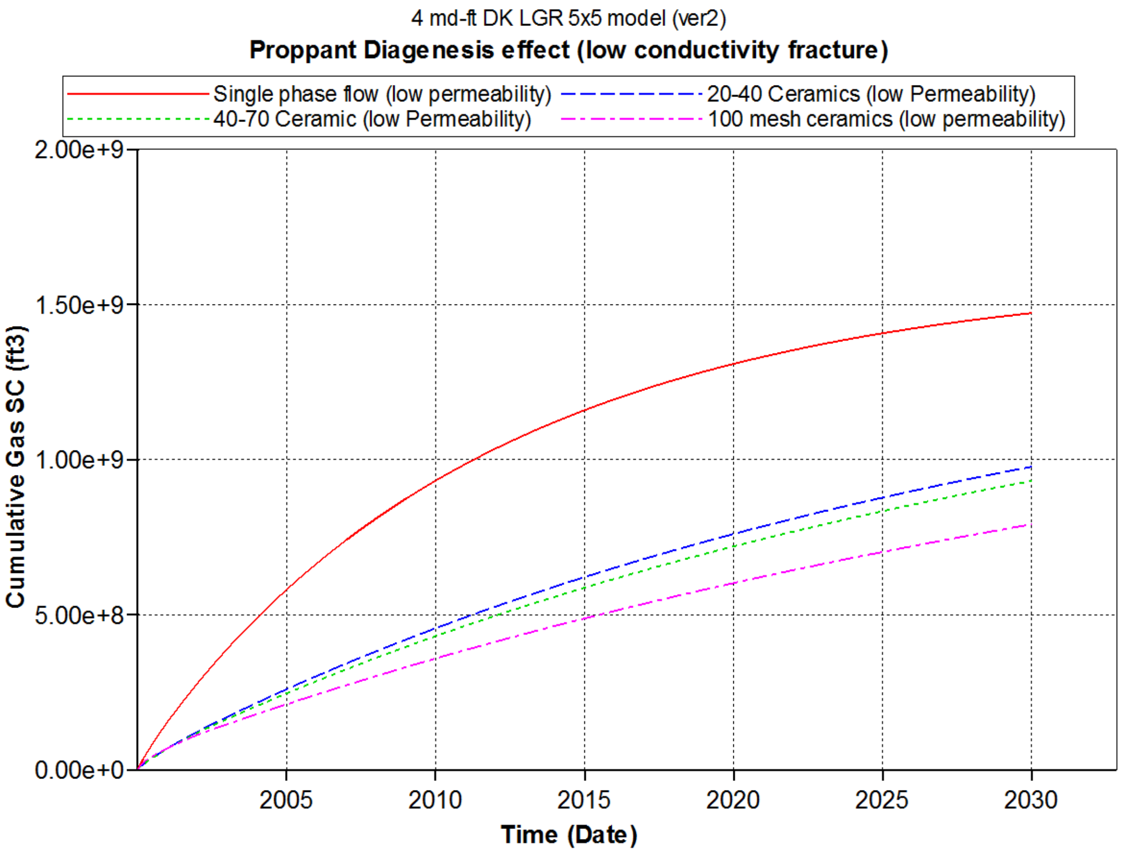

Figure 29: Proppant diagenesis effect on selected proppants (lowly conductive hydraulic fracture).

Overall gas produced using the ideal single phase model shows 1.5 BCF gas production. When proppant diagenesis is modeled using the 3 kind of proppants producing low hydraulic fracture conductivity, we see a significant decrease in overall gas recovered. Gas production drops from 1.5 BCF to 1 BCF when 20-40 ceramic proppant is used. Production further drops to 0.8 BCF and 0.6 BCF when 40-70 ceramic proppant and 100 mesh ceramic proppant are used.

The effect of proppant diagenesis is more pronounced when a low conductivity hydraulic fracture is created. When high conductivity hydraulic fracture is created, the difference in overall production is less significant as compared to difference in overall gas production when lowly conductive hydraulic fracture is created.

The gas flow rates associated with the 3 proppant for case of low and high hydraulic fracture conductivity are shown in Figure 30 and Figure 31

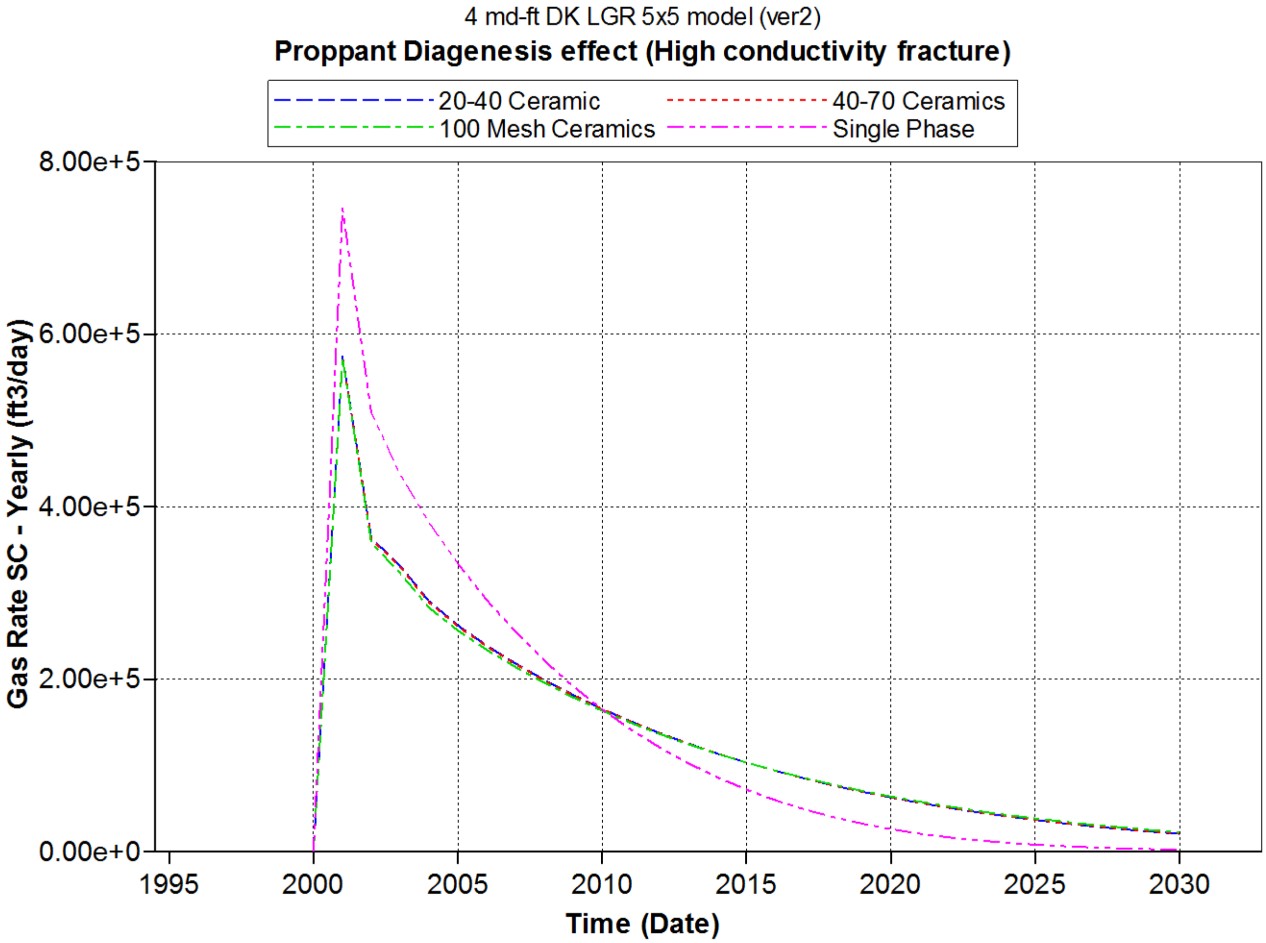

Figure 30: Gas flow rate of selected proppants (High conductivity hydraulic fracture).

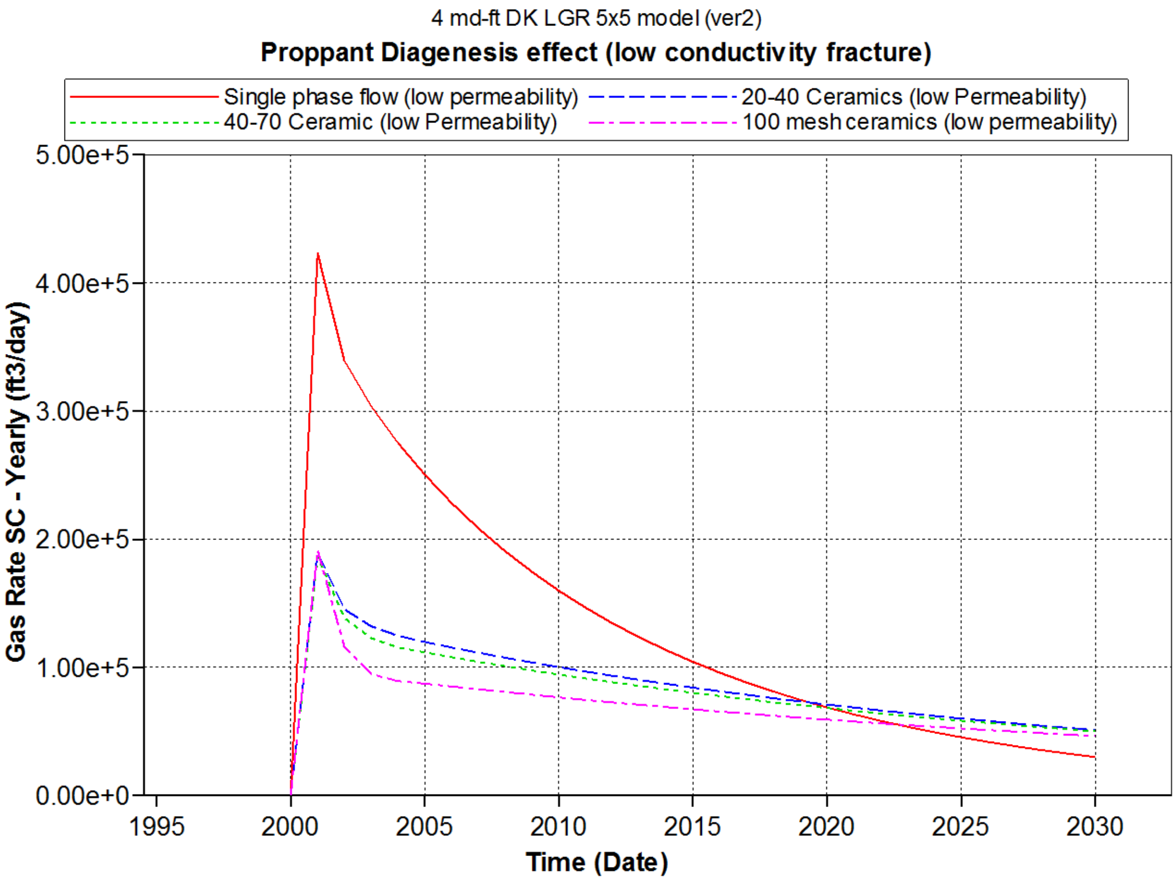

Figure 31: Proppant diagenesis effect on selected proppants (low conductivity hydraulic fracture).

For a high conductivity hydraulic fracture, the drop in the gas production rate is not significant. The effect of proppant diagenesis on gas flow rate is magnified for a low conductivity hydraulic fracture. Figure 30 and Figure 31 both show that the gas production rate when compared for the 3 different proppant is higher at early times and lower at later times of production for 20-40 ceramic proppant.

In conclusion, out of the three ceramic proppant used in our simulation study, 20-40 Carbo-Econoprop ceramic proppant will give the maximum overall gas production for a Marcellus shale gas well when the effect of proppant diagenesis is examined.

5.5 The Effect of Reservoir Compaction on Production

As production proceeds from a gas well in the Marcellus shale reservoir, the effective stress of the formation increases with the decrease in pore pressure. Using compaction data derived from lab experiments from Reyes (2000), we developed a model to simulate the effect of reservoir compaction/permeability change on production. We are able to do this by incorporating matrix permeability and natural fracture permeability change with decrease in pore pressure. We are able to derive a net pressure vs. reservoir permeability multiplier table applicable to the Marcellus shale.

Net Pressure (psi)	Matrix and Natural fracture permeability multiplier
0	1
688	0.3968
1068	0.0682
1558	0.034
2034	0.0194
2443	0.0094
2943	0.007
3389	0.0038
3892	0.0027
4251	0.0023
5250	0.0021
6252	8.88E-04
7253	7.25E-04

Table 10: Permeability multiplier table employed in modeling compaction effect

Table 10 show the percent decrease in the initial permeability of reservoir matrix and natural fracture apertures as effective stress the reservoir is subjected to increases as compaction proceeds.

We conducted simulation runs for cases of low and high conductivity hydraulic fracture as was done for the ideal single phase flow effect. For the highly conductive hydraulic fracture, proppant pack permeability values for 20-40 mesh carbolite ceramic proppant, 40-70 mesh carbolite ceramic proppant, 100 mesh carbolite ceramic proppant, 20-40 mesh multicoated sand proppant, 40-70 mesh multicoated sand proppant, and 100 mesh multicoated sand proppant were entered into our model. For the low conductive hydraulic fracture case, proppant pack permeability of 200 MD was used in our model. The cumulative gas production and gas flow rate results are shown below.

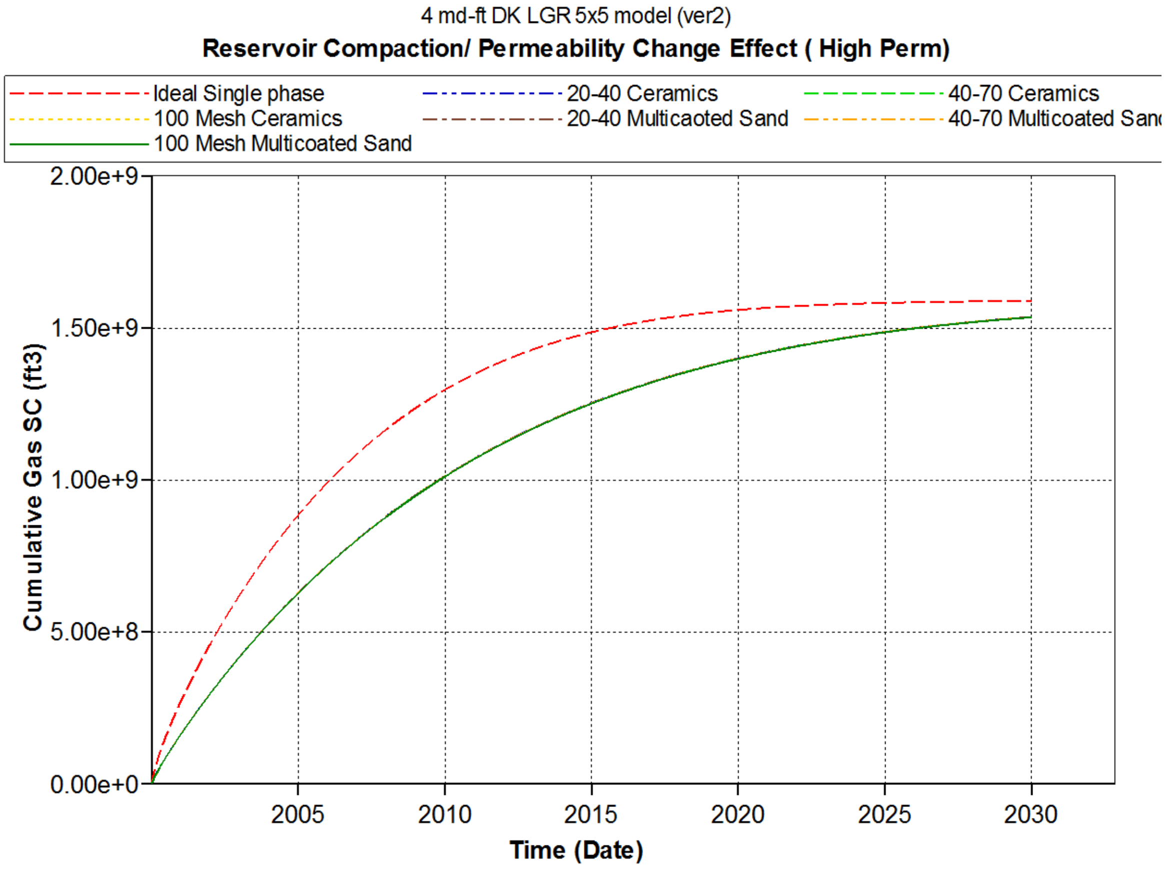

Figure 32: Reservoir compaction effect on selected proppants (Highly conductive hydraulic fracture).

The comparison of overall gas recovered for the ideal single phase model and reservoir compaction model shows the decrease in total production. The difference in production is approximately 0.1 BCF. This decrease is not significant because of the high conductivity of the hydraulic fracture. The impact of reservoir compaction is easily noticeable when low hydraulic fracture conductivity is used in our model. The difference in production is approximately 0.2 BCF of gas.

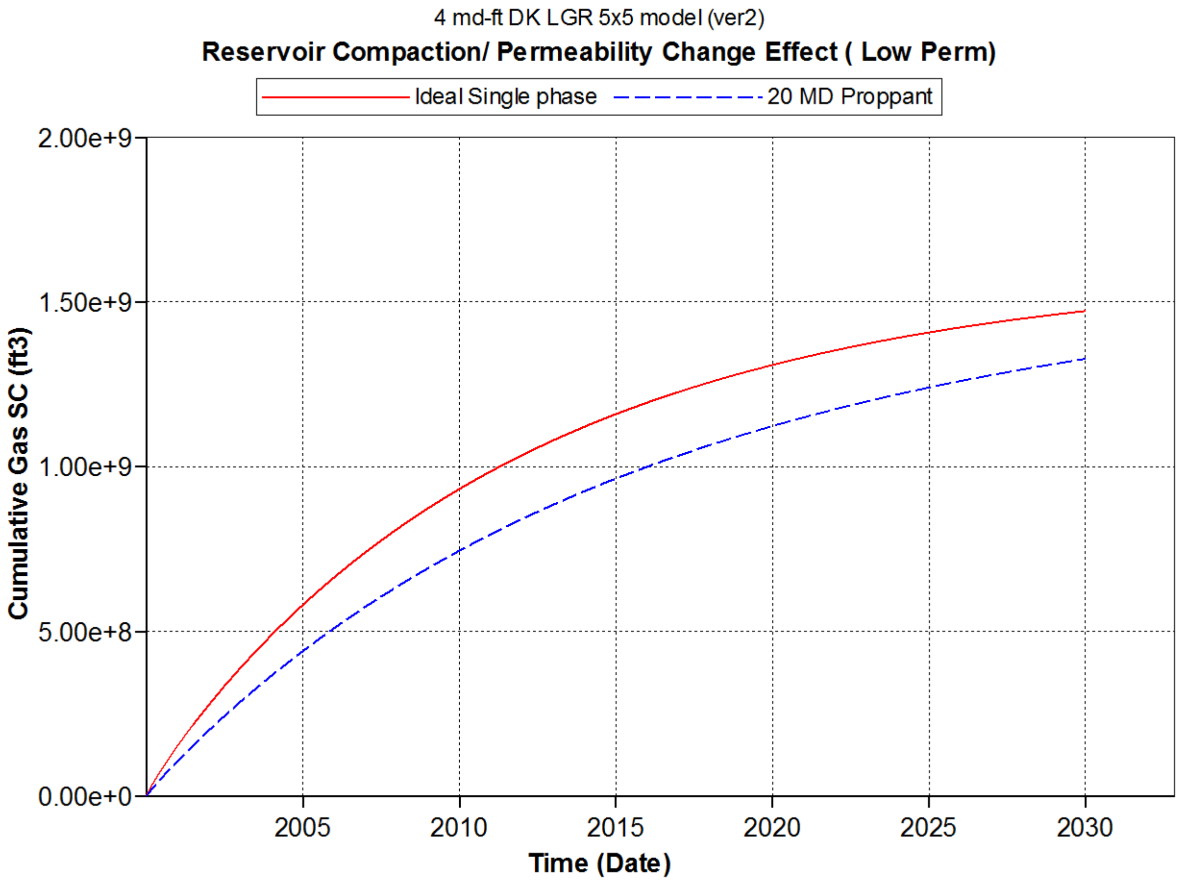

Figure 33: Reservoir compaction effect on selected proppants (low conductive hydraulic fracture).

Figures 34 below show the equivalent gas flow rates for the two cases we have simulated. Similar to the above trend, the impact of reservoir compaction on gas flow rates is more significant when low hydraulic fracture conductivity value is used in the model.

In conclusion, any of the six proppants used in our simulation when used in a Marcellus shale reservoir will achieve the same overall gas recovery when reservoir compaction/ permeability change effect is considered. This is because reservoir compaction affects the natural fractures and the matrix permeability of the reservoir.

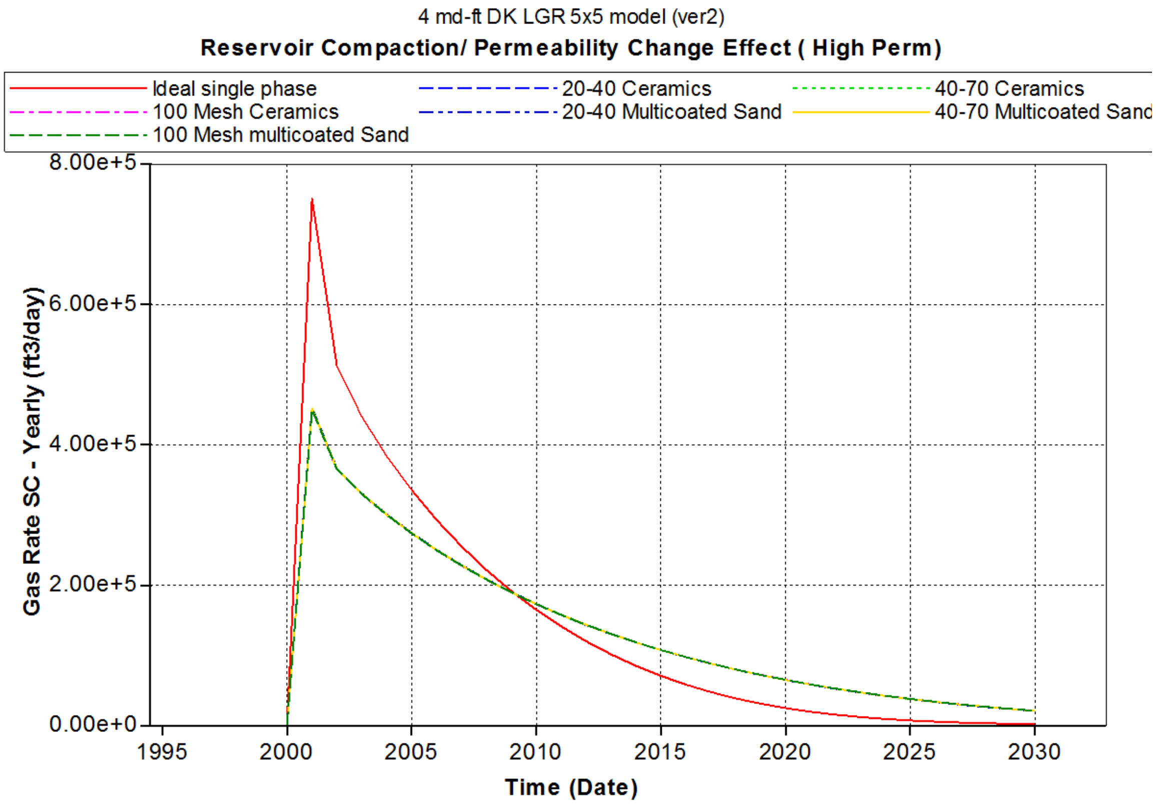
4 md-ft DK LGR 5x5 model (ver2)
Reservoir Compaction/ Permeability Change Effect (High Perm)
Ideal single phase
20-40 Ceramics
40-70 Ceramics
100 Mesh Ceramics
20-40 Multicoated Sand
40-70 Multicoated Sand
100 Mesh multicoated Sand
Gas Rate SC - Yearly (ft3/day)
8.00e+5
6.00e+5
4.00e+5
2.00e+5
0.00e+0
1995
2000
2005
2010
2015
2020
2025
2030
Time (Date)

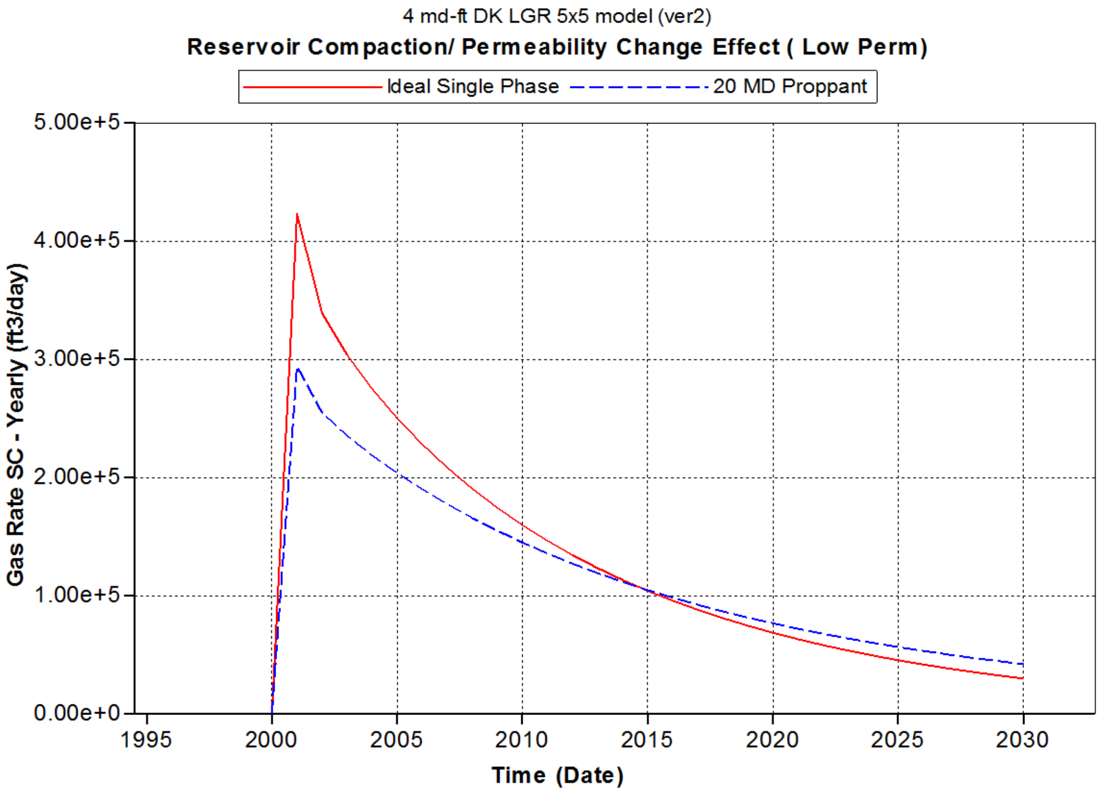

Figure 34: Reservoir compaction effect on yearly gas production rate for selected proppants (high and low conductivity hydraulic fracture).

5.6 The Effect of Operational Condition on Production

Using our model, we are able to study the effect of operational conditions on the overall gas production and overall water production from the Marcellus shale gas reservoir. We included all the various factors that we have studied above into our model to realistically simulate the effect of operational condition. Since the reservoir simulation software we have used in our studies has a limitation in terms of not allowing the specification of a constant water flow back rate, we employ the use of different constant bottom hole pressure constraint in controlling the flow from the reservoir into the well. The bottom hole pressure specifications that we have used in this study include 300 psi, 500 psi, 1000 psi, 1500 psi, and 2000 psi. We ran simulation runs for the high conductivity hydraulic fracture case and the low conductivity hydraulic fracture case. The results associated with our simulation runs are shown below.

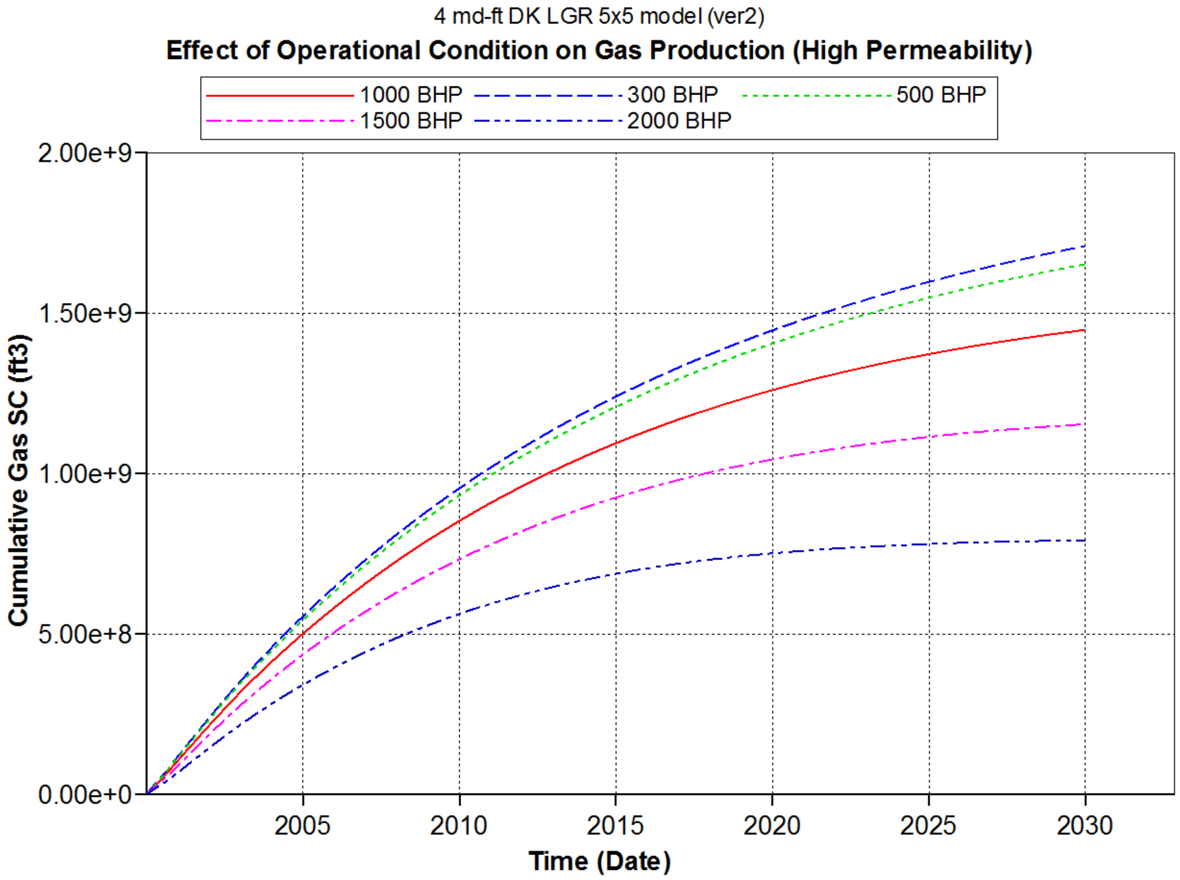

Figure 35: Effect of several BHP on overall gas production (high permeability fracture)

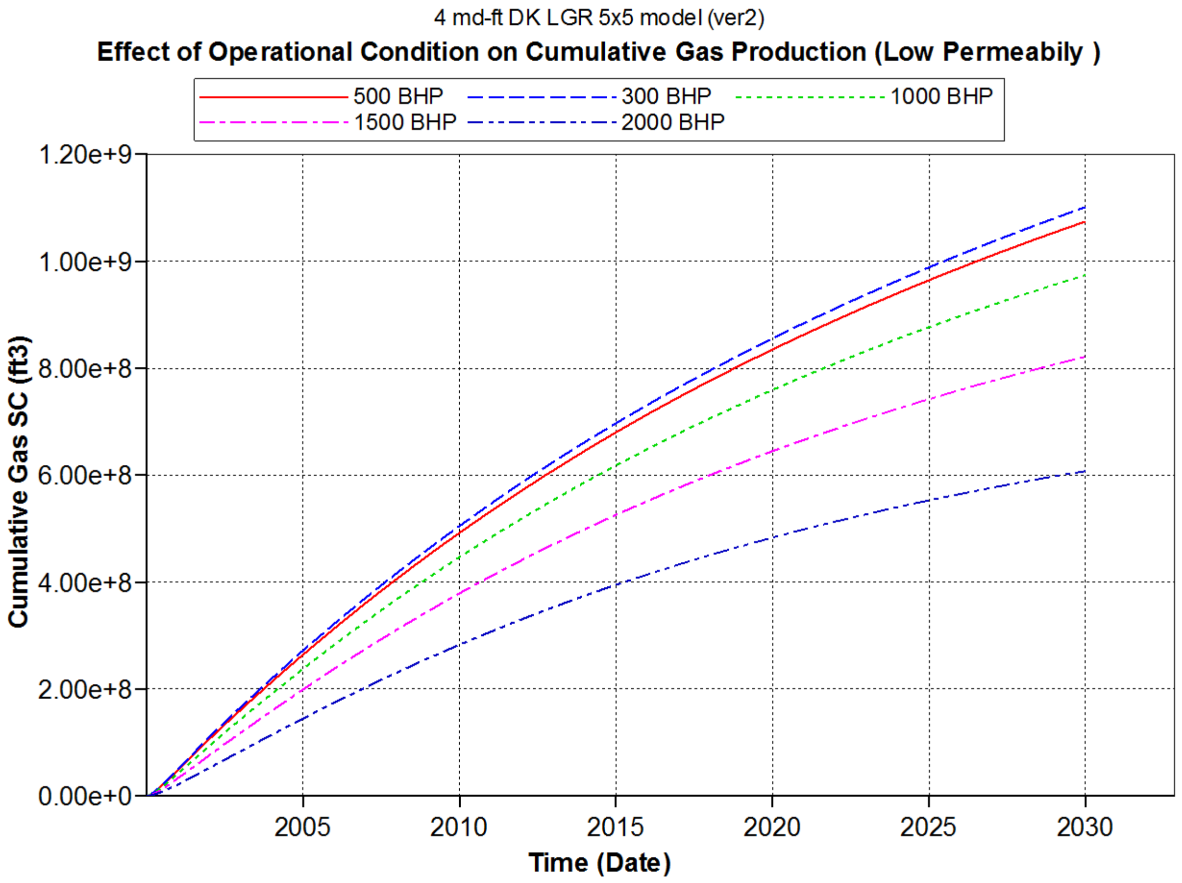

Figure 36: Effect of several BHP on overall gas production (low permeability fracture)

From Figure 35 and Figure 36, we can see that as the bottom hole pressure is decreased, the cumulative gas production increases. At a bottom hole pressure of 1000 psi, we begin to see significant drop in gas production. The cases of a high permeability hydraulic fracture and a low permeability fracture both show the same production behavior.

We also consider the effect of operational condition on flow back water production. Figure 37 and Figure 38 show the cumulative water produced from our production well over a period of 30 years. For a high permeability fracture case, after 200 days of production, we are able to flow back 40% volume of the fracture fluid injected during the hydraulic fracturing process. Over a 30 year period, we are able to flow back about 54 % of the injected fracture fluid. Producing the well at a low BHP allows more fracture fluid to be flown back at 200 days of production as compared to producing the well at other BHP. Over a 30 year period, the cumulative water volumes produced at different BHPs are similar.

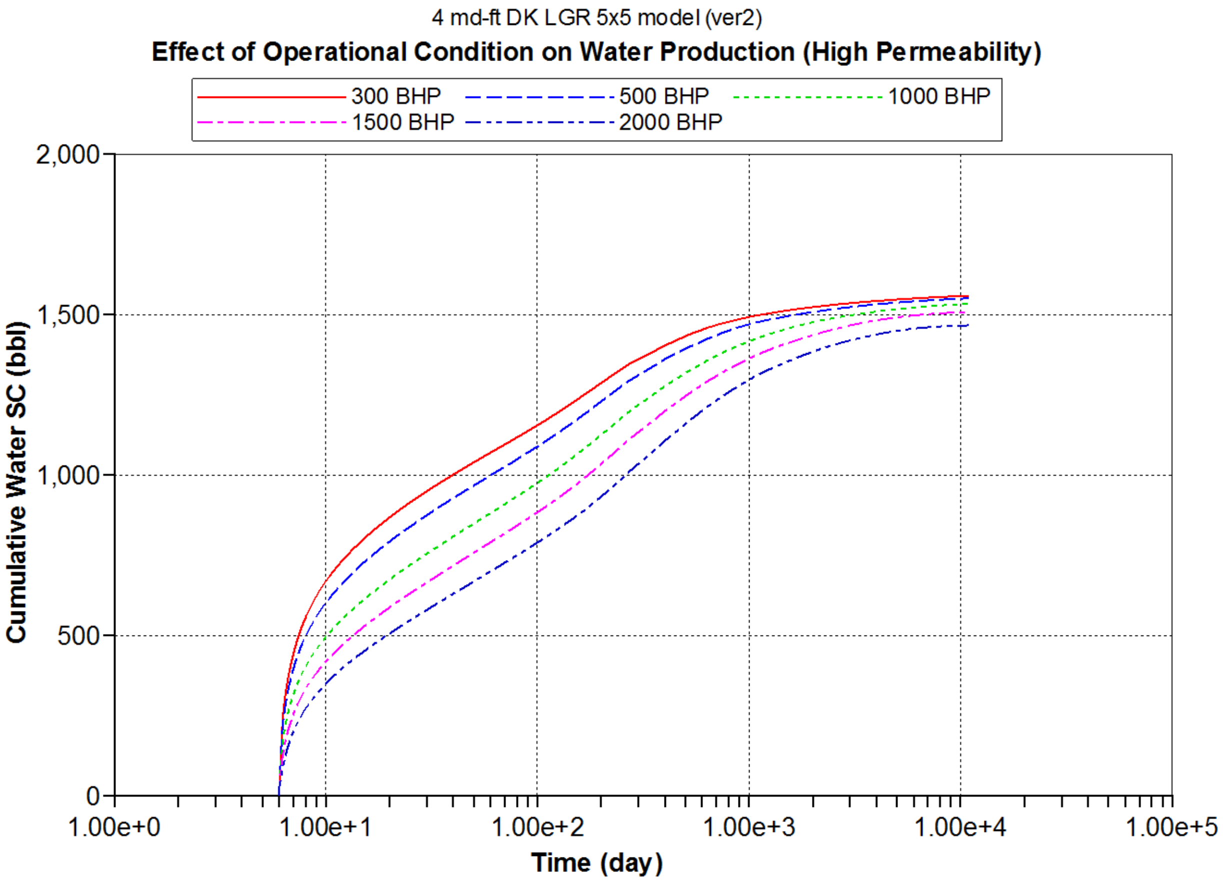

Figure 37: Effect of several BHP on overall water production (high conductivity fracture)

For a low permeability fracture case, after 200 days of production, we are able to flow back 42% of the fracture fluid injected during the hydraulic fracturing process. Over a 30 year period, we are able to flow back about 76 % of the injected fracture fluid. Producing the well at a low BHP allows more fracture fluid to be flown back at early days of production as compared to producing the well at other BHP. Over a 30 year period, the difference in cumulative water produced at different BHP is minimal.

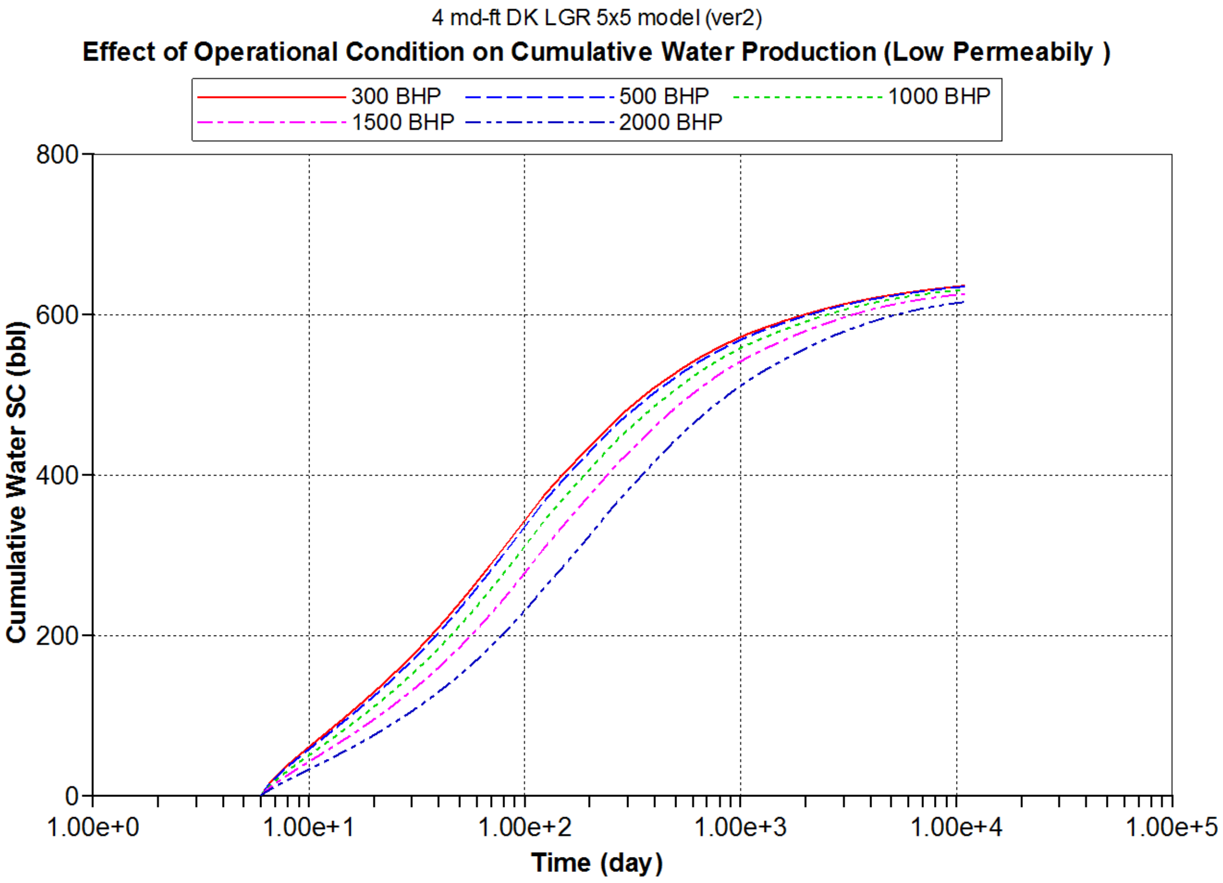

Figure 38: Effect of several BHP on overall water production (low conductivity fracture)

In conclusion, to produce more gas and flow back more fracture fluid, the fractured well should be flown at a low bottom hole pressure. From simulation result, we observe that, at a lowly conductive hydraulic fracture, we flow back more fracture fluid over a 30 year period as compared to the fluid flown back when we have a highly conductive hydraulic fracture. Also at early times, both cases of hydraulic fracture conductivity flow back approximately 40% of injected fracture fluid. It is recommended to create a highly conductive hydraulic fracture and to produce at low bottom hole pressure to recover more gas and to flowback more fluid at early times of production.

5.7 The Effect of Addition of All Factors on Production

Next step in our simulation process to combine all the effects we have simulated in Sections 5.1 to 5.6 and quantify their combined impact on production from a hydraulically fracture well in the Marcellus shale gas. We have divided each step into sections. Starting from the ideal single phase flow which we call scenario-1, we will modify our model by incorporating the multiphase flow process, this model we call scenario-2. Then to scenario-2 model, we will incorporate the impact of proppant crushing which we call scenario-3. Scenario-4 will be able to model the impact of multiphase flow, proppant crushing and proppant diagenesis. Scenario-5 model consist of the required modifications that can model the impact of multiphase flow, proppant crushing and proppant diagenesis, along with the reservoir compaction effect.

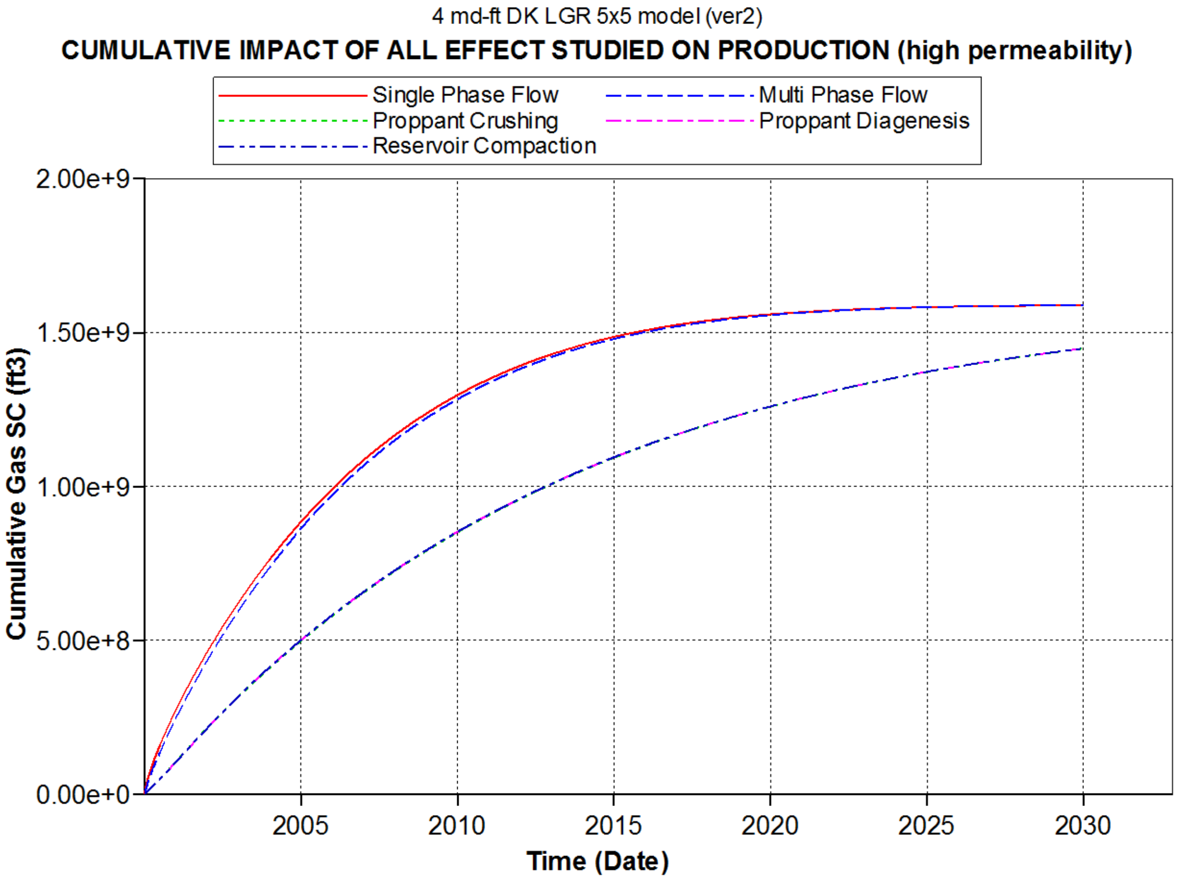

Figure 39: Cumulative impact of various effects on overall gas recovery.

The purpose of a cumulative study is to quantify how much impact each additional post hydraulic fracture effect has on production. We have simulated these effects using the two cases of which we have used in the past, the low conductivity hydraulic fracture case and the high conductivity hydraulic fracture case. Figure 39 above shows the cumulative gas production associated with scenario-1, scenario-2, scenario-3, scenario-4, and scenario-5 for the highly conductive hydraulic fracture. From the plot, it is observed that production decreases slightly when multiphase flow is added to the ideal single phase model. When proppant crushing is added to the single and multiphase factors, we see a significant decrease in production. When proppant diagenesis and reservoir compaction factors are added to the single phase, multiphase and proppant crushing factors, we see no decrease in production (plot of scenario-3, scenario-4 and scenario-5 lies underneath one another). The reason for this is because; the permeability of the hydraulic fracture is significantly high that additional decrease in permeability due to proppant diagenesis and reservoir compaction is not significant enough to further reduce gas production. The gas flow rate associated with each scenario is shown in Figure 40.

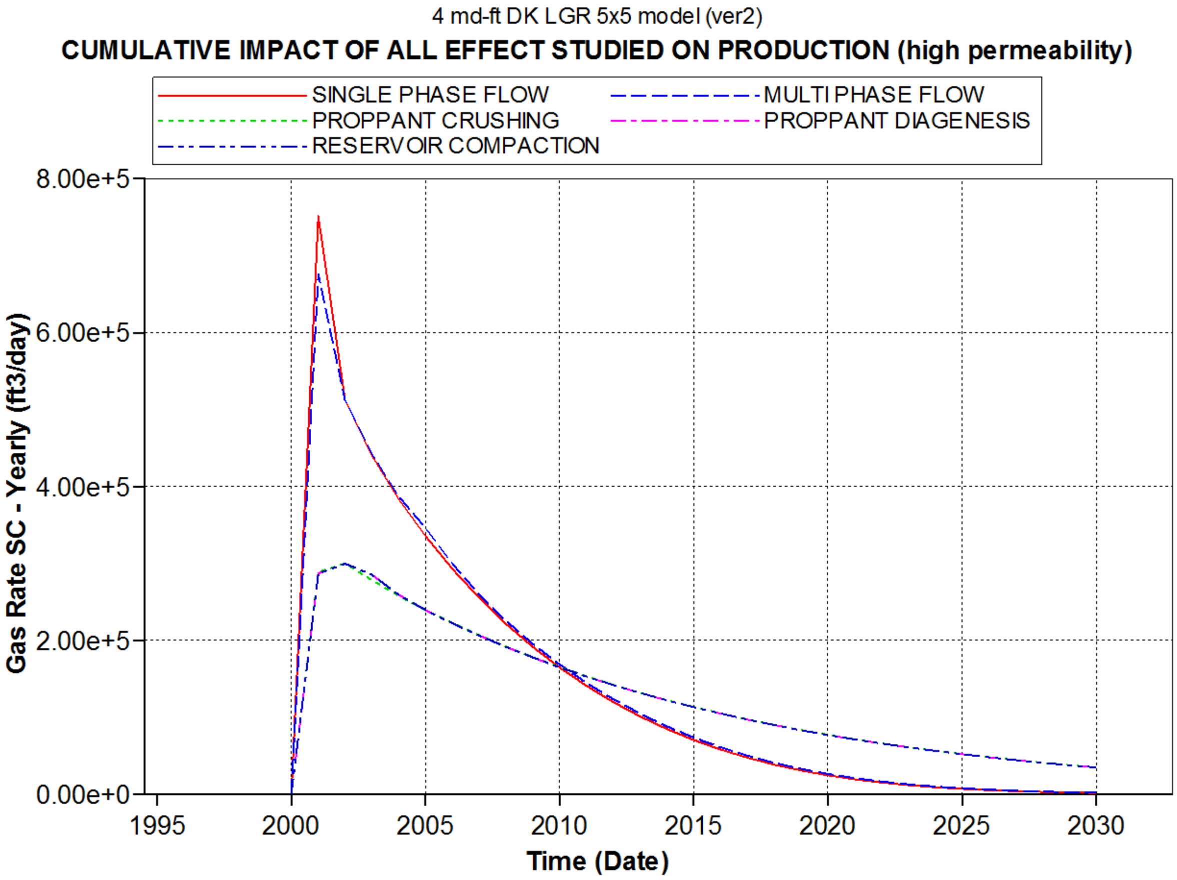

Figure 40: Cumulative impact of various effects on gas production rate.

As expected, early time flow rate is high for scenarios 1 and 2, while the early time flow rates for scenarios 3, 4, and 5 are lower. Toward the later period of production, the flow rates associated for scenarios 1 and 2 decreases significantly while the flow rates associated for scenarios 3, 4, and 5 decreases steadily towards the later times of production. It should be noted that scenarios 3, 4, and 5 all yield the same curve.

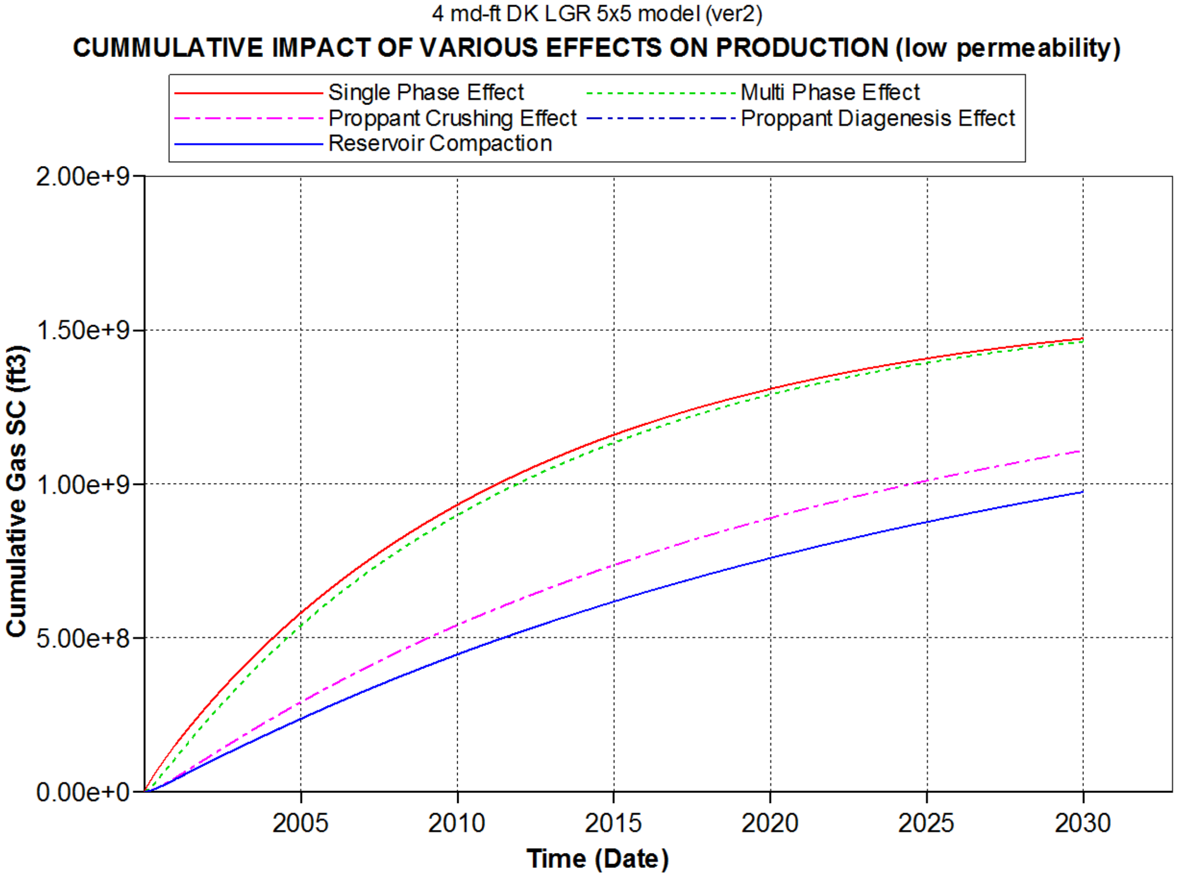

Figure 41: Cumulative impact of various effects on overall gas recovery.

Figure 41 shows the cumulative production associated with scenarios 1, 2, 3, 4, and 5 when the conductivity of the hydraulic fracture created is low. The impact of the addition of more factors into the initial single phase model is better illustrated when low conductive hydraulic fracture is employed in the model.

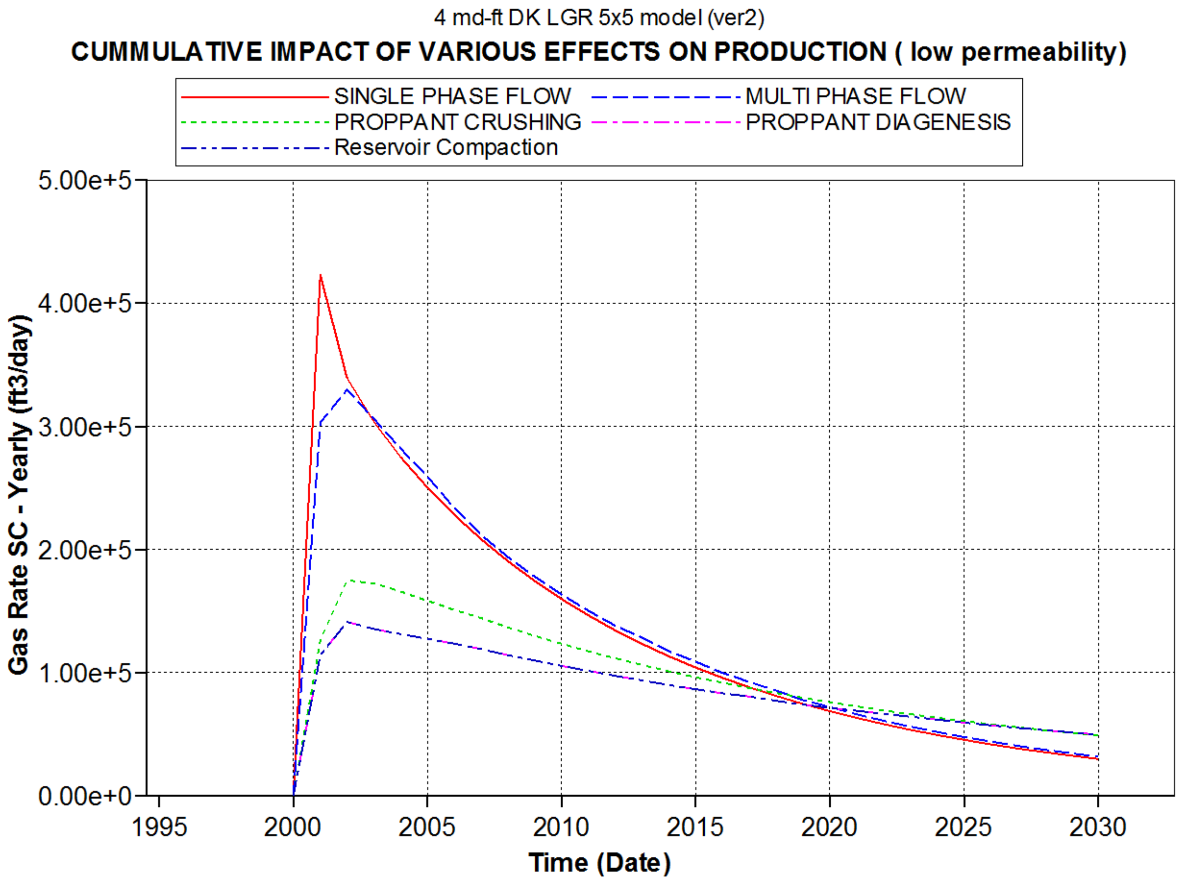

Figure 42: Cumulative impact of various effects on gas production rate.

As one can see from Figure 42, when each scenario is modeled, there is a continuous decrease in production as a new post hydraulic fracture effect is added into the base model. The decrease in production from scenario 1 to scenario 2 is minimal, but when proppant crushing effect is added to the single phase and multiphase flow effects, we see a significant decrease in production. The decrease in production due to the addition of proppant diagenesis is not as significant as the change experience from scenario-2 to scenario-3. We see approximately 0.1 BCF decrease in production from scenario-3 to scenario-4. Scenario-5 does not show any decrease in production from scenario-4.

The gas flow rate associated with each scenario is illustrated in figure 42; the trend in gas flow rate decrease is similar to the decrease experienced in the cumulative gas production for the case of lowly conductive hydraulic fracture.

5.8 The Effect of Proppants on Gas Recovery

We studied the effect of four kinds of proppants on overall gas recovery. The proppants used in this study includes 20-40 ceramic proppant, 20-40 sand proppant, 40-70 ceramic proppant and 40-70 sand proppants. We conducted simulations runs to predict the how much gas will be produced when factors such as multi phase flow effect, proppant crushing effect and reservoir compaction effect are experience in a Marcellus shale gas well. Proppant diagenesis effect is not include in our analysis because we do not have enough data for all of the four proppant we used.

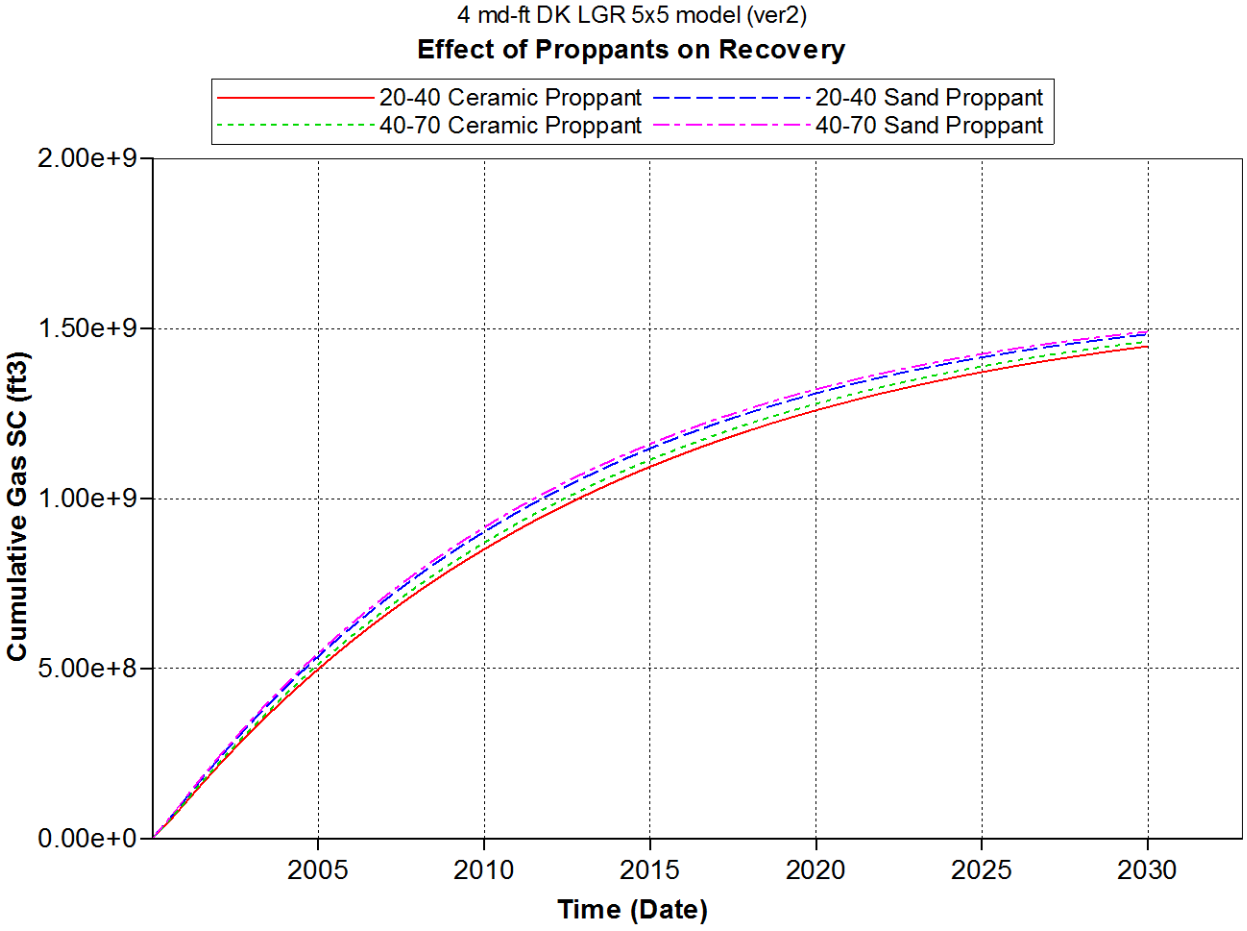

Figure 43: Effects of proppants on overall gas production.

Figure 43 shows that 20-40 ceramic proppant will give the minimum gas recovery out of the four proppants we used. 40-70 multi coated sand proppant will the maximum gas recovery out of the four proppant. Even though the difference in production associated with the four proppants is not significant, the difference is still noticeable.

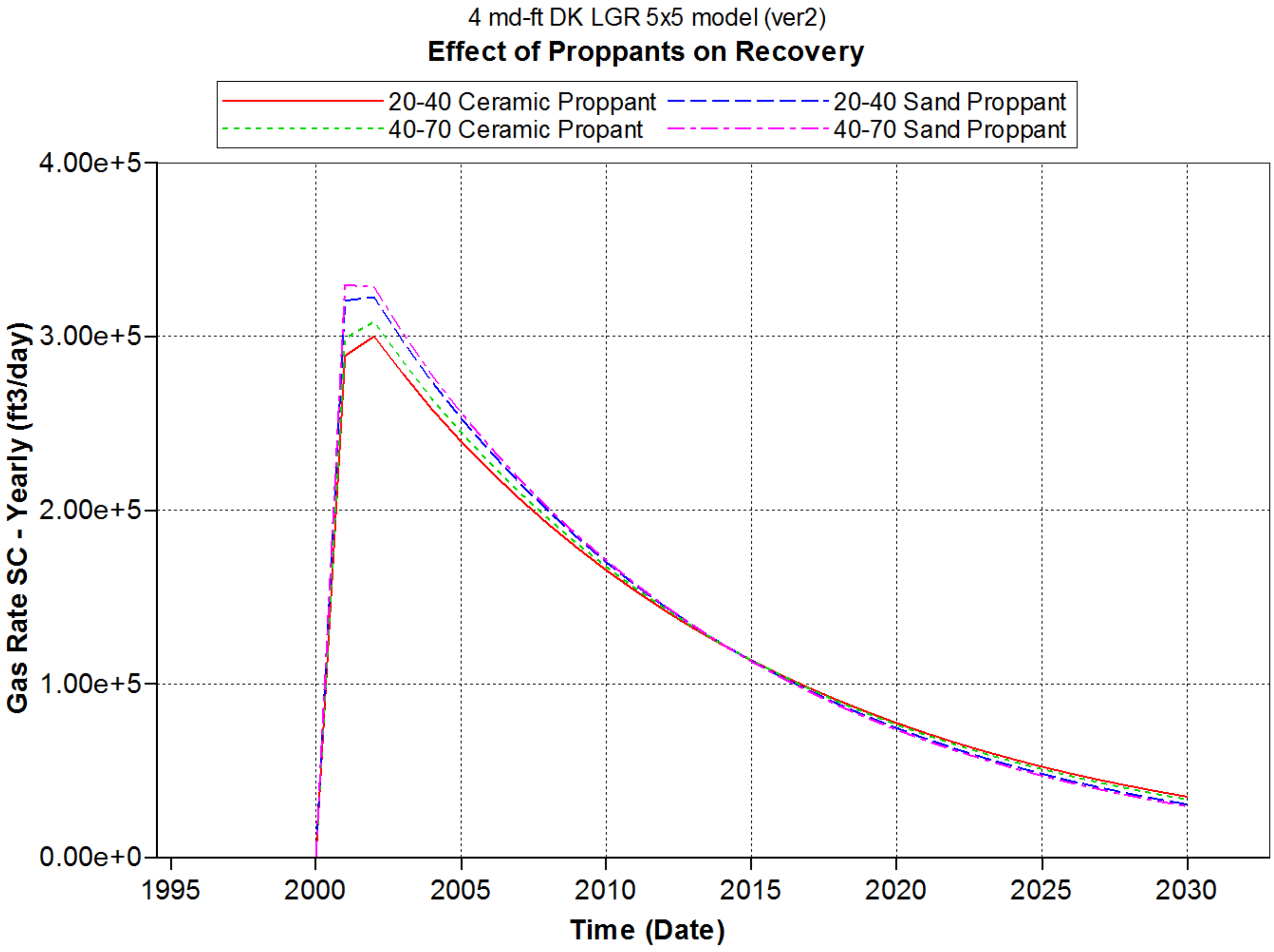

Figure 44: Effects of proppants on gas production rate.

Figure 44 shows the gas production rate associated with the use of four different proppants in creating a hydraulic fracture in the Marcellus shale. Gas production is higher at early time when 40-70 multi coated sand proppant is used, and gas production is highest at later time when 20-40 ceramic proppant is used. In conclusion, it is suggest that to produce more gas and to produce at higher rate at earlier time, 40-70 multi coated sand proppants is recommended to be used in the Marcellus shale gas well when factors such as multi phase flow, proppant crushing and reservoir compaction effects are taken into consideration.

Table 11 below shows the gas recovery associated with the 20-40 ceramic proppant, 20-40 sand proppant, 40-70 ceramic proppant and 40-70 sand proppants when we take into consideration factors such as multi phase flow, proppant crushing and reservoir compaction effects.

Proppant type	**Single phase effect Recovery**	**Cumulative effect recovery**
20-40 Ceramic	1.60 BCF	1.44 BCF
20-40 Multicoated Sand	1.60 BCF	1.48 BCF
40-70 Ceramic	1.60 BCF	1.46 BCF
40-70 Multicoated Sand	1.60 BCF	1.49 BCF

Table 11: Table showing overall gas recovery associated with 4 proppants.

CHAPTER 6

CONCLUSIONS AND RECOMMENDATION

We have studied several post hydraulic fracture effects that impact the productivity of a gas well in the Marcellus shale. We conducted reservoir simulation study on the various effects such as the ideal single phase flow, multiphase flow effect, proppant crushing effect, proppant diagenesis effect, reservoir compaction effect, and operational condition effect. The reservoir model we use help quantifies how much impact each post hydraulic fracture effect has on overall gas production both when an individual case by case scenario is model and when the combination of several effects are modeled. From literature review of all published article in connection to Marcellus shale to the reservoir simulation work that we have conducted, we are able to use the vast scholarly resources in our disposal to draw several observations and several conclusion from our work. The main conclusions are:

1. Using expensive proppants or bigger proppants does not necessary imply significant increase in the ultimate gas recovery, a proppant that will create a hydraulic fracture conductivity of approximately 1639 md-ft should be used in creating the hydraulic fracture in the Marcellus shale gas well.
2. When a 12,500 md-ft conductive hydraulic fracture is created, the impact of all the factors we have studied on ultimate gas recovery is less minimal as to when a 0.4 md-ft conductive hydraulic fracture has been created.
3. Proppant diagenesis effect when compared to other effects has the most significant impact on production regardless of the conductivity of the hydraulic fracture created. As stated above, decrease in production due to proppant diagenesis is intensified when 0.4 md-ft conductivity hydraulic fracture is created. From our simulation results, out of all the 3 ceramic proppant we used 20-40 Carbo-Econoprop ceramic proppant will give the maximum overall gas production for a Marcellus shale gas well when proppant diagenesis effect is considered.
4. Reservoir compaction effect causes decrease in overall gas production. Regardless of whatever proppant we use, the same result overall gas recovery is achieved.

The reason for this is because; reservoir compaction affects the natural fracture and matrix permeability properties of the reservoir.

5. To produce more gas and flow back more fracture fluid, the fractured well should be flown at a low bottom hole pressure of 300 psi or less. It is recommended to create a highly conductive hydraulic fracture in the range of 200 md-ft and to produce at low bottom hole pressure of 300 psi or less to recover more gas and to flowback more fluid at early times of production.
6. When all the post hydraulic fracture effects are simulated by adding one effect after the other to the base model, there is a steady decrease in production with the addition of another case, the drop in production by adding proppant crushing to the multiphase flow and single phase effect is more significant than any other introduction of a post hydraulic fracture effect.

REFERENCES

Balhoff M.T, Matthew J.M. "An Analytical Model for Cleanup of Yield-Stress Fluids in Hydraulic Fractures." *SPE*, 2005.

Blauch M.E, Myers R.R, Moore T.R, Lipinski B.A, Houston N.A. "Marcellus Shale Post-Frac Flowback Waters - Where is All the Salt Coming From and What are the Implications?" *SPE*, 2009.

Blauch Matt. "Geochemical Fixes Boost Shale Completion Efficient." *Shale Energy*, 2010.

Cheng, Y. "Impact of Water Dynamics inFractures on the Performance of Hydraulically Fracture Wells in Gas Shale Reservoirs." *SPE*, 2010.

Cipolla C.L, Lolon E.P, Erdle J.C, Tathed V. "Modeling Well Performance in Shale Gas Reservoirs." *SPE*, 2009.

Cipolla C.L, Lolon E.P, Mayerhofer M.J. "Reservoir Modeling and Production Evaluation in Shale Gas Reservoirs." *IPTC*, 2009.

Cipolla C.L., Lolon E.P, Erdle J.C, Rubin B. "Reservoir Modeling in Shale Gas Reservoir." *SPE*, 2009.

Cipolla, Craig. "Modeling Production and Evaluating Fracture Performance in Unconventional Gas Reservoirs." *JPT*, 2009: 84-90.

Cooke Jr C.E. "Conductivity of Fracture Proppants in Multiple Layers." *JPT*, 1973.

Crafton, James W. "Modeling Flowback Behavior or Flowback Equals "Slowback"." *SPE*, 2008.

Davies D.R, Kulper T.O.H. "Fracture Conductivity in Hydraulic Fracture Stimulation ." *JPT*, 1988: 550-552.

Davies J.P. "Stress Dependent Permeability: Characterization and Modeling." *SPE*, 1999.

Fabrice Cuisiat, Lars Grande, Kaare Hoeg. "Laboratory Testing of Long Term Fracture Permeability in Shale." *SPE/ISRM*, 2002.

Fatt I, Davis D.H. "Reduction in Permeability With Overburden Pressure." *Petroleum Transaction*, 1952.

Fredd C.N, McConnell S.B, Boney C.L, England K.W. "Experimental Study of Fracture Conductivity for Water Fracturing and Conventional Fracturing Application." *SPE*, 2001.

Holditch S.A. "Factors Affecting Water Blocking and Gas Flow From Hydraulically Fractured Gas Wells." *JPT*, 1979: 1515-1524.

Holditch S.A. "Stimulation of Tight Gas Reservoirs Worldwide." *OTC*, 2009.

Houston N, Blauch M, Weaver D, Miller D, O'Hara D. "Fracture Stimulation in the Marcellus Shale - Lesson Learned in Fluid Selection and Execution." *SPE*, 2009.

Kaufman P, Penny G.S, Paktinat J. "Critical Evaluations of Additives Used in Shale Slickwater Fracs." *SPE*, 2008.

LaFollete R, Carman P,. "Proppant Diagenesis: Result So Far." *SPE*, 2010.

Lee D.S, Elsworth D, Yasuhara H, WeaverJ, Rickman R. "An Evaluation of the Effects of Fracture Diagenesis on Fracture Treatments: Modeled Response." *ARMA*, 2009.

Luna J.B, Soriano E, Garcia R, Galvan J, Barrera C. "Sustaining Fracture Conductivity Increases Cumulative Production in Tight-Gas Reservoir - A Case History." *SPE*, 2008.

Mckee C.R, Bumb A.C, Koenig R.A. "Stress-Dependent Permeability and Porosity of Coal and Other Geologic Formations." *SPE*, 1988.

Nguyen P.D, Dewprashad B.T, Weaver J.D. "New Approach for Enhancing Fracture Conductivity." *SPE*, 2000.

Palisch T, Duenckel R, Bazan L, Heidt H, Turk G. "Determining Realistic Fracture Conductivity and Understanding its Impact on Well Performance - Theory and Field Examples." *SPE*, 2007.

Putra E, Muralidharan V, Schechter D. "Overburden Pressure Affects Fracture Aperture and Fracture Permeability in a Fractured Reservoir." *Suadi Aramco Journal of Technology*, 2003: 58-63.

Reyes L, Osisanya S.O. "Empirical Correlation of Effective Stress Dependent Shale Rock Properties." *Petroleum Society*, 2000.

Settari. "Reservoir Compaction." *Distinguished Author Series*, 2002.

Sherman J.B, Holditch S.A. "Effect of Injected Fracture Fluids and Operating Procedures on Ultimate Gas Recovery." *SPE*, 1991.

Soeder, Daniel J. "Porosity and Permeability of Eastern Devonian Gas Shale." *SPE*, 1988.

Tao Q, Ehlig-Economides C.A, Ghassemi A. "Modeling Variation of Stress and Permeability in Naturally Fractured Reservoirs Using Displacement Discontinuity Method." *ARMA*, 2009.

Tao Q, Ehlig-Economides, Ghassemi A. "Investigation of Stress-Dependent Fracture Permeability in Naturally Fracture Reservoirs Using a Fully Coupled Poroelastic Displacement Discontinuity Model." *SPE*, 2009.

Wang F.P, Reed R.M,. "Pore Networks and Fluid Flow in Gas Shales." *SPE*, 2009.

Wang J.Y, Holditch S.A. "Simulation of Gel Damage on Fracture Fluid Cleanup and Long Term Recovery in Tight Gas Reservoirs." *SPE*, 2008.

Wang J.Y, Holditch S.A, McVay D.A. "Modeling Fracture Fluid Cleanup in Tight Gas Wells." *SPE*, 2009.

Weaver J, Parker M, Batenburg D, Nguyen P. "Fracture-Related Diagenesis May Impact Conductivity." *SPE*, 2007.

Weaver J, Rickman R, Luo H. "Fracture Conductivity Loss Due to Geochemical Interaction Between Man-Made Proppants and Formation." *SPE*, 2008.

Weaver J, Rickman R, Luo H, Loghry R. "A study of Proppant-Formation Reactions." *SPE*, 2009.

Weaver J.D, Nguyen P.D, Parker M.A,Van Batenburg D. "Sustaining Fracture Conductivity." *SPE*, 2005.

Weaver J.D, Rickman R.D, Luo H, Elsworth D. "Fracture-Conductivity Loss Caused by Geochemical Interactions Between Man-Made Proppants and Formations." *ARMA*, 2009.

APPENDIX

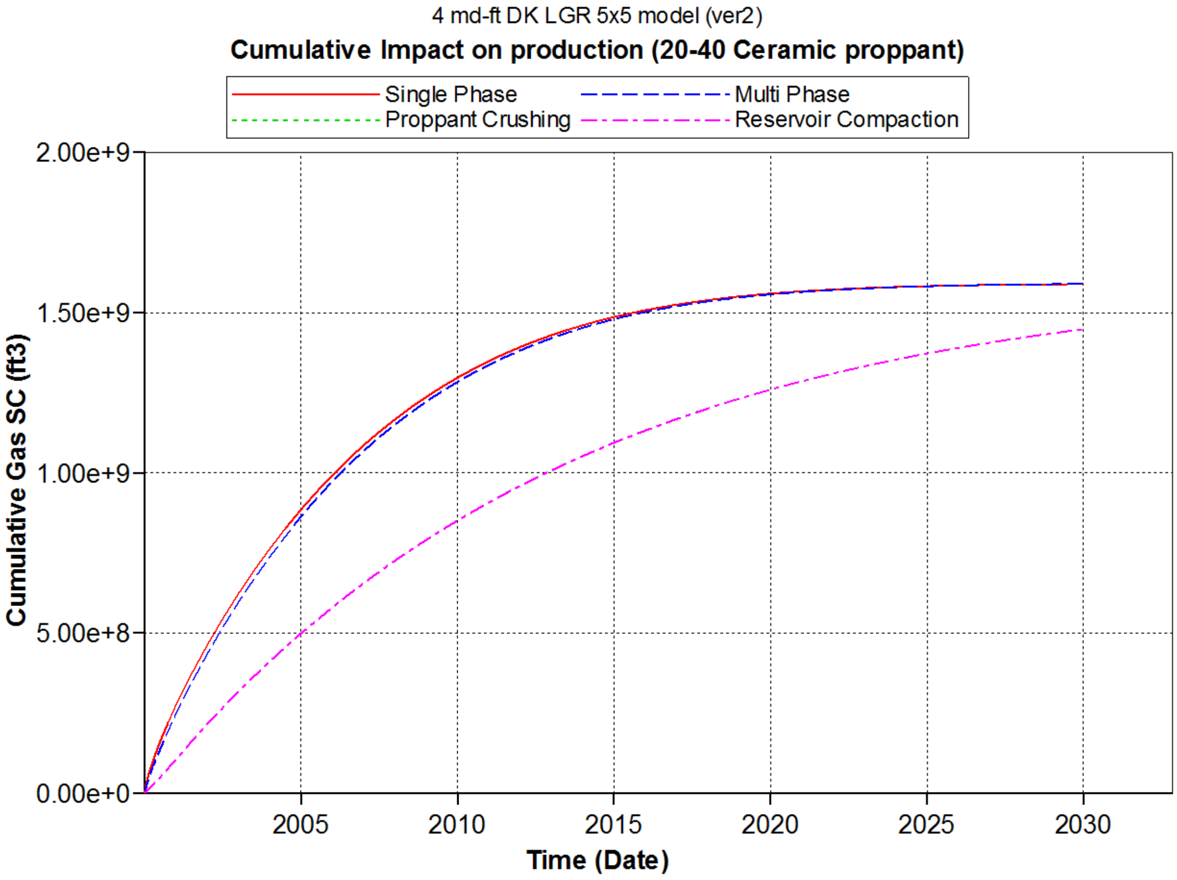

Figure 45: Effect of 20-40 ceramic proppant on cumulative production

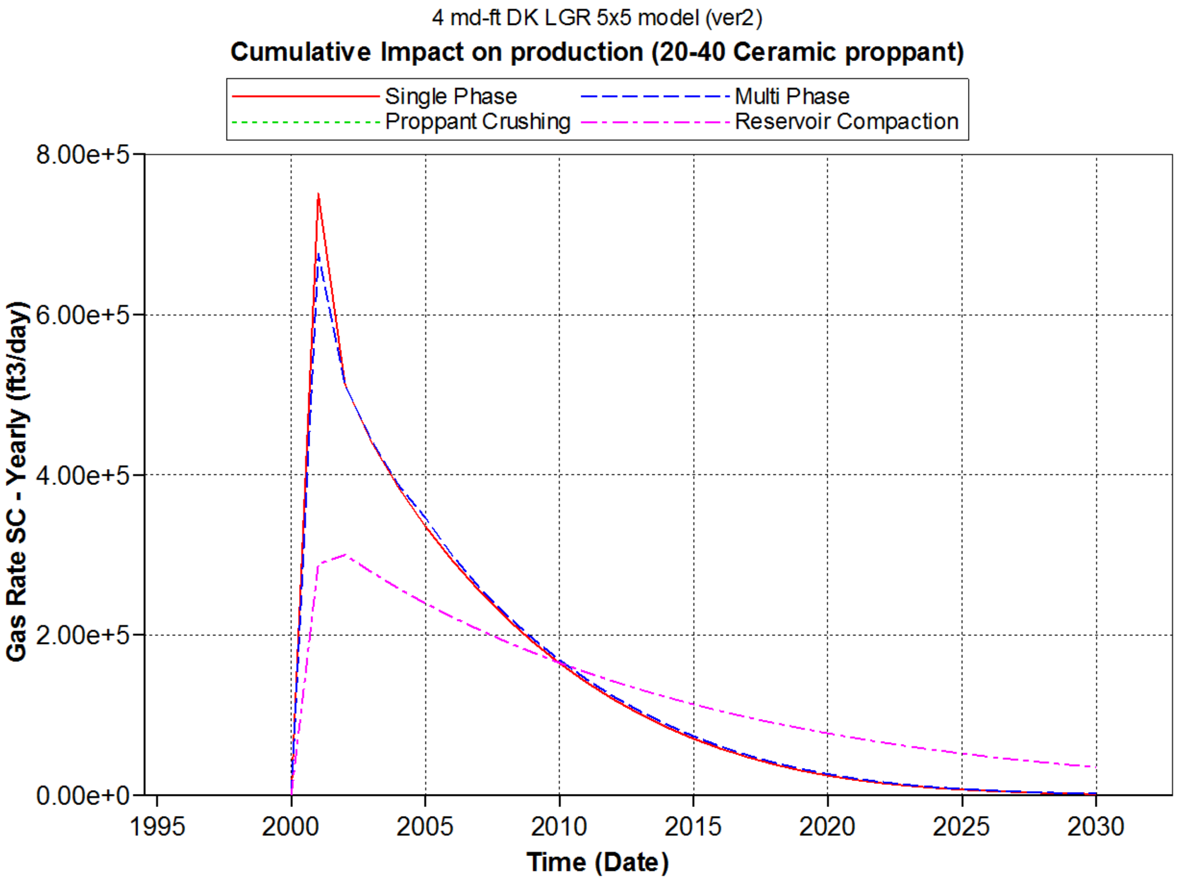

Figure 46: Effect of 20-40 ceramic proppant on gas production rate

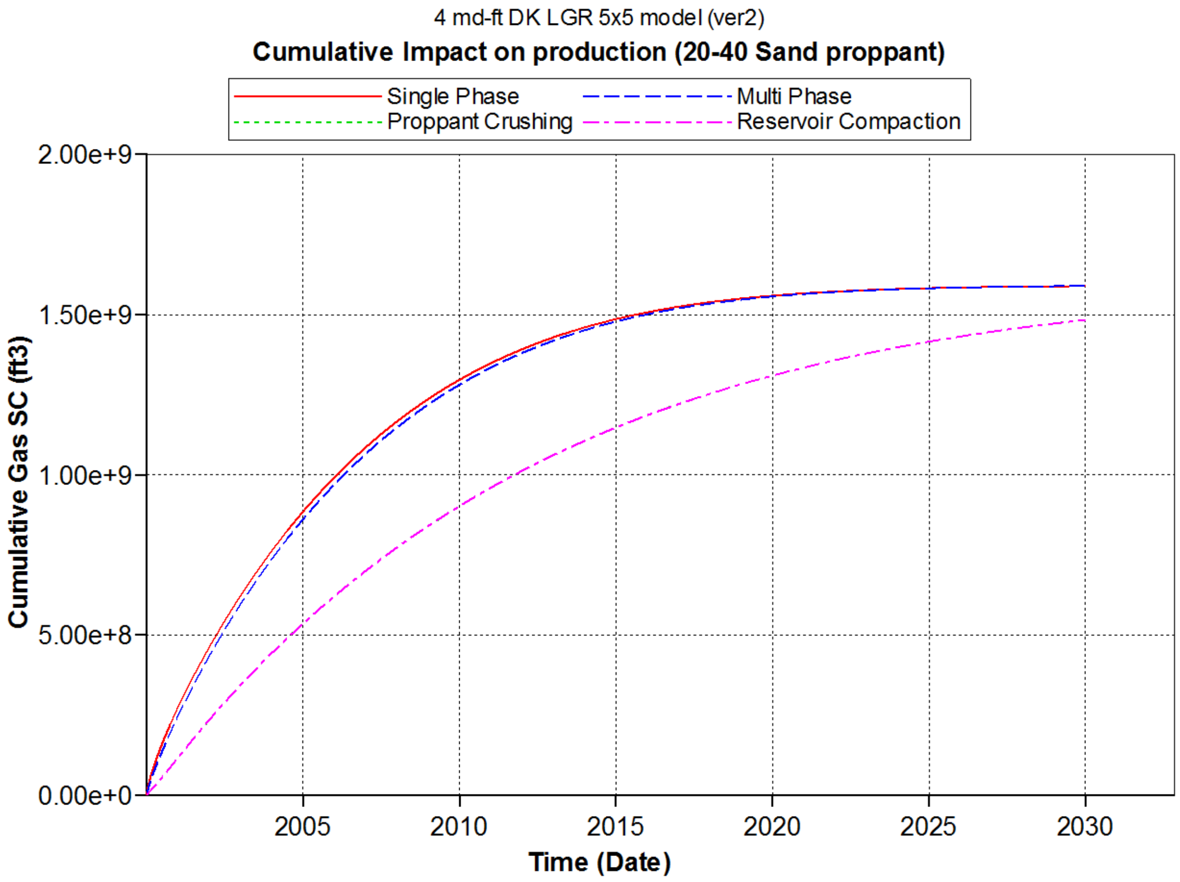

Figure 47: Effect of 20-40 multicoated sand proppant on cumulative gas production

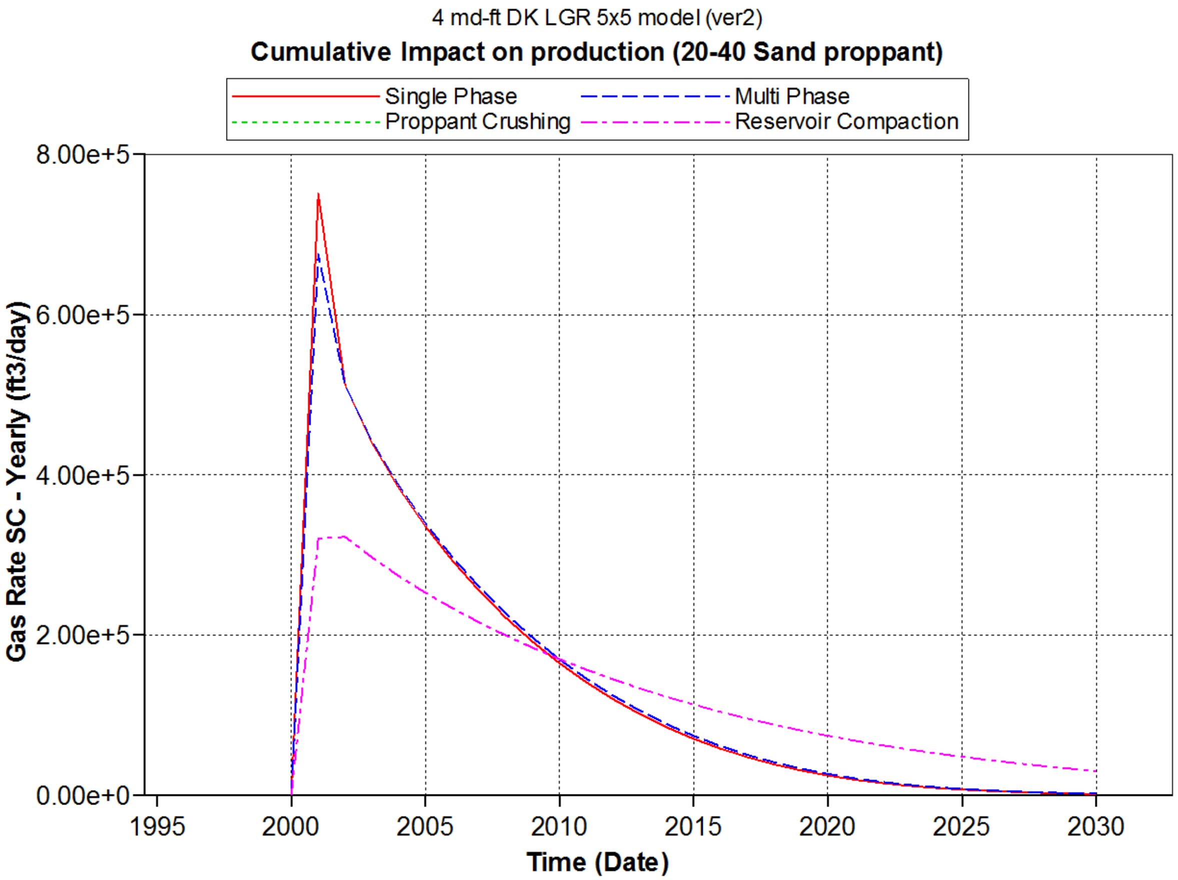

Figure 48: Effect of 20-40 multicoated sand proppant on gas production rate

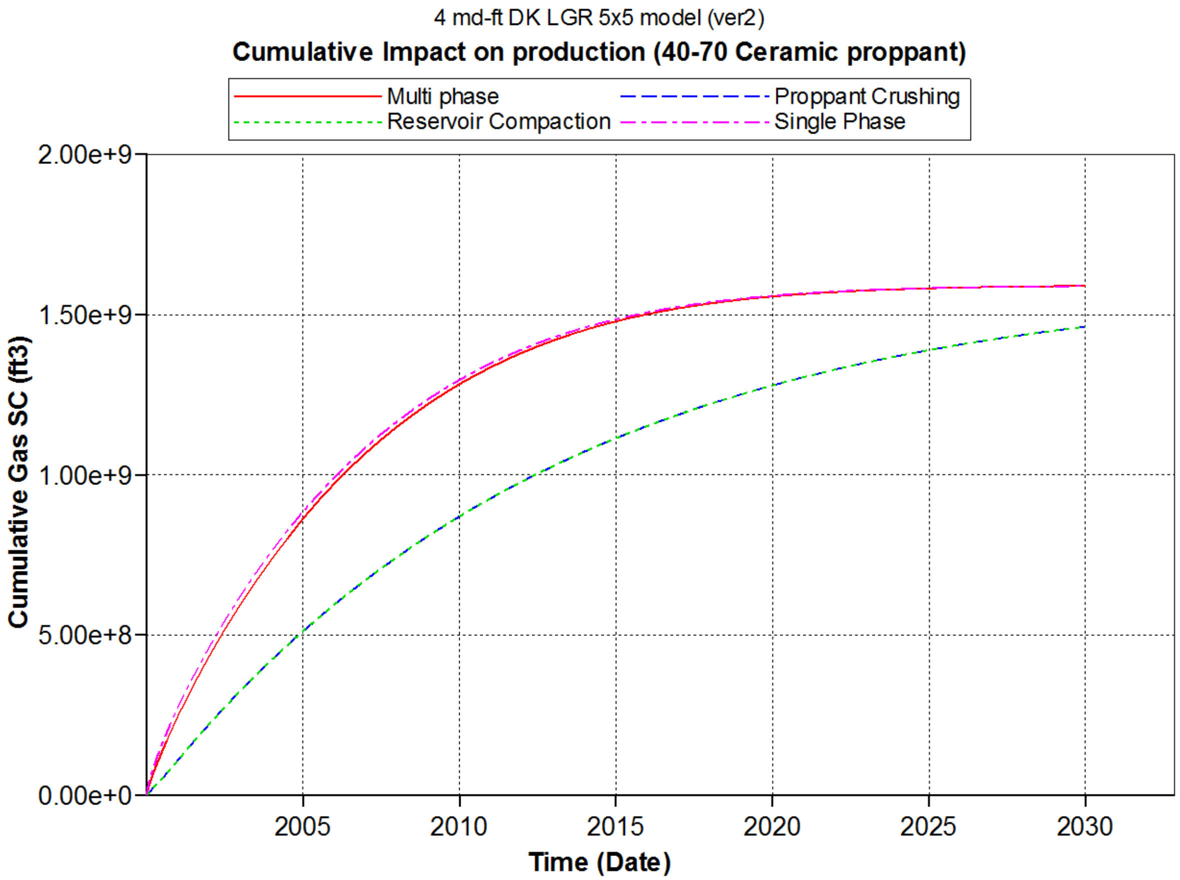

Figure 49: Effect of 40-70 Ceramic proppant on cumulative gas production

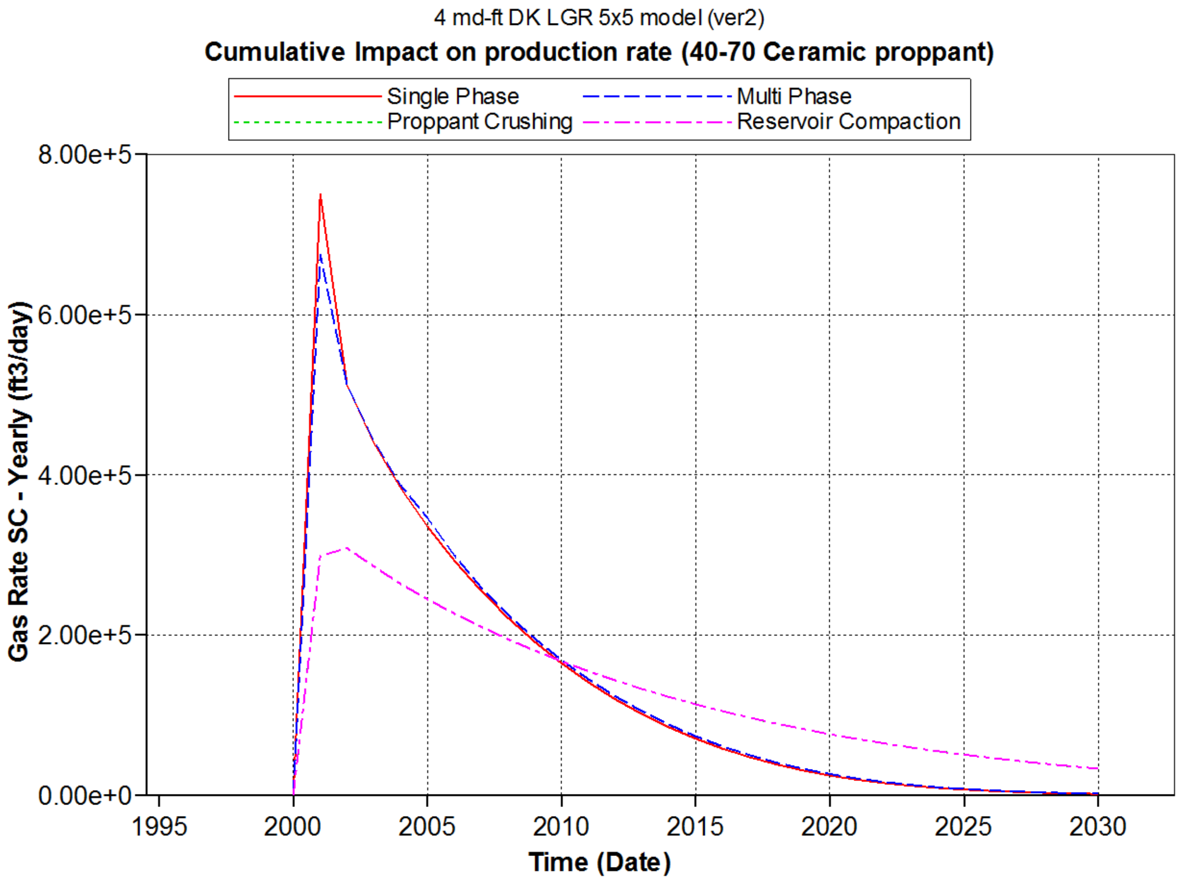

Figure 50: Effect of 40-70 ceramic proppant on gas production rate

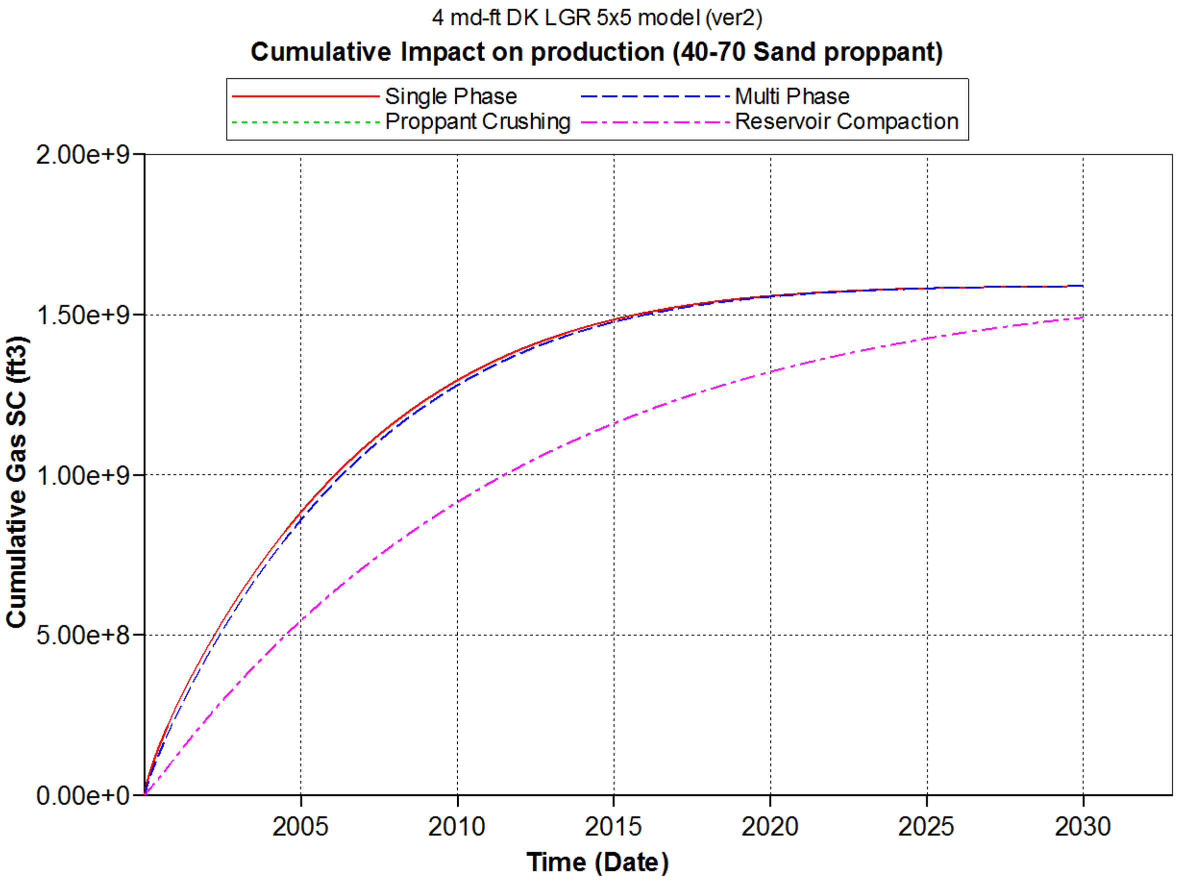

Figure 51: Effect of 40-70 multicoated sand proppant on cumulative gas production

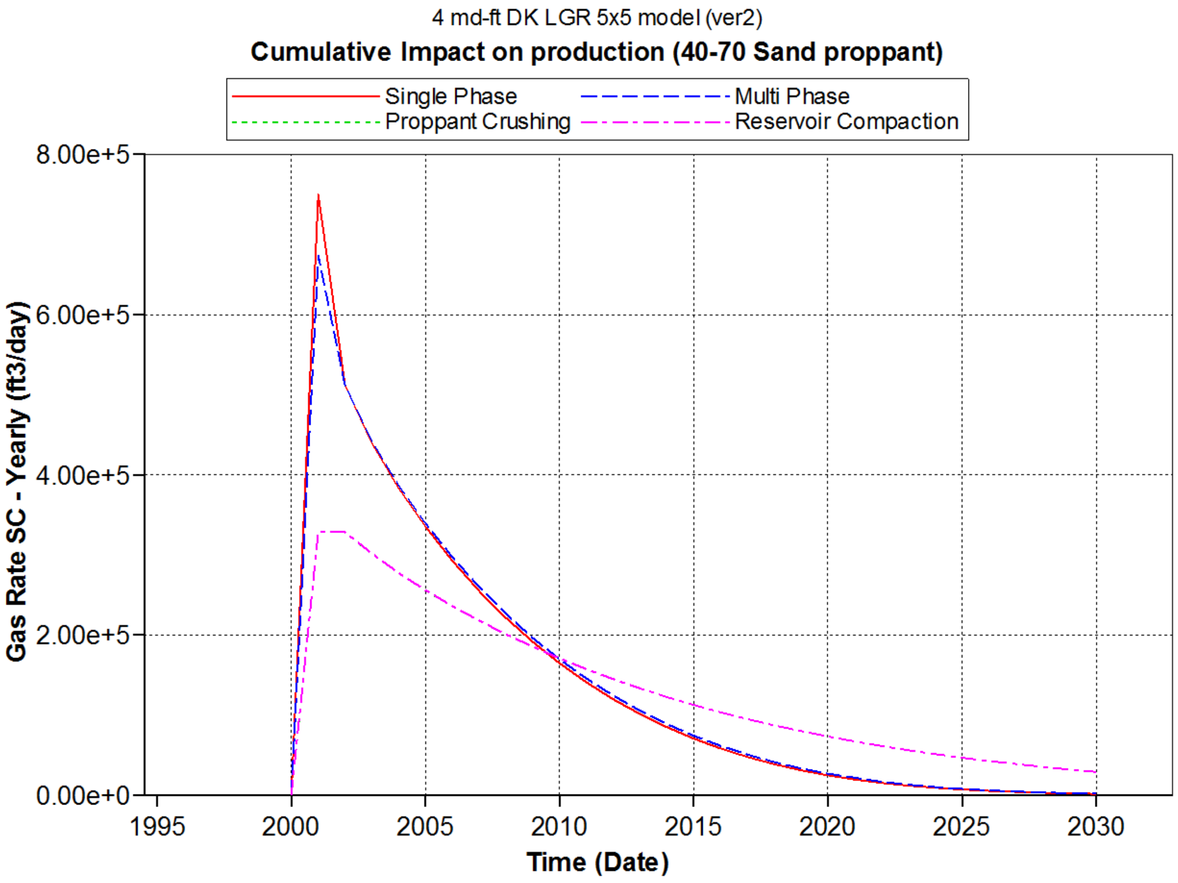

Figure 52: Effect of 40-70 multicoated sand proppant on gas production rate